Summer 8-4-2011

Topochemical Manipulation of Layered Perovskites

Elisha A. Josepha
University of New Orleans, ejosepha@uno.edu

Topochemical Manipulation
of Layered Perovskites

A Dissertation

Submitted to the Graduate Faculty of the
University of New Orleans
in partial fulfillment of the
requirements for the degree of

Doctor of Philosophy
in
Chemistry
Solid State

by

Elisha A. Josepha

B.S., University of West Florida, 2004
M.S., University of New Orleans, 2009

August, 2011

To those who know how to get back up after a great fall,
my parents, my dearest friend, and Bay

Acknowledgements

I would like to extend my great appreciation to my advisor Professor John B. Wiley. I will forever be indebted to him for everything he has done for me through the years. He has been an advisor, a mentor, an example, a true human being, and a friend. Thank you for your guidance in my chemistry career, thank you for teaching me how to be a better and more patient person, thank you for your great advices. You have given me the room to make my mistakes and to learn from them while encouraging me along the way. I walked into your office many times and said: "I quit!" and yet you knew exactly how to bring me back on board. I already knew you were a great person but the memorable "Katrina-time" made you so much greater in my eyes. You have been one of the most influential individuals in my life and I look up to you. If I had to do this again, I WOULD DO IT ALL OVER AGAIN WITH YOU!!

To some of my past and current group members; Liliana, Doina, Xiao, Feng, Bo, Larisa, Choi, Sanjaya, Chaubey, Jin, Piku (little one), Yuantje, Jianxia, Debo, Dariush, Lea, Andrew, Brit; Thank You!!!. Thanks for the support, the help with some of the work presented herein, the educational discussions, the laughs, the good times and the bad ones too, and for every opportunity that I spend learning about your cultures.

I would like to thank some of my friends, who were very supportive in many ways during my graduate career; The French Guy, The Greeco-N, Jurema, Keysha, Dudu, Jill, Jean-Ann, Dyainsie, and James. I appreciate your support and your understanding along the way.

Table of Contents

List of Figures

List of Tables

Abstract

Topochemical strategies, techniques that allow one to effectively manipulate the structures of nonmolecular solids once a crystal lattice is established, are effective in the low temperature (< 500 °C) modification of solid state structures, allowing the preparation of nonmolecular compounds not accessible by standard synthetic routes. Some of the techniques, ion exchange, intercalation/deintercalation, have proven to be excellent synthetic methods for preserving specific frameworks. The combination of these techniques can allow one to create a multistep approach that can be used to design new compounds with interesting properties.

As an expansion to the field of topotactic reactions, a multistep approach was developed towards the synthesis of the new compounds $(A_xM_{0.5}Cl_y)LaNb_2O_7$ (where A = Rb, Cs; M = Fe, Ni; $x \approx 1.5$; $y \approx 1$) at temperatures below 400^oC. The first reaction step involved the ion exchange of the host materials ($ALaNb_2O_7$, A = Rb, Cs) to form the products $M_{0.5}LaNb_2O_7$ (where M = Fe, Ni), a structure open to further chemistry. The next step involved reductive intercalation with Rb or Cs metal to form the air sensitive mixed-valence products with the nominal compositions, $A_{1.5}M_{0.5}LaNb_2O_7$. The last step involved the oxidative intercalation of chlorine using chlorine gas to obtain the final compounds. This multistep approach is a design to form mix-metal halide layers, specifically those with divalent cations, within layered perovskites, opening the doors to compounds that can have interesting properties.

This reaction series was also applied to the tantalate layered oxides, leading to the formation of the new compound $Ni_{0.5}LaTa_2O_7$ through ion exchange. The further multistep

topochemical manipulation of this new compound was not successful and was indicative of the difference in chemical behavior of the tantalates versus the niobates.

We have also investigated the oxidative intercalation of halogens into a series of Ruddlesden-Popper (R-P) ruthenate oxides with the formula $Ae_{n+1}Ru_nO_{3n+1}$ (Ae = Ca, Sr; n = 1, 2, 3) using several sources of fluorine, chlorine, and bromine. A new method was developed to intercalate chlorine into layered systems; this new approach avoids the use of chlorine gas which is highly toxic. The new phase $Sr_3Ru_2O_7Cl_{0.7}$ was synthesized by the new method and further topotactic manipulations were explored. The chemistry was not limited to the n = 2 phase but was also applied to the n = 3 phase, $Sr_4Ru_3O_{10}$.

Keywords: topotactic manipulation, layered perovskites, synthesis, oxides, oxyhalides, ruthenates, niobates, tantalates, ion exchange, intercalation, chlorine, fluorine

Chapter 1: Introduction and Background

1.1 Perovskites and Layered Perovkites.

Perovskite oxides have obtained much attention over the years due to their range of important properties such as high-temperature superconductivity,[1] colossal magnetoresisitance,[2] catalytic activity,[3] and ferroelectricity.[4] Colossal magnetoresistance (CMR) for example has been seen in several mixed valence manganese oxides,[2,5-8] ferroelectric behavior in barium titanates,[9,10] and high temperature superconductivity in layered cuprates.[11-13] The further development of this class of compounds may therefore lead to new technologically significant materials.

The ideal perovskite structure has the general formula ABO_3 where B is a transition metal ion and A is a large cation, typically an alkali metal, an alkaline earth, or a rare earth metal ion.[14] Figure 1.1 illustrates the ideal cubic perovskite structure[15] of corner sharing BO_6 octahedra with the A cation sitting in a twelve coordination (AO_{12}) site (body center).[16]
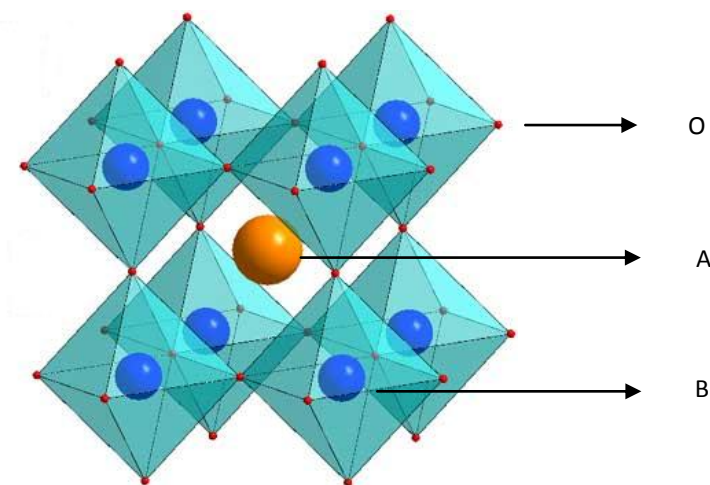
Figure 1.1 Ideal perovskite structure

A close-packed illustration of the structure can also be seen in Figure 1.2 and is described as a cubic close-packed array of O anions and A cations with the B cations filling one fourth of the interstitial octahedral sites.[16]
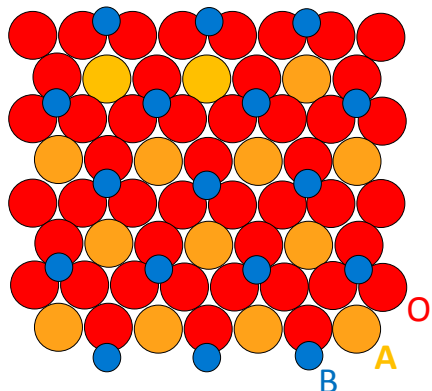
Figure 1.2 Cubic close-packed combinations of A cations and O anion in the ABO_3 structure.

Three common perovskite-related layered structures studied in our group include the Dion-Jacobson (DJ), Ruddlesden-Popper (RP), and Aurivillius (AV) phases. Layered perovskites are intergrowths of perovskite and other structures, and they consist of two-dimensional perovskite slabs interleaved with cations or cationic structure units. The DJ[17] series is described by the general formula $A[A'_{n-1}B_nO3_{n+1}]$, and the RP[18] series by $[A_2[A'_{n-1}B_nO_{3n+1}]$ where A is often an alkali metal or alkaline earth metal, A' is a rare earth metal, B is a transition metal, and n is the number of perovskite layers. The structural similarity, Figure 1.3 a and 1.3 b, between the two series is that they both contain perovskite sheets that are separated by A cations; and the difference resides in the number of A (alkali metals) interconnecting them – one A cation for the DJ series and two for the RP series.[19,20] The AV phases can be defined by the general formula (Bi_2O_2) A $[A'_{n-1}B_nO3_{n+1}]$. Their structure (Figure 1.3 c) also contains perovskite layers but the interlayer is generally composed of (Bi_2O_2) sheets.
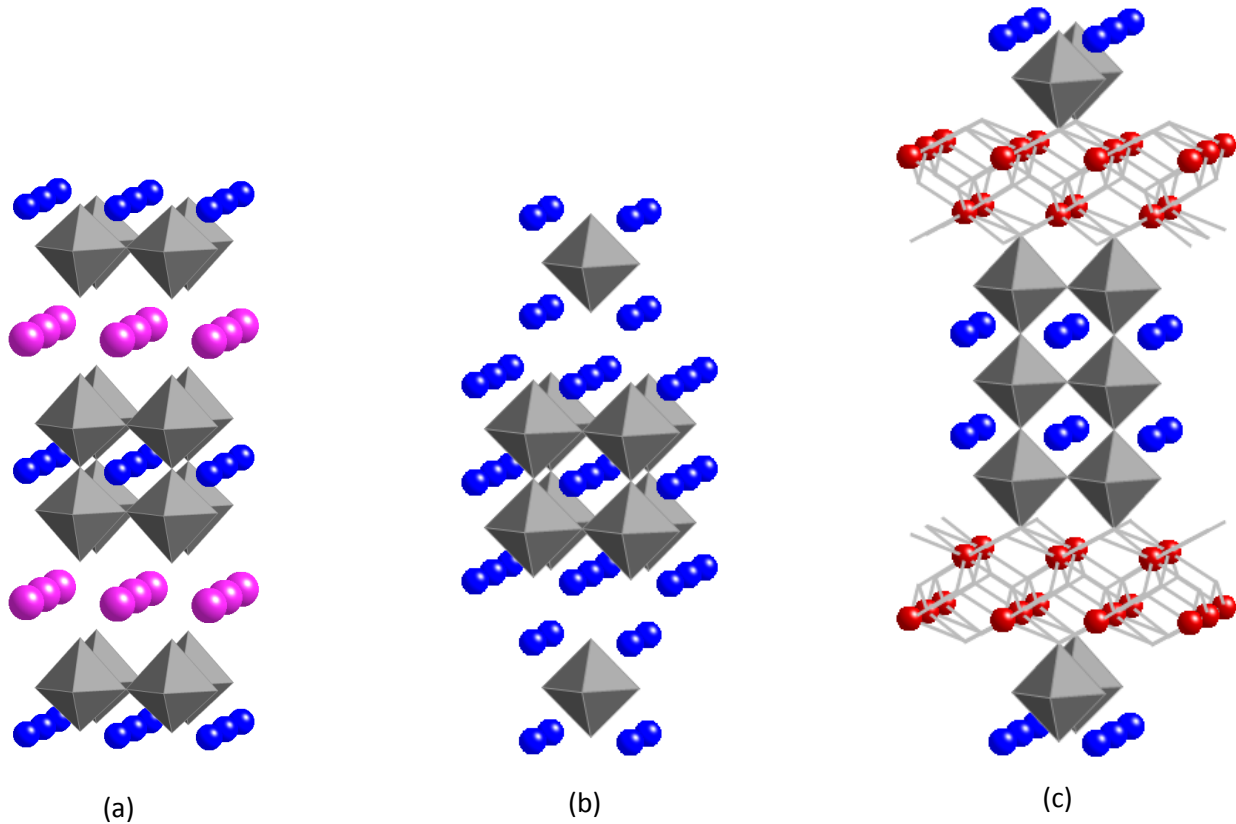
Figure 1.3 Examples representing each layered perovskite structure, (a) Dion-Jacobson, $CsLaNb_2O_7$; (b) Ruddlesden-Popper, $Sr_3Ru_2O_7$; (c) Aurivillius, $Bi_2O_2Sr_2TiNb_2O_{10}$.

Layered perovskites have received great attention in recent years due to two main reasons: 1. their properties, 2. their chemical variations. It is the electronic state of the B ion that most greatly contributes to the electronic and magnetic properties observed. With the use of topochemical techniques, structural modifications can be executed within the interlayers, as well as the actual perovskite layers, that can lead to new compounds with interesting properties.

1.2 Solid State Synthetic Technique: Topotactic Methods

Solid state chemists have in recent years adapted a new and more controlled way of synthesizing new compounds that were previously hard to obtain due to the harsh conditions known before. The traditional and common "heat and beat" ceramic method used in solid state synthesis has to be carried out under high temperatures (> 1000 ^{o}C), long time frames, and requires fine mixing since ceramic reactions are diffusion limited. The input of energy in these reactions is large and as such, do not favor the formation of metastable compounds. Such high temperatures allow for bond reformation so that one has no control over the structure and phase purity in the extended non-molecular solids, something organic chemists have great control over in their corresponding molecular systems.

Topotactic methods, a type of soft chemical methods (*chimie douce*), allow for the manipulation of solid-state compounds at low temperatures (< 500 ^{o}C).[21] A general goal in this research is to create or improve topochemical strategies for the formation of new-layered compounds that cannot be thermodynamically obtained at high temperatures, while maintaining their overall structural features at a kinetic level. The techniques used towards these goals are ion exchange,[22] intercalation/deintercalation,[23] layer extraction, grafting, exfoliation, layer construction, pillaring, and substitution reactions (Figure 1.4). All these methods have proven to be excellent synthetic techniques for preserving specific frameworks.
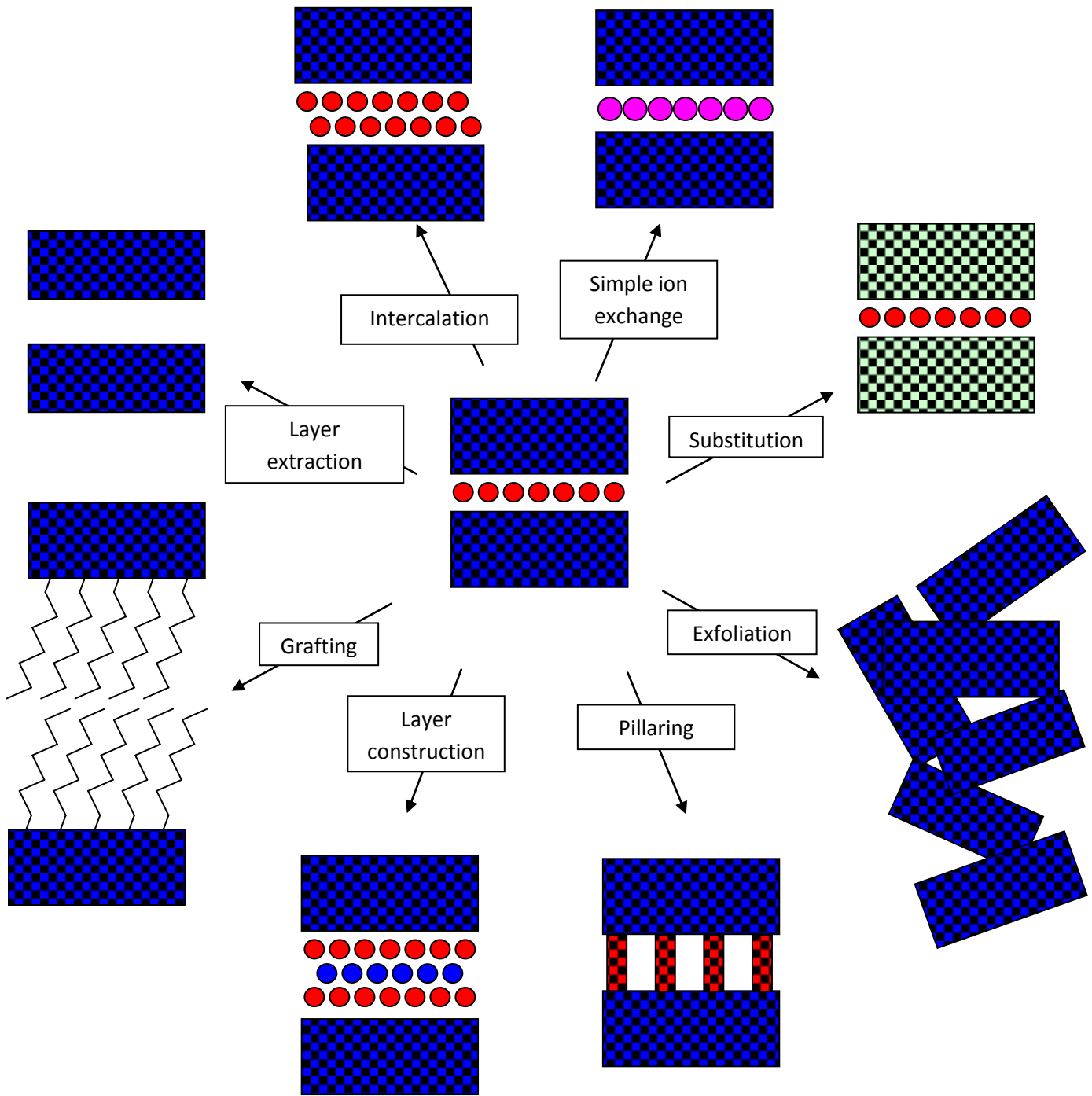
Figure 1.4 Cartoon representing the basic idea of topochemical manipulations.[24]

Ion exchange: For years, ion exchange has been a very well-known and used technique in the chemistry world. The idea is the exchange of weakly bonded cations (or anions) for other ionic species, and is not limited to monovalent ions but also extends to aliovalent ones (Figure 1.5).
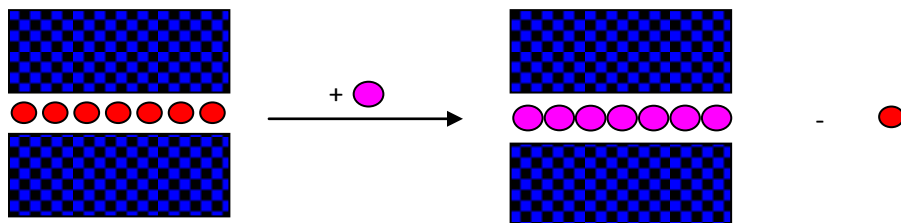
Figure 1.5 Cartoon showing the overall idea of ion exchange

A couple of important factors need to be taken into account for these reactions to be favorable and effective; reactions can occur more favorably when carried out in molten or aqueous media to aid in the diffusion to the solids and ions of comparable sizes exchange more readily.

In the perovskites, this topochemical technique has been mostly studied in DJ and RP perovskites. In the DJ compound $RbLaNb_2O_7$[25] for example, the Rb cation can be exchanged for other alkali metal cations (Li, Na, K) and a structural change is seen to accommodate for the smaller size of the exchanged ion. On that same note, the Rb cation can be substituted for transition metal ions like Fe and Ni to form $M_{0.5}LaNb_2O_7$ (where M = Fe, Ni).[26] One can also control the amount of exchange by altering the reaction conditions as reported by Galven *et al.*,[27] where the RP compound $LiHSrTa_2O_7$ was exchanged from $Li_2SrTa_2O_7$ under aqueous conditions.

Intercalation and deintercalation: These methods have been studied extensively and are popular because of the ability to obtain products with mixed-valency, which can be significant in technological applications. The reactions involved in these processes are oxidation or reduction involving the addition or removal of cationic or anionic species within the interlayer of the host used while still maintaining the overall structure of the host. These reactions can be

| (a) | (b) | (c) |

Figure 1.6 Scheme showing intercalation going from a to b, and deintecalation from b to c

carried out chemically or electrochemically,[28,29] and as in ion exchange, interlayer spacing of the host and the size of the intercalant are important to the thermodynamics and kinetics of the reactions.[25,26]

Some of the first reports on intercalation were in graphite with its capability to be receptive to different intercalants.[30]   An example is the reductive intercalation of rubidium metal to form RbC_8. Alkali metals are often used as reagents for reductive intercalations because they are strong reducing agents. This basic technique has been extended to many other systems, which include layered perovskites. As long as there are vacant A sites in the interlayer of the perovskite, the chemistry will allow for simple intercalants like alkali metals to be inserted e.g.,

the intercalation of Li into $LiLaNb_2O_7$ to form $Li_2LaNb_2O_7$.[31] It is to be noted that this chemistry is limited to the DJ and AV phases since the RP phases typically have "room constraints."

Oxidative Intercalation is similar to reductive intercalation but now the reaction involves the oxidation of the B site ion while allowing the anionic intercalant to occupy an interstitial site in the interlayer of the perovskite. Greaves *et al.* have shown that fluorine ions can be inserted in the cationic layers between the perovskite blocks as in the compounds $Sr_3Ru_2O_7$ to produce $Sr_3Ru_2O_7F_2$ and $LaSrMnO_4$ to produce $LaSrMnO_4F$.[32,33] Often in this chemistry, one can also see what is considered a substitution reaction, where the intercalant actually replaces one of the anions in the perovskite block. It can also be explained as a combination of an oxidative intercalation with a simultaneous deintercalation reaction. An example of such reaction is the formation of $RbLaNb_2O_6F$[34] from the reaction between host compound $RbLaNb_2O_7$ and polyvinylidene fluoride (PVDF) or polytetrafluoroethylene (PTFE) in air.

Multi-step Topochemical Manipulation: Our group has investigated the formation of alkali metal halide layers within Dion-Jacobson (DJ) perovskites by two-step techniques.[35] The combination of oxidative and reductive intercalation is well studied and will be further discussed in some of the work presented later; especially with respect to the combination of the two methods.[36] Combined with each other or with other techniques like ion-exchange (multistep approach) is how one can also develop a low temperature solid-state synthetic route. Reductive intercalation with an alkali metal, followed by oxidative intercalation with chlorine gas, lead to the formation of the compounds of general formula, $(A_2Cl)LaNb_2O_7$ (A = Rb, Cs).[35]

One area where topochemical reactions are expected to be especially important is in the controlled construction of metal-nonmetal layers. The routine formation of layers consisting of combinations of transition metal-main group species within receptive hosts could lead to a variety of new important compounds. Multistep ion exchange reactions have also been used to facilitate the construction of transition-metal halide arrays.[36] In the synthesis of mixed valence compounds, earlier studies have shown that aliovalent ion exchange followed by reductive intercalation allows for the formation of semiconducting perovskites from insulating hosts.[37,38] Mixed-metal oxides with the perovskite structure, including layered perovskites, are already known to exhibit a range of important properties. For example, layers of Cu-O, Fe-As, and Mn-O, are common to compounds exhibiting superconductivity or magnetoresistive properties. The ability to build such layers within a particular host or to explore completely new combinations of metal-nonmetal species, could lead to significant advances in the fabrication of materials with important properties. The routine design and synthesis of new compounds with specific properties could serve to greatly expand access to important materials such as superconductors, ferromagnetics, ferroelectrics, multiferroics, thermoelectrics, magnetoresistive materials, optical materials, catalysts, ionic conductors, battery and fuel cell components, etc.

1.3 Characterization of Layered Perovskites

Crystallography

Sample characterization of new solid state materials is essential to identify and confirm if the desired compounds were prepared. First of all, one has to obtain the identification or structural determination based on the crystal structure.[16] A solid that is built through regular arranged atoms that are on specific points in three dimensions is defined as the crystal structure. The grouped atoms are represented by a unit cell as can be seen in Figure 1.7 and each unit cell is described by the vectors a, b, c and the angles α, β, γ which are referred
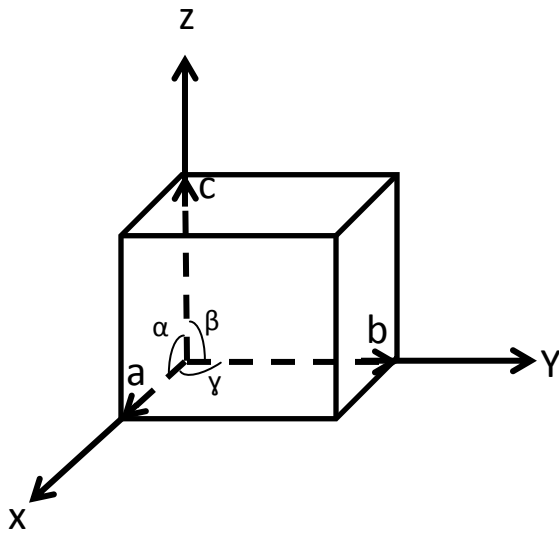
Figure 1.7 Unit Cell and parameter description

to as the lattice parameters. The atoms which can be represented as points (lattice points) will arrange in a certain way to minimize the electrostatic interaction among them and/or to maximize the symmetry of the crystal structure (or lattice). There are 7 crystal systems and they can be seen in Figure 1.8 below from which August Bravais, a French crystallographer,

showed that there are 14 three dimensional unit cells possible (Table 1.1) based on where the

atoms are placed with a specific unit cell.[39,40] These unit cells are very much dependent on the

lattice parameters that govern what crystal system the compound will adapt.

Cubic   Tetragonal   Orthorhombic

Triclinic   Hexagonal   Monoclinic

Trigonal or Rhombohedral
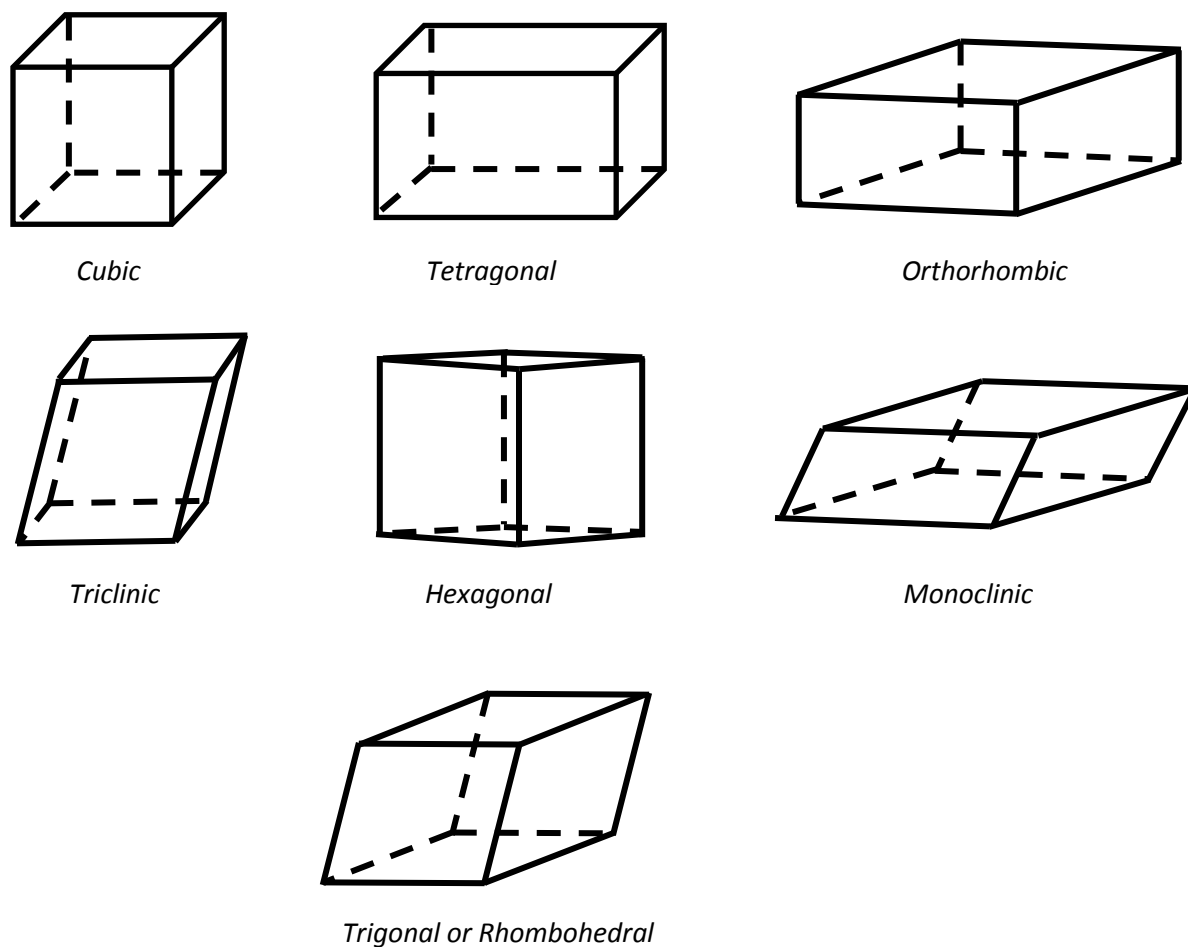
Figure 1.8 Unit cells of the seven crystal systems

Table 1.1 The 14 Bravais lattices and their description

Crystal System	Description of Coordinates	Essential Symmetry	Allowed Lattices
Cubic	$a = b = c, \alpha = \beta = \Upsilon = 90^{o}$	$4 \times C_3$	P, F, I
Tetragonal	$a = b \neq c, \alpha = \beta = \Upsilon = 90^{o}$	$1 \times C_4$	P, I
Orthorhombic	$a \neq b \neq c, \alpha = \beta = \Upsilon = 90^{o}$	$3 \times C_2$ or mirror planes	P, F, I, A (B or C)
Hexagonal	$a = b \neq c, \alpha = \beta = 90^{o}, \Upsilon = 120^{o}$	$1 \times C_6$	P
Trigonal (a)	$a = b \neq c, \alpha = \beta = 90^{o}, \Upsilon = 120^{o}$	$1 \times C_3$	P
(b)	$a = b = c, \alpha = \beta = \Upsilon \neq 90^{o}$	$1 \times C_3$	R
Monoclinic	$a \neq b \neq c, \alpha = \Upsilon = 90^{o}, \beta \neq 90^{o}$	$1 \times C_2$ or mirror plane	P, C
Triclinic	$a \neq b \neq c, \alpha \neq \beta \neq \Upsilon \neq 90^{o}$	None	P

A crystal structure can also be seen as an agglomerate of imaginary equally distant periodic parallel planes (lattice planes) that intersect with at least three non-collinear lattice points.[16] Lattice planes are denoted by Miller indices (hkl), a set of three numbers that are reciprocals of the points where the plane intercepts with the x, y, z axis. Figure 1.9 shows an example of t

a) (1 0 0)   b) (2 0 0)   c) (1 0 0)
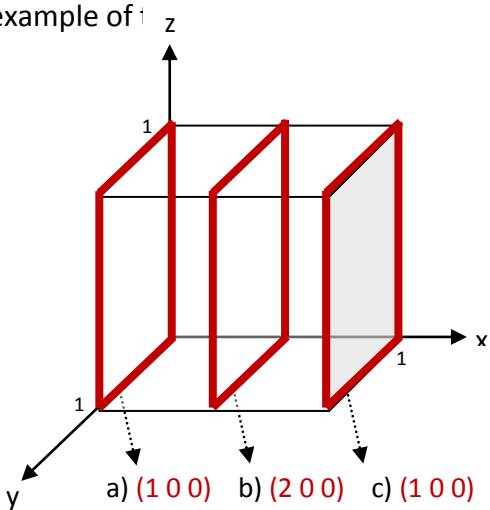
Figure 1.9 Derivation of the Miller indices and their corresponding planes in a P cubic cell

(1 0 0) plane in a primitive cubic cell. In the figure, the edge of the primitive cube will be used as coordinate axes and as is noted, the middle plane (b), for example, intercepts the axes at 1/2, ∞,∞. After taking the reciprocate of each number and thus getting, 2/1, 0, 0 we end up with the Miller indices (2 0 0) of plane c. A set of planes with the same hkl's are represented by the Miller indices but instead of using parenthesis one would use the curly brackets. For example, plane "a" and plane "c" in Figure 1.6 are considered a set of planes and will be written {1 0 0}. Regular brackets, [], are used to indicate the direction of the Miller indices.[16]

X-ray Diffraction

Two techniques that are widely used as initial tools towards structure characterization and phase recognition are X-ray diffraction and neutron diffraction. The latter, where neutrons interact with the atomic nuclei, will not be covered herein since it was not used in the research projects. A monochromatic, intense beam of X-rays produced by a cathode ray tube (Cu or Mo) is collimated to interact with a sample and diffracted (scattered) by the electrons surrounding the nuclei, producing constructive interference when Bragg's law:

$$n\lambda = 2d \sin (2\theta/2) \tag{1}$$

 is satisfied depending on the wavelength of the X-rays (λ) and the distance between the atoms present in the sample (Figure 1.10 and 1.11). The X-rays scattered are in phase with each other
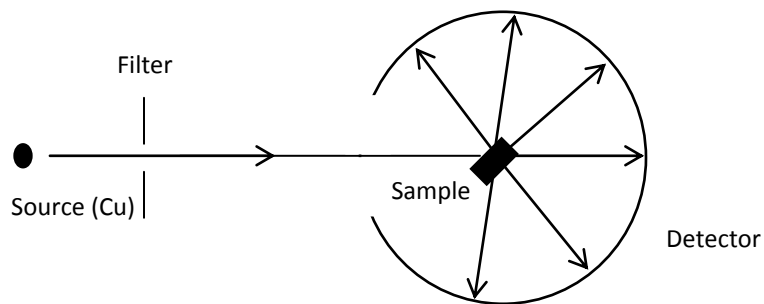
Figure 1.10 Scheme of powder diffraction experiment

therefore there is constructive interference, but can also be out of phase, cancelling each other

out (destructive interference).[16] The incident beam makes an angle θ with the atomic planes

that are parallel to each other separated by a distance "d" and "n" is nothing but an integer
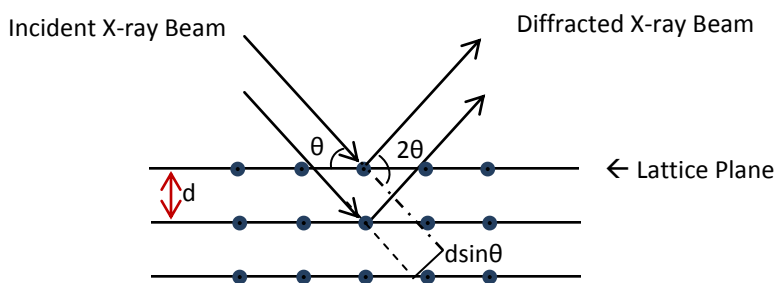
Figure 1.11 Scheme of diffraction of X-rays in the lattice planes of a solid

that defines the order of the reflection and is usually set to be 1. It is important to highlight here that the scattering of the X-rays is very dependent on the electron density of the atoms present in the sample; heavier atoms scatter more than lighter ones, so for that matter it is hard to locate lighter atoms in the presence of heavier atoms. Each electron present contributes to the scattering intensity. The intensity of peaks depend not only on the scattered intensity of the electrons and the atoms but is also dictated by interference effects (destructive interference) and thermal motion. Each reflection has an intensity that depends on the what kind of atom there is present and where it is in the unit cell, so planes that go through atoms with high electron density can give intense reflections.

Powder diffraction is important when it comes to the qualitative identification of crystalline compounds or phases and is one of the tools used in the determination of the crystal structure and unit cell parameters of a material. Every crystalline phase is unique when it comes to its powder pattern based on the peak positions which are governed by specific hkl's (dictated by the planes present for each unit cell distinctively). Looking back at Figure 1.8, the d-spacing (d), defined by the hkl's, can be determined through Bragg's law using the measured angle 2-theta (obtained from the XRD pattern output). The shape of the unit cell is d-spacing specific for each of the seven Bravais lattices and is mathematically defined for each in Table 1.2.

Table 1.2 Formulae for the d-spacing for the seven Bravais lattices

Unit Cell	Formula
Cubic	$\dfrac{1}{d^2} = \dfrac{h^2 + k^2 + l^2}{a^2}$
Tetragonal	$\dfrac{1}{d^2} = \dfrac{h^2 + k^2}{a^2} + \dfrac{l^2}{c^2}$
Orthorhombic	$\dfrac{1}{d^2} = \dfrac{h^2}{a^2} + \dfrac{k^2}{b^2} + \dfrac{l^2}{c^2}$
Hexagonal	$\dfrac{1}{d^2} = \dfrac{4}{3}\dfrac{h^2 + hk + k^2}{a^2} + \dfrac{l^2}{c^2}$
Monoclinic	$\dfrac{1}{d^2} = \dfrac{1}{\sin^2\beta}\left[\dfrac{h^2}{a^2} + \dfrac{k^2 \sin^2\beta}{b^2} + \dfrac{l^2}{c^2} - \dfrac{2hl\cos\beta}{ac}\right]$
Triclinic	$\dfrac{1}{d^2} = \dfrac{1}{V^2}[h^2 b^2 c^2 \sin^2\alpha + k^2 a^2 c^2 \sin 2\beta + l^2 a^2 b^2 \sin 2\gamma + 2hkabc^2(\cos\alpha\cos\beta - \cos\gamma) + 2kla^2 bc(\cos\beta\cos\gamma - \cos\alpha) + 2hlab^2 c(\cos\alpha\cos\gamma - \cos\beta)]$

1.4 References

1. Bednorz, J.G.; Müller, K.A.Z. *Phys. B* **1986**, *64*, 189.
2. Maignan, A.; Martin, C,; Damay, F.; Raveau, B. *Chem. Mater.* **1998**, *10*, 950.
3. Moritomo, Y.; Asamitsu, A.; Kuwahara, H.; Tokura, Y. *Nature* **1996**, *380*, 141.
4. Horn, J.; Zhang, S.C.; Selvaraj, U.; Messing, G.L.; Trolier-McKinstry, S. *J. Am. Ceram. Soc.* **1999**, *82*, 921.
5. Battle, P.D.; Cox, D.E.; Green, M.A.; Millburn, J.E.; Radaelli, P.G.; Rosseinky, M.J.; Vente, J.F. *Chem. Mater.* **1997**,*9*, 1042.
6. Battle, P.D.; Green, M.A.; Laskey, N.S.; Millburn, J.E.; Spring, L.E.; Sullivan, S.P.; Rosseinky, M.J.; Vente, J.F. *Chem. Mater.* **1997**, *9*, 1042.
7. Damay, F.; Maigan, A.; Nguyen, N.; Raveau, B. *J. Solid State Chem.* **1996**, *124*, 385.
8. Raveau, B.; Maigan, A.; Caignaert, V.J. *Solid State Chem.* **1995**, *117*, 424.
9. von Hippel, A.; Breckenridge, R.G.; De Bretteville, A.T.; Brownlow, J..M.; Chesley, F.G.; Oster, G.; Tisza, L.; Westphal, W.B. *Nat. Def. Res. Comm. Report* No. 300, **1944**.
10. Chen, S.N.; Ramakrishnan, E.S.; Grannemann, W.W. J. Vac. Sci. Technol. A **1985**, *3,* 678.
11. Raveau, B.; Studer, F.; Pelloquin, D. Physica C Supercond. **1995**, *242* (1/2), 1.

12. Bednorz, J.G.; Müller, K.A.; *Z. Phys*. B64 **1986**, *187*.

13. Regueiro, M.N.; Tholence, J.L.; Antipov, E.V.;Capponi, J.J.; Marezio, M. **Science 1993**, *262*, 97.

14. Galasso, F.S. *Structure, Properties and Preparation of Perovskite-type Compounds*; Pergamon Press: Oxford, 1969.

15. http://www.princeton.edu/~cavalab/tutorials/public/structures/perovskites.html.

16. West, A.R. *Solid State Chemistry and its Applications*; John Wiley & Sons Ltd, 1987.

17. Dion, M.; Ganne, M.; Tournoux*, M.; *Mater. Res. Bull*., **1981**, *16*, 1429; Jacobson, A. J.; Johnson, J. W.; Lewandowski, J. T.; *Inorg. Chem*., **1985**, *24*, 37.

18. Ruddlesden, S. N. and Popper, P.; *Acta Crystallogr*., **1957**, *10*, 538.

19. Dion, M.; Ganne, M.; Tournoux*, M. *Mater.Res.Bull*., **1981**, *16*, 1429;

20. Dion, M.; Ganne, M. ; Tournoux, M.; Revez, J. *Rev. Chim. Miner.* **1984**, *21*, 92.

21. Smart Lesley E., Moore Elaine A. 2005. Solid State Chemistry: An Introduction 2005. 3rd edition. Boca Raton, Florida. CRC Press.

22. (a)Jacobson, A. J.; Johnson, J. W.; Lewandowski, J. T.; *Inorg. Chem*, **1985**, *24*, 3729; (b) Gopalakrishnan, J.; Uma, S.; Bhat, V.; *Chem. Mater*., **1993**, *5*, 132; (c) Cushing, B. L.; Wiley, J. B.; *Mater. Res. Bull*, **1999**, *34*, 271.

23. Jones, R.; McKinnon, W. R.; *Solid State Ionics*, **1991**, *45*, 173; (b) Gomez-Romero, P.; Palacin, M.R.; Casan, N.; Fuerts, A.; *Solid State Ionics*, **1993**, *63-65*, 424; (c) Armstrong, A. R.; Anderson, P. A.; *Inorg. Chem*., **1994**, *33*, 4366.

24. Ranmohotti, K.G.S.; Josepha, E.; Choi, J.; Zhang, J.; Wiley, J.B. *Adv. Mater*. **2011**, 23, 442-460.

25. Gopalakrishnan, J., Bhat, V., Raveau, B. *Mater. Res. Bull.* **1987**, *22*, 413

26. Viciu, L.; Liziard, N.; Golub, V.; Kodenkandath, T. A.; Wiley, J. B. *Mater. Res. Bull.* **2004**, *39*, 2147.

27. Galven, C.; Fourquet, J. L.; Suard, E.; Crosnier-Lopez, M. P.; Le Berre, F. *Dalton Trans.* **2010**, *39*, 3212.

28. Mizushima, K.; Jones, P. C.; Wiseman, P. J.; Goodenough, J. B. *Mater. Res. Bull.* **1980**, *15*, 783.

29. Menetrier, M.; Saadoune, I.; Levasseur, S.; Delmas, C. *J. Mater. Chem.* **1999**, *9*, 1135

30. Bartlett, N., McQuillan, B. W. In *Intercalation Chemistry*; Whittingham, M. S., Jacobson, A. J., Ed.; Academic Press: New York, 1982.

31. Whittingham, M. S., Jacobson, A. J. In *Intercalation Chemistry*; Academic Press: New York, 1982.

32. Greaves C.; Li R.K., *Physical Review B* **2000**, 62, 3811.

33. Greaves C.; McCabe E.E., *J of Fluorine Chem.* **2007**, 128, 448-458.

34. Kobayashi, Y.; Tian, M.; Eguchi, M.; Mallouk, T. E. *J. Am. Chem. Soc.* **2009**, *131*, 9849.

35. Viciu, L.; Kodenkandath, T. A.; Wiley, J. B. *J. Solid State Chem.* **2007**, *180*, 583.

36. Choi, J.; Zhang, X.; Wiley, J. B. *Inorg. Chem.* **2009**, *48*, 4811.

37. Viciu, L.; Caruntu, G.; Royant, N.; Koenig, J.; Zhou, W. L. L.; Kodenkandath, T. A.; Wiley, J. B. *Inorg. Chem.* **2002**, *41*, 3385.

38. McIntyre, R. A.; Falster, A. U.; Li, S. C.; Simmons, W. B.; O'Connor, C. J.; Wiley, J. B. *J. Am. Chem. Soc.* **1998**, *120*, 217.

39. Lalena, J. N.; Cushing, B. L.; Falster, A. U.; Simmons, W. B.; Seip, C. T.; Carpenter, E. E.; O'Connor, C. J.; Wiley, J. B. *Inorg. Chem.* **1998**, *37*, 4484.

40. R. Jenkins and R. L. Snyder, *Introduction to X-ray Powder Diffractometry,* John Wiley & Sons Ltd., **1996**.

41. David, W. I. F.; Shankland, K.; McCusker, L.B. and Baelocher, Ch. *Structure Determination from Powder Diffraction Data;* Oxford University Press, **2002**.

Chapter 2

New Layered Oxides ($A_xM_{0.5}Cl_y$)$LaNb_2O_7$ (where A = Rb, Cs; M = Fe, Ni; x ≈ 1.5; y ≈ 1) Prepared through a Multistep Approach

2.1 Introduction

Topotactic methods, part of soft chemical methods (*chimie douce*), allow for the formation of new compounds at low temperatures (< 500 ^{o}C) while maintaining salient structural features.[1] Some of the techniques, ion exchange, intercalation/deintercalation, have proven to be excellent synthetic methods for preserving specific frameworks. A further expansion in the field of topotactic reactions towards the development of specific compounds is the sequential application of these techniques. By combining such methods, one can design a multistep approach that leads to the formation of products not obtainable through traditional solid state techniques. By using a low temperature solid-state synthetic route one can preserve the main framework of the host material while creating new materials with possibly interesting properties. Multistep reaction design using topochemical techniques on layered perovskite hosts, like Dion-Jacobson (DJ), $A[A'_{n-1}B_nO_{3n+1}]$ and Ruddlesden-Popper (RP) $A_2[A'_{n-1}B_nO_{3n+1}]$ where A is an alkali metal; A' is an alkaline or rare earth metal; and B is a transition metal, has been recently studied. DJ compounds are quite receptive to combinations of ion exchange[2-5] as well as reductive and oxidative intercalation.[1,6-12] Viciu et al. showed the formation of metal halide layers within Dion-Jacobson (DJ) layered perovskites through a two-step approach by performing a co-exchange followed by a reductive intercalation to form (Li_2Cl)$LaNb_2O_7$.[13] Choi

et al. also showed the ability to form metal halide layers with DJ compounds by performing

reductive followed by oxidative intercalation to obtain $(A_2Cl)LaNb_2O_7$ (A = Rb, Cs).[12] Other

researchers have also used this approach on perovskite compounds beyond those of the DJ

series.[14-16] The work presented herein further demonstrates the ability to manipulate layered

perovskites topochemically through a multistep approach (Figure 2.1). Step-by-step
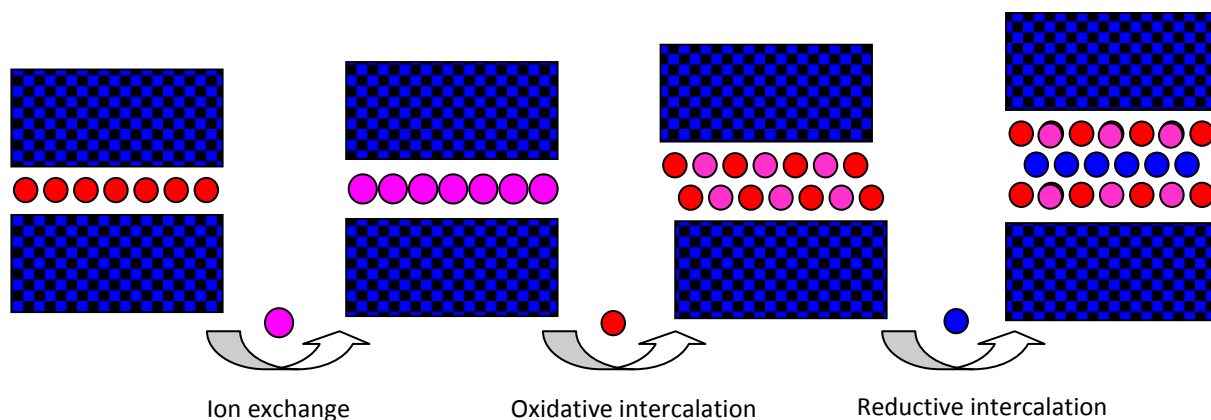
Figure 2.1 Scheme of Multistep Approach

synthesis and characterization starting with the ion exchange of $ALaNb_2O_7$ to lead to

$M_{0.5}LaNb_2O_7$, followed by the reductive intercalation of the alkali metals (A) to form

$A_xM_{0.5}LaNb_2O_7$, and finally oxidative intercalation to yield the final compounds

$(A_xM_{0.5}Cl_y)LaNb_2O_7$ (A = Rb, Cs; M = Fe, Ni), also referred to later as AM-0.5Cl,will be provided.

2.2 Experimental

2.2.1 Synthesis

Starting materials: ALaNb$_2$O$_7$ (A = Rb, Cs;) were synthesized as reported in the literature.[2,12] Stoichiometric quantities, weighed out in an argon filled glovebox, of Rb$_2$CO$_3$ (Alfa Aesar, 99%), or Cs$_2$CO$_3$ (Alfa Aesar, 99%), La$_2$O$_3$ (Alfa Aesar, 99.99%, dried for overnight at 1050°C to remove all hydroxide and carbonate impurities), and Nb$_2$O$_5$ (Alfa Aesar, 99.9985%) were ground together with a 25% molar excess of A$_2$CO$_3$ to compensate for that alkali-metal oxide lost due to volatilization. The mixtures were ground well, placed in alumina crucibles, and heated first at 850 ^{o}C for 12 hours for the full conversion of the carbonates to pure oxides, and then again ground and heated at 1050 ^{o}C for 24 hours. After the reaction, the products were cooled, washed with copious amounts of distilled water, and isolated in a Büchner funnel through suction filtration. Samples were then rinsed with acetone before drying them in an oven at 150 ^{o}C for a minimum of 30 minutes.

*Ion Exchange:*The synthesis of the intermediate compounds, M$_{0.5}$LaNb$_2$O$_7$ (M = Fe, Ni), further indicated as M-0.5, was carried out using ALaNb$_2$O$_7$ (where A = Rb, Cs) and anhydrous MBr$_2$ (M = Fe, Ni). RbLaNb$_2$O$_7$ and CsLaNb$_2$O$_7$ is reacted with NiBr$_2$ (Alfa Aesar, 99% anhydrous) and FeBr$_2$ (Alfa Aesar, 99.995% anhydrous), respectively, at a 1:2 molar ratio following a method similar to that reported by Viciu et al.,[17] Stoichiometric amounts of reagents were weighed out and ground for about 30 minutes using a mortar and pestle. The homogenous mixture was pressed into pellets with a hand press. Pellets were sealed under vacuum (< 10^{-4}

Torr) in Pyrex tubes. Reactions were carried out at 400 $^{\circ}$C for 1 week. The final products were washed with copious amounts of distilled water in combination with suction filtration to get rid of the alkali-metal bromide byproducts; samples were then rinsed with acetone dried at 150 $^{\circ}$C for a minimum of 30 minutes. The Fe-05 was olive green in color and Ni-0.5 was light yellow.

Reductive Intercalation: Rb (Alfa Aesar, 99.75%) and Cs (Alfa Aesar, 99.75%) was intercalated into the exchange products, $M_{0.5}LaNb_2O_7$ (where M= Fe, Ni) but only Fe-0.5 was reacted with Cs using the same techniques reported by Choi et al.[12] Reactions were carried out at 1:1.6 molar ratios based on the vacancies present after ion-exchange. $M_{0.5}LaNb_2O_7$ compounds were pressed into pellets with a hand press, placed in a Pyrex tube (12 mm o.d.) before flame drying the samples under dynamic vacuum. Then calculated amounts of alkali metals were weighed out in a small glass ampoule (6 mm o.d.) and this was combined with the $M_{0.5}LaNb_2O_7$ pellet. ***Note:*** *Caution should be taken when handling and disposing of alkali metals due to their violent reaction when in contact with moisture.* The reaction tube was then sealed under vacuum (< 10^{-4} Torr) and placed in a tube furnace at 250°C and 290°C, for rubidium and cesium metal, respectively. The reactions were carried out for 4 days, during which time the pellets turned black in color and crumbled on reaction due to volume changes in the products. After 4 days, to remove any unreacted metals, a temperature gradient was applied by sliding one end of the Pyrex tube outside of the tube furnace close to room temperature.

Oxidative Intercalation: In the last part of the multistep synthesis, the products obtained after reductive intercalation underwent oxidative intercalation using chlorine gas (Matheson 99.99%). ***Note:*** *Chlorine gas should be handled using an appropriate apparatus and protective*

equipment due to its corrosive and toxic nature. The chlorination procedure was similar to that

followed by Choi et al.[12] A Schlenk line, like that described by Jolly,[18] was set up in a fume hood.

Concentrated sulfuric acid was used as a scrubber and a saturated aqueous AOH solution (A =

Na, or K) was used to convert the un-reacted chlorine gas into KCl/NaCl. $A_{1.5}M_{0.5}LaNb_2O_7$

samples were loaded into scintillation vials fitted with TFE/silicone septum caps. The vials were

placed in a water bath then connected to the Schlenk line system via 18G stainless steel

needles. The Schlenk line was flushed with chlorine gas before the reaction vial containing the

sample was connected to make sure that the line was free of air. Chlorine flow was then

maintained for about an hour and the system was purged for at least 4 hours under nitrogen to

remove excess chlorine gas. The reactions for the cesium samples were much faster than those

of the rubidium; the cesium containing samples were reacted at room temperature and

changed color after a couple of minutes of chlorine exposure, but were still kept under gas flow

for about 30 min to an hour, and the rubidium samples, cooled in an ice bath, were reacted for

about an hour, though after 15 minutes one could see the change in color.

2.2.2 Characterization

Compounds were characterized by X-ray powder diffraction using a Philips X'Pert PW 3040

MPD system equipped with a graphite monochromator (Cu Kα radiation, λ = 1.5448Å). Routine

scans were collected in continuous mode for one hour over a 2θ range of 3 to 75° with a scan

speed of 0.02 deg/sec. Air-sensitive samples were prepared for X-ray data collection in an

argon-filled glovebox and sealed under a polypropylene film with silicone grease. CHECKCELL[19]

was used to refine the lattice parameters after the peak positions were determined using the

program PROFILE FIT.[20] Crystal structure refinements of the final compounds were investigated by the Rietveld technique with the FullProf program.[21]

Compositions were examined by energy dispersive spectroscopy (EDS) on a JEOL JSM 5410 scanning electron microscope (SEM) equipped with an EDAX-DX PRIME microanalytical system. All ratios were normalized to lanthanum. Residues of rubidium and cesium were observed in both the nickel and the iron compounds for the tantalate series, respectively. Field emission SEM, Leo 1530 VP field emission scanning electron microscope, was used to look at the morphology of the parent and the final products.

Thermal behavior was monitored using a differential scanning calorimeter (DSC) on a Netzsch 404S thermal analysis instrument in flowing argon and a TA-SDTQ600 thermal analyzer in the temperature range 25-1000 ^{o}C under nitrogen atmosphere. Samples were heated in alumina pans to 1000 ^{o}C at a rate of 10-50°C/min. Thermogravimetric analysis data was collected on TA Instruments Thermal Analyst-2000 apparatus using a platinum boat under argon flow heated to 1000 ^{o}C.

2.3 Results

As a further expansion of topochemical manipulation for the design of new compounds, we investigated the synthesis of $(A_{1.5}M_{0.5}Cl)LaNb_2O_7$ where A = Rb, Cs and M = Fe, Ni. $M_{0.5}LaNb_2O_7$ (M = Fe, Ni) was synthesized as reported by Viciu et $al.$[17] through ion exchange from the parent compounds $ALaNb_2O_7$ (A = Rb, Cs) and were confirmed through XRD data. EDS indicated that a residual amount of the alkali metal from the starting material is still present; this is consistent

with what was previously reported in the synthesis of these compounds.[17] All the peaks of both

compounds were indexed on a tetragonal cell with space group $P4/mmm$ and the unit cell

parameters were refined (Table 2.1); the c-parameters, however, were larger than the reported

values. Figure 2.2 shows a

Table 2.1 Unit cell parameters of $M_{0.5}LaNb_2O_7$

		Experimental	Literature values[17]
$Fe_{0.5}LaNb_2O_7$	a(Å)	3.880(4)	3.885(3)
	c(Å)	10.999(3)	10.680(7)
$Ni_{0.5}LaNb_2O_7$	a(Å)	3.879(4)	3.863(6)
	c(Å)	10.829(2)	10.61(2)
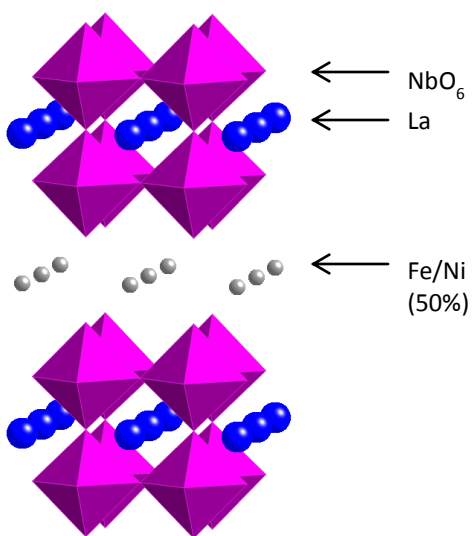
Figure 2.2 Proposed model structure of $M_{0.5}LaNb_2O_7$.

simulated model of the proposed crystal structure of the parent compounds with the transition

metal in the interlayer.

The M-0.5 host compounds underwent reductive intercalation with Rb and/or Cs metal and both compounds showed evidence of intercalation. Figure 2.3 shows a comparison of the XRD data collected for the Rb intercalated samples. Because both parents are isostructural with each other, only one parent was shown for comparison purposes. Cs intercalation was not attempted with Ni-0.5. An increase in the c-parameter was observed for the alkali inserted samples, which was expected due to the size of the alkali intercalant; a loss of crystallinity is also observed. In Table 2.2, the refined unit cell parameters are presented to show the variation

Table 2.2 Unit cell parameters for the reductive intercalation

Compound	a (Å)	b (Å)	c (Å)	Layer Spacing (Å)
$Fe_{0.5}LaNb_2O_7$	3.880(4)	3.880(4)	10.999(3)	10.68
$Rb_xFe_{0.5}LaNb_2O_7$	22.60(2)	5.677(5)	5.662(6)	11.30
$Ni_{0.5}LaNb_2O_7$	3.879(4)	3.879(4)	10.829(2)	10.61
$Rb_xNi_{0.5}LaNb_2O_7$	22.37(5)	5.698(5)	5.676(5)	11.19
$Rb_2LaNb_2O_7$[7]	22.30955(9)	5.69748(10)	5.69365(10)	11.15

in unit cell sizes. Products changed to black from their original color, which is usually indicative of a change in oxidation state (mix valency), in this case, on the niobium.[7] All the compounds were sensitive to air when handled outside the drybox and would lose their black color and decompose in a matter of minutes. Diffraction data showed a large increase in the c-parameter after air exposure, possibly due to the uptake of oxygen and/or water. Due to the extreme air sensitivity of the Cs intercalated Fe-0.5 sample, XRD data and the subsequent lattice
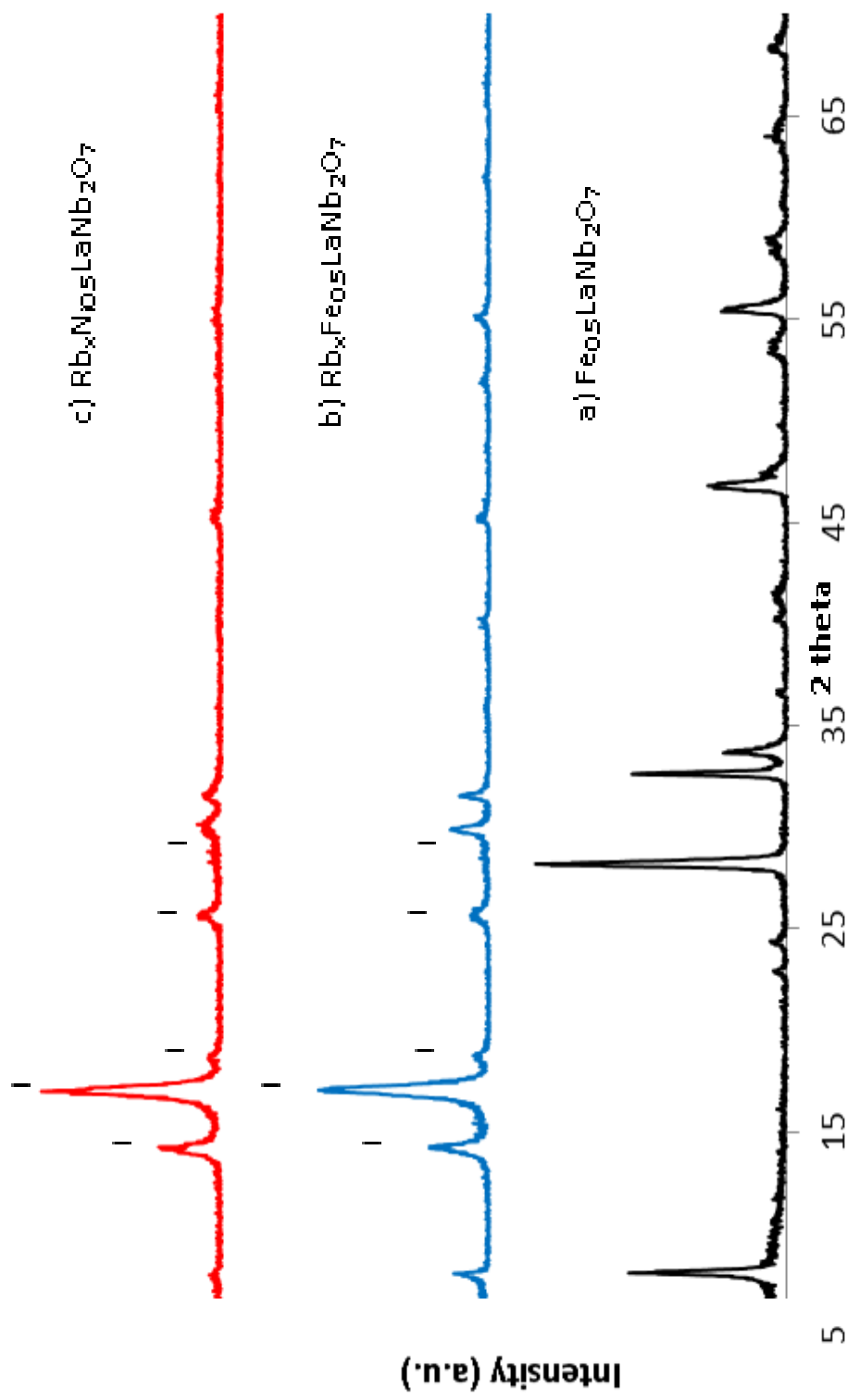
Figure 2.3 XRD patterns for a) $Fe_{0.5}LaNb_2O_7$, b) $Rb_xFe_{0.5}LaNb_2O_7$, and c) Rb intercalated Fe-0.5, and c) Rb intercalated Ni-0.5. The air-sensitive products were covered with a polypropylene and the corresponding peaks are indicated with the symbol (|).

parameters could not be obtained. It was assumed that the reaction was successful based on the black color of the sample and the XRD data collected after exposure to air (subsequent oxidative intercalation results are consistent with this conclusion, see below). As a final step of the multistep approach, the intermediate compounds $A_xFe_{0.5}LaNb_2O_7$ (A = Rb, Cs) were oxidatively intercalated with chlorine gas. The XRD data collected for the Rb at sample can be seen in Figure 2.4. The cesium containing compounds clearly underwent intercalation at room temperature (Figure 2.5). The rubidium compounds, to minimize the formation of an unwanted
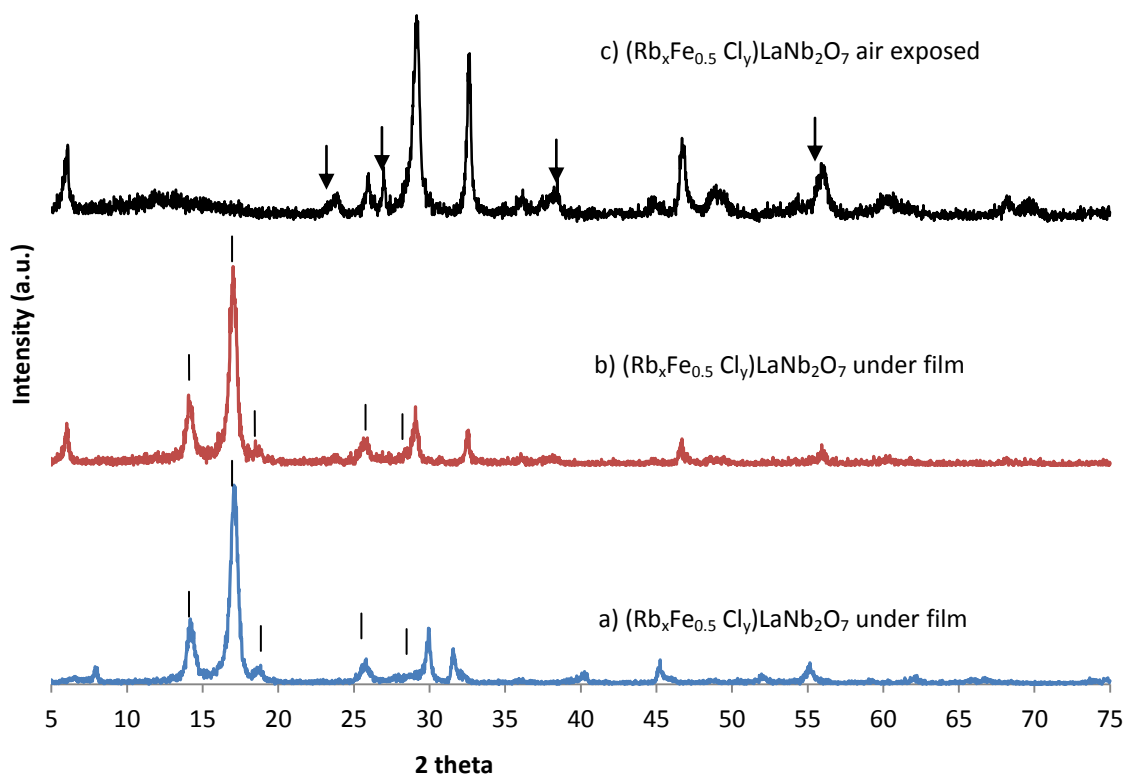
Figure 2.4 XRD patterns for a) $Rb_xFe_{0.5}LaNb_2O_7$, b) $(Rb_xFe_{0.5}Cl_y)LaNb_2O_7$ under polypropylene film, and c) $(Rb_xFe_{0.5}Cl_y)LaNb_2O_7$ air exposed. The air-sensitive products were covered with a polypropylene and the corresponding peaks are indicated with the symbol (I). The trace amount of the RbCl impurity is indicated by the arrow (↓).

28

ACl byproduct, had to be cooled in an ice-bath for about 30 min before chlorination.[12] An

expansion is seen in the c-parameters of both products indicating that intercalation was

successful and this was confirmed by EDS where chlorine was observed. The samples

were also analyzed without the polypropylene film to check for air stability (Fig. 2.4 c); the

compounds are air stable well over 6 months but a small amount of RbCl and CsCl is observed.

Table 2.3 contains the unit cell parameters refined using the CHECKCELL program. The products

are isostructural to $(A_2Cl)LaNb_2O_7$; as seen from the diffraction data and the cell parameters are

consistent as structural analogues of these compounds.

Table 2.3 Refined unit cell parameters for $(A_xFe_{0.5}Cl)LaNb_2O_7$

Compounds	a(Å)	b (Å)	c (Å)	Layer Spacing (Å)
$Rb_xFe_{0.5}LaNb_2O_7$	22.6(1)	5.68(2)	5.66(2)	11.30
$(Rb_xFe_{0.5}Cl)LaNb_2O_7$	3.890(5)	3.890(5)	15.103(5)	15.10
$(Rb_2Cl)LaNb_2O_7$[12]	3.887(1)	3.887(1)	14.913(1)	14.91
$(Cs_xFe_{0.5}Cl)LaNb_2O_7$	3.92(2)	3.92(2)	15.413(3)	15.41
$(Cs_2Cl)LaNb_2O_7$[12]	3.9218(1)	3.9218(1)	15.3107	15.31

Efforts were made at Rietveld refinement of $(Cs_xFe_{0.5}Cl_y)LaNb_2O_7$ on the tetragonal cell

P4/mmm based on a proposed model. While the refinement only reached an agreement factor

of $\approx$ 20%, the proposed model of the product is quite consistent with the diffraction data. The

evaluation of this model could be greatly improved by the availability of better diffraction data

sets. Figure 2.5 shows the XRD pattern of the proposed model against that experimentally

obtained through XRD and in Figure 2.6 the corresponding structure model is shown. EDS data
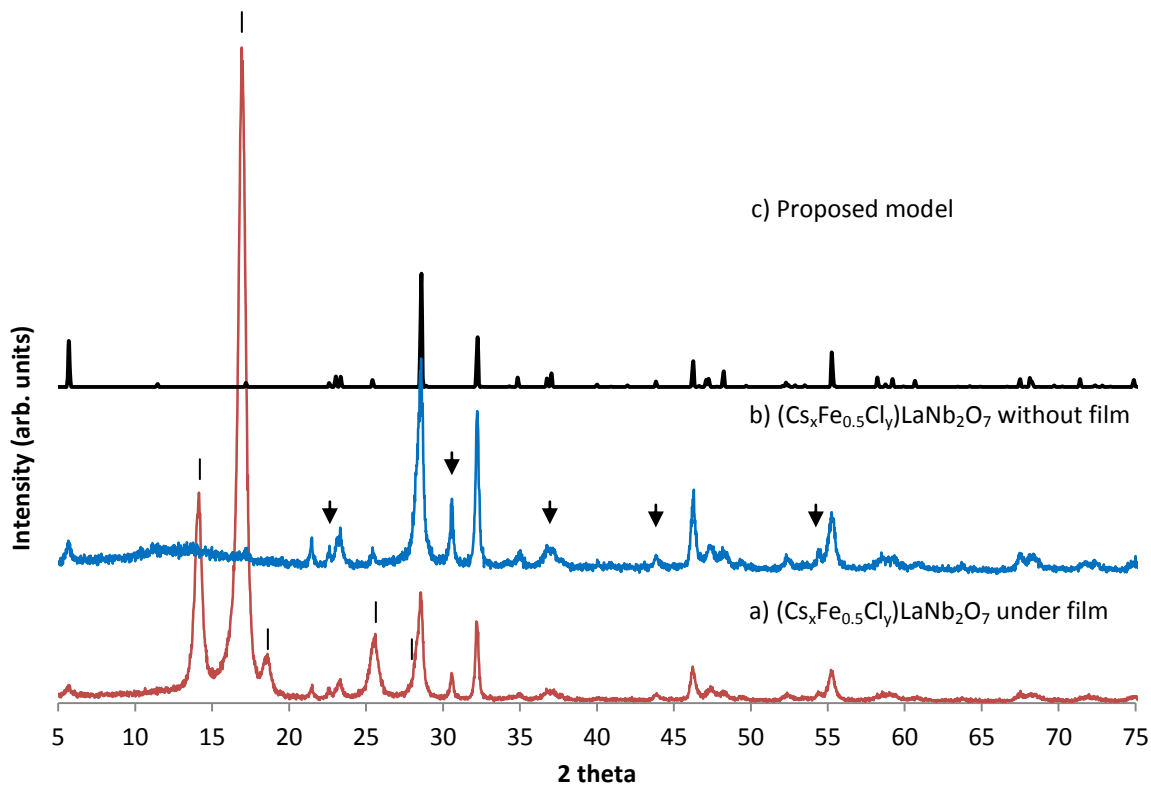
Figure 2.5 XRD patterns for a) $(Cs_xFe_{0.5}Cl_y)LaNb_2O_7$ under polypropylene film, b) $(Cs_xFe_{0.5}Cl_y)LaNb_2O_7$ in air, and c) calculated pattern based on proposed model. Polypropylene film peaks are indicated with the symbol (l). The impurity CsCl impurity is indicated by the down arrow (▼).
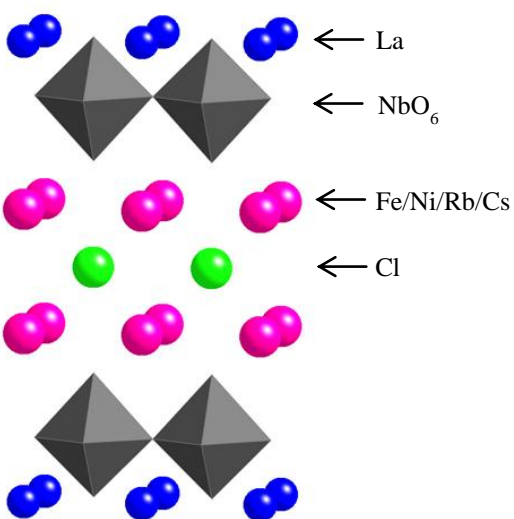
Figure 2.6 Proposed model structure of $(A_{1.5}M_{0.5}Cl)LaNb_2O_7$.

obtained to pin point the composition of the compounds were inconclusive. There is a large

deviation in the atomic percentages; possible reasons include the intrinsic limitations of the EDS

method or a large compositional variance within the sample. Unfortunately, ICP measurements

are not effective with these systems due to the poor dissolution of the metals in different acids.

However we can project, based on the synthetic route used, that the nominal composition of

the final products is $(A_{1.5}Fe_{0.5}Cl)LaNb_2O_7$, where A is Rb or Cs.

FESEM images (collected by Ms. Yuan Yao), show the morphology of crystallites (1 to 5 μm

in size) exhibit only minor changes in going from Fe-0.5 to the end product AFe-0.5Cl of the

multistep approach. Figure 2.7 shows the FESEM images of the parent Fe-0.5 and the products
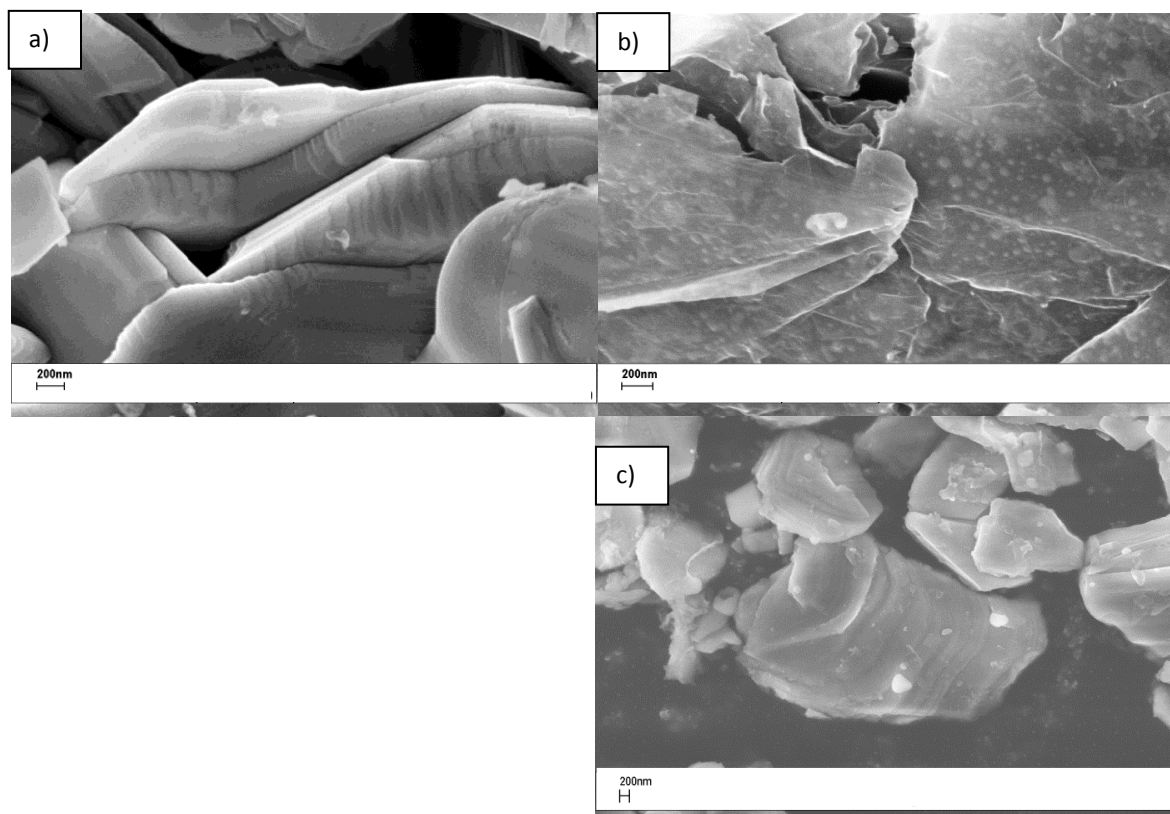
Figure 2.7 FESEM images showing the plate-like morphology of a) $Fe_{0.5}LaNb_2O_7$, b) $(Rb_{1.5}Fe_{0.5}Cl)LaNb_2O_7$, and c) $(Cs_{1.5}Fe_{0.5}Cl)LaNb_2O_7$.

RbFe-0.5Cl and CsFe-0.5Cl and it can be noted that the crystallites of both compounds are plate like indicating that the product has the same morphology after treatment.

An onset of major decomposition around 700 ^{o}C is observed in TGA under nitrogen. The latter is also seen in other metal-halide systems with the loss of the metal-halide.[22] XRD analysis of the DSC/TGA products shows that after decomposition, RbFe-0.5Cl and CsFe-0.5Cl decompose to $RbLaNb_2O_7$ and $CsLaNb_2O_7$, respectively. This supports the loss of the corresponding metal-halide.

2.4 Discussion

A topochemical multistep approach was used as a method to build layers within layers. The combination of ion exchange, reductive intercalation, and oxidative intercalation to manipulate the double layered Dion Jacobson $ALaNb_2O_7$ (A = Rb, Cs) was shown to be an effective and promising route to insert transition-metal containing metal-halide layers within layered perovskites. Other reaction strategies to build layers have been reported.[22-27] Previously, transition-metal-halide layers were fabricated using a one-step ion exchange process (Eq. 1).

$ALaNb_2O_7 + MX_2$ ➔ $(MX)LaNb_2O_7 + AX$ (M = V, Cr, Co, Fe, Cu; X = Cl, (Br for Cu))   (1)

Two-step methods have also been used to build alkali-metal layers. In one case, ion exchange was combined with intercalation (Eqs. 2 and 3),

$$RbLaNb_2O_7 + CuCl_2 \rightarrow (CuCl)LaNb_2O_7 + RbCl \tag{2}$$

$$(CuCl)LaNb_2O_7 + A^o \rightarrow (A_xCl)LaNb_2O_7 + Cu^o \quad (A = Li, Na) \tag{3}$$
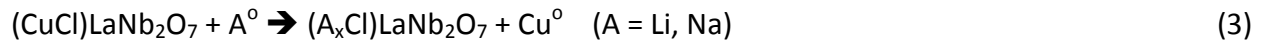
in another case a combination of reductive intercalation and oxidative intercalation was used as seen in Equations 4 and 5.

$$ALaNb_2O_7 + A^o_{(g)} \rightarrow A_2LaNb_2O_7 \quad (A = Rb, Cs) \tag{4}$$

$$A_2LaNb_2O_7 + \tfrac{1}{2}\,Cl_{2(g)} \rightarrow (A_2Cl)LaNb_2O_7 \tag{5}$$
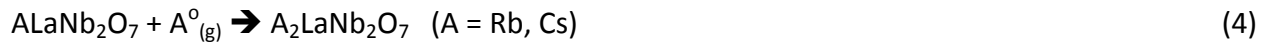
The reaction strategies initiated in the current study were directed towards the construction of mixed metal-halide layers by a 3 step reaction process involving ion exchange, reductive and oxidative intercalation (Eqs 6-8).

$$ALaNb_2O_7 + MBr_2 \rightarrow M_{0.5}LaNb_2O_7 \qquad (A = Rb, Cs; M = Fe, Ni)^{[17]} \tag{6}$$

$$M_{0.5}LaNb_2O_7 + A^o_{(g)} \rightarrow A_{1.5}A_{0.5}LaNb_2O_7 \quad (A = Rb, Cs) \tag{7}$$

$$A_{1.5}M_{0.5}LaNb_2O7 + \tfrac{1}{2}Cl_{2(g)} \rightarrow (A_{1.5}M_{0.5}Cl)LaNb_2O_7 \tag{8}$$
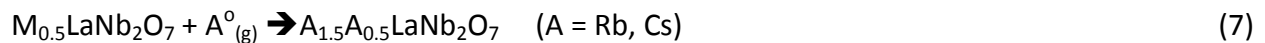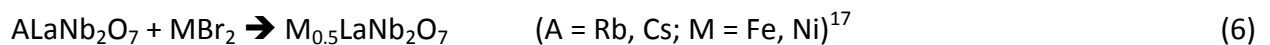
This 3 step approach focused on the niobates of iron and nickel. This approach was also investigated in other systems including the tantalates (Chapter 3).

Divalent transition-metal ion exchange was carried out to produce the isostructural compounds $M_{0.5}LaNb_2O_7$ as has been reported in literature.[17] The c-parameter is larger than

previously reported and EDS indicated that some of the alkali was still present after the exchange; the presence of residual alkali metal in the perovskite host could contribute to this size difference.

The $M_{0.5}LaNb_2O_7$ compounds underwent the second step, being reductively intercalated to produce the RP phases $A_{1.5}M_{0.5}LaNb_2O_7$. An increase in the layer spacing is observed (Table 2.2) and the intermediate products are isostructural to each other (Figs. 2.3b and 2.3c) and also to $Rb_2LaNb_2O_7$ (Fig 2.8). Based on the observed similarity, the unit cell was assumed to be orthorhombic as in $Rb_2LaNb_2O_7$ and cell parameters were refined on the *Cmcm* space group.[7] This indicates that a major structural shift of the perovskite layers has occurred to accommodate the insertion of the alkali metal with a simultaneous decrease in niobium's formal charge. It has to be mentioned that with the lack of composition measurements on the parent compounds it is hard to be conclusive that the intercalation product has Rb to Fe ratio of 1.5:0.5 but based on the reaction conditions used, the nominal composition of the intermediate step should be close to this. With the smaller divalent metal now in the interlayer, the interaction between interlayer and perovskite slab is likely quite different compared to interaction of only rubidium in $Rb_2LaNb_2O_7$. However no conclusive details can be given on the structure of the intermediate compounds since no further attempts to analyze the samples were made since it was difficult due to their high sensitivity to air/moisture.

The final step of the multistep approach was the intercalation of chlorine gas into the intermediate compounds $A_{1.5}M_{0.5}LaNb_2O_7$ where A = Rb, Cs and M = Fe, Ni. XRD (Figure 2.9) does indicate that upon oxidative intercalation, based on the similarity to the $(A_2Cl)LaNb_2O_7$
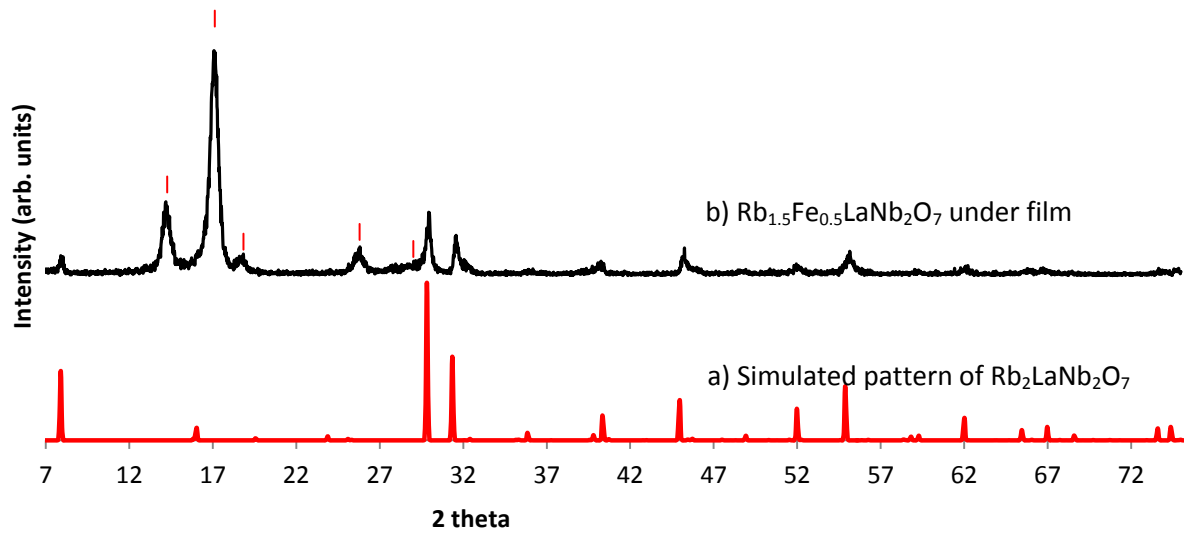
Figure 2.8 Diffraction data showing the calculated pattern for a) $Rb_2LaNb_2O_7$ and the experimental pattern of b) $Rb_{1.5}Fe_{0.5}LaNb_2O_7$ under polypropylene film (I)
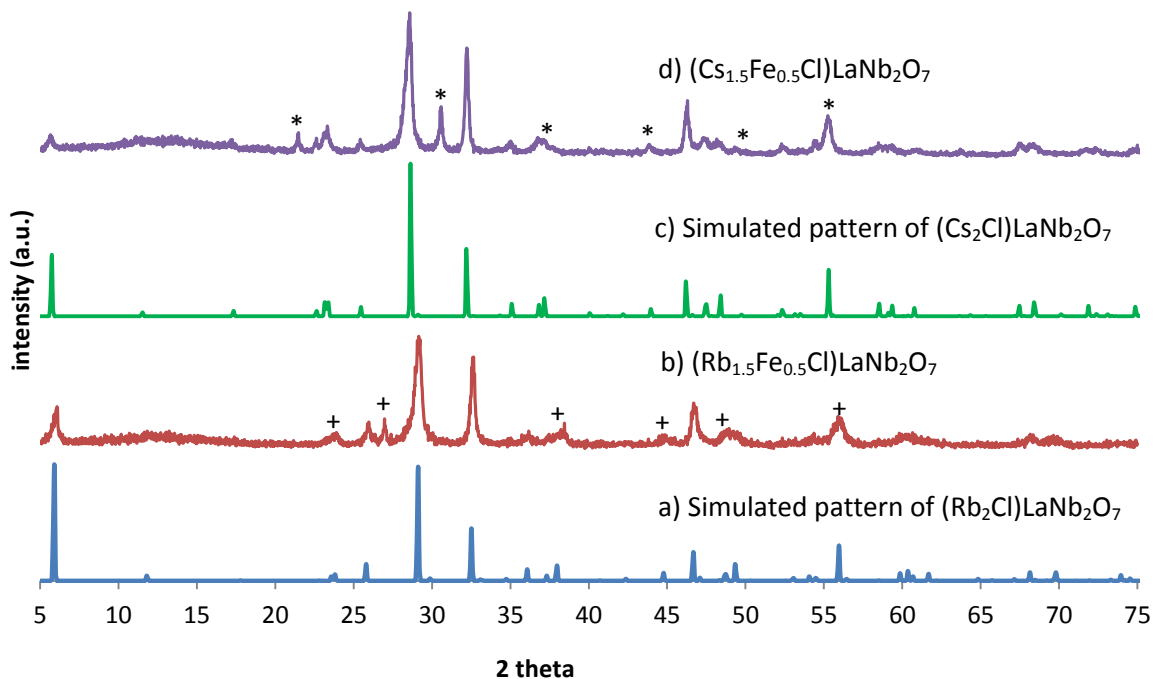
Figure 2.9 Diffraction pattern of a) Simulated pattern of $(Rb_2Cl)LaNb_2O_7$ versus b) $(Rb_{1.5}Fe_{0.5}Cl)LaNb_2O_7$ showing that they are isostructural and c) Simulated pattern of $(Cs_2Cl)LaNb_2O_7$ versus d) $(Cs_{1.5}Fe_{0.5}Cl)LaNb_2O_7$ indicating that they are also isostructural to each other. The CsCl impurity peaks were labeled (∗), and the RbCl impurity peaks were labeled (+)

structure goes back to a tetragonal cell with eclipsed layers. The trace amount of ACl observed in the diffraction data could be explained by either surface Rb that is left over from the reductive step that gets chlorinated or the deintercalation of the A to form ½ ACl to produce the compound $(AFe_{0.5}Cl)laNb_2O_7$. Figure 2.6 shows the simulated structure after chlorination based on the proposed model where the chlorine sits within the Fe/Cs layer.

2.5 Conclusions

A new multistep approach has been developed to build metal-halide layers within perovskites slabs. This approach, based on ion exchange followed by reductive intercalation and oxidative intercalation, allows for the incorporation of transition metals into the construction of these layers. While earlier methods of ion exchange allow for the production of single metal halide layers, this new approach produces double-layered structures (Fig. 2.6) with nominal composition $(A_{1.5}Fe_{0.5}Cl)LaNb_2O_7$, where A is Rb or Cs. This method is a new way of introducing transition metals within the interlayer of layered perovskites and building upon these layers with other topotactic techniques to form nixed metal-halide layers i.e. building layers within layers. It is a new approach that further expands the library of reaction strategies available for the construction of metal-nonmetal arrays within receptive perovskite hosts. Using such techniques, researchers can more effectively and rationally design and produce new technologically significant materials such as those used in magnetics and electronics.

2.6 References

1. Ranmohotti, K. G. S.; Josepha, E.; Choi, J.; Zhang, J. X.; Wiley, J. B. *Adv. Mater.* **2011**, *23*, 442.
2. Gopalakrishnan, J.; Bhat, V.; Raveau, B. *Mater. Res. Bull.* **1987**, *22*, 413.
3. Sato, M.; Abo, J.; Jin, T. *Solid State Ionics* **1992**, *57*, 285.
4. Sato, M.; Kono, Y.; Jin, T. *Nippon Seramikkusu Kyokai Gakujutsu Ronbunshi-J. Cer Soc Jap* **1993**, *101*, 980.
5. Toda, K.; Teranishi, T.; Ye, Z. G.; Sato, M.; Hinatsu, Y. *Mater. Res. Bull.* **1999**, *34*, 971.
6. Jones, R.; McKinnon, W. R. *Solid State Ionics* **1991**, *45*, 173.
7. Armstrong, A. R.; Anderson, P. A. *Inorg. Chem.* **1994**, *33*, 4366.
8. Sato, M.; Jin, T.; Ueda, H. *Chem. Lett.* **1994**, 161.
9. Takano, Y.; Takayanagi, S.; Ogawa, S.; Yamadaya, T.; Mori, N. *Solid State Commun.* **1997**, *103*, 215.
10. Greaves, C.; Francesconi, M. G. *CURR OPIN SOLID ST M* **1998**, *3*, 132.
11. Francesconi, M. G.; Slater, P. R.; Hodges, J. P.; Greaves, C.; Edwards, P. P.; Al-Mamouri, M.; Slaski, M. *J. Solid State Chem.* **1998**, *135*, 17.
12. Choi, J.; Zhang, X.; Wiley, J. B. *Inorg. Chem.* **2009**, *48*, 4811.
13. Viciu, L.; Kodenkandath, T. A.; Wiley, J. B. *J. Solid State Chem.* **2007**, *180*, 583.
14. Schaak, R. E.; Mallouk, T. E. *J. Am. Chem. Soc.* **2000**, *122*, 2798.
15. Choy, J. H.; Park, N. G.; Hwang, S. J.; Kim, Y. I. *Synth. Met.* **1995**, *71*, 1551.
16. Choy, J. H.; Kim, Y. I.; Hwang, S. J.; Yang, I. S. *J. Solid State Chem.* **1999**, *147*, 328.
17. Viciu, L.; Liziard, N.; Golub, V.; Kodenkandath, T. A.; Wiley, J. B. *Mater. Res. Bull.* **2004**, *39*, 2147.
18. Jolly, W. L. *The Synthesis and Characterization of Inorganic Compounds*; Prentice-Hall Inc.: NJ, . 1970.
19. Laugier, J.; Bochu, B.; http://www.inpg.fr/LMGP: Domaine Universitaire BP 46, 38402 Saint Martin d'Hères, France.
20. ProFit; Philips Analytical X-ray: Netherlands, 1996.
21. Carvajal, R. *Commission on Powder Diffraction (IUCr)* **2001**, *26*, 12.
22. Viciu, L.; Koenig, J.; Spinu, L.; Zhou, W. L.; Wiley, J. B. *Chem. Mater.* **2003**, *15*, 1480.
23. Kodenkandath, T. A.; Lalena, J. N.; Zhou, W. L.; Carpenter, E. E.; Sangregorio, C.; Falster, A. U.; Simmons, W. B.; O'Connor, C. J.; Wiley, J. B. *J. Am. Chem. Soc.* **1999**, *121*, 10743.
24. Kodenkandath, T. A.; Kumbhar, A. S.; Zhou, W. L.; Wiley, J. B. *Inorg. Chem.* **2001**, *40*, 710.
25. Viciu, L.; Caruntu, G.; Royant, N.; Koenig, J.; Zhou, W. L. L.; Kodenkandath, T. A.; Wiley, J. B. *Inorg. Chem.* **2002**, *41*, 3385.
26. Tsujimoto, Y.; Kageyama, H.; Baba, Y.; Kitada, A.; Yamamoto, T.; Narumi, Y.; Kindo, K.; Nishi, M.; Carlo, J. P.; Aczel, A. A.; Williams, T. J.; Goko, T.; Luke, G. M.; Uemura, Y. J.; Ueda, Y.; Ajiro, Y.; Yoshimura, K. *Phys. Rev. B* **2008**, *78*, 214410.
27. Tsujimoto, Y.; Baba, Y.; Oba, N.; Kageyama, H.; Fukui, T.; Narumi, Y.; Kindo, K.; Saito, T.; Takano, M.; Ajiro, Y.; Yoshimura, K. *J. Phys. Soc. Jpn.* **2007**, *76*, 063711.

Chapter 3

Synthesis and Reactivity of Transition-Metal Tantalate Oxide Layered Perovskites Prepared through Ion Exchange

3.1 Introduction

Ion exchange is a very simple and effective method of topochemical manipulation. In perovskite systems, ion exchange has mostly focused on DJ and RP phases. Compounds such as $RbLaNb_2O_7$,[1] $CsCa_2Nb_3O_{10}$,[2] $RbLa_2Ti_2NbO_{10}$,[3] $RbSrNb_2O_6F$,[4] $NaLaTiO_4$,[5] $K_2SrTa_2O_7$,[6-8] and $K_2La_2Ti_3O_{10}$ [9-10] have been extensively studied. Ion exchange reactions readily involve the replacement of interlayer cations in these compounds with other alkali metals, Ag^+, NH_4^+, and protons.[11] Additionally, aliovalent ion exchange is known with alkaline earths[12-16] and transition metal cations.[17-18] Neiner *et al.* has shown the exchange VO^{2+} into different titanate systems that gave rise to new magnetic properties.[19-20] Aliovalent exchange of $RbLaNb_2O_7$ with calcium results in a compound isostructural with $KLaNb_2O_7$.[16] The compounds formed by exchange with divalent transition metals (M = Fe, Ni)[18,21-22] appear to be isostructural with $RbLaNb_2O_7$. Also, reactions involving the partial exchange of cations have been described. [21-22]

Herein we report an investigation of the synthesis of a series of different metal-0.5 tantalates, $M_{0.5}LaTa_2O_7$, specifically those where M = VO^{2+}, Fe, Ni, Cu through ion-exchange. The synthesis and characterization of $Ni_{0.5}LaTa_2O_7$ is greatly explored and further topotactic manipulation like reductive followed by oxidative intercalation with chlorine is also discussed in detail.

3.2 Experimental

3.2.1 Synthesis

Starting materials: $ALaTa_2O_7$ (A = Na, K, Rb, Cs) were synthesized as reported in literature.[23-25] Stoichiometric quantities, measured in an argon-filled glovebox, of A_2CO_3 (Alfa Aesar, 99.99%; A = Rb, Cs), La_2O_3 (Alfa Aesar, 99.99%; dried for overnight at 1050 ^{o}C to decompose any hydroxides and carbonates), and Ta_2O_5 (Alfa Aesar, 99.85%) were ground together with a 25% molar excess of A_2CO_3 to compensate for that alkali-metal oxide lost due to volatilization. The mixtures were ground well, placed in alumina crucibles, and heated to at 1100 ^{o}C for 4 hours and 12 hours for $RbLaTa_2O_7$ and $CsLaTa_2O_7$, respectively. After the reaction, the products were cooled, washed with copious amounts of distilled water, isolated in a Büchner funnel through suction filtration, and rinsed with acetone before drying them in an oven at 150 ^{o}C for 24 hours. $NaLaTa_2O_7$ and $KLaTa_2O_7$ was prepared through ion exchange by mixing $RbLaTa_2O_7$ with $NaNO_3$ (Alfa Aesar, 99.999%) and KNO_3 (Alfa Aesar, 99.994%) in a 1:10 molar ratio and heated at 400 and 350°C for 24 hours in air for the sodium and the potassium compounds, respectively. The melts were washed with copious amounts of distilled water in a Büchner funnel through suction filtration to remove byproducts, and the collected products were rinsed with acetone and placed in the furnace at 150 ^{o}C for 24 hours. Because the Na sample readily formed a hydrate, it was stored in an argon filled glove box. For the synthesis of $(CuCl)LaTa_2O_7$,[26] $RbLaTa_2O_7$ was mixed and ground with anhydrous $CuCl_2$ (Alfa Aesar, 99.99%) at a 1:2 molar ratio in an argon filled glovebox and the mixture was pressed into pellets that were sealed in evacuated (< 10^{-4} Torr) Pyrex tubes. The reaction tubes were heated at 325 ^{o}C for one

week. The products were washed with copious amounts of distilled water to remove the RbCl product, rinsed with acetone and heated overnight in a drying oven at 150 $^{\circ}$C.

Synthesis of M$_{0.5}$LaTa$_2$O$_7$: The synthesis of the compounds, M$_{0.5}$LaTa$_2$O$_7$ where M is Fe or Ni, was carried out using CsLaTa$_2$O$_7$ and RbLaTa$_2$O$_7$ with FeBr$_2$ (Alfa Aesar, 99.995% ultra-dry) and NiBr$_2$ (Alfa Aesar, 99%, anhydrous), respectively, at a 1:2 molar ratio. The methods used follow ones similar to those reported by Viciu *et al.*[18] for the niobates (M$_{0.5}$LaNb$_2$O$_7$, M = Fe, Ni). Starting compounds were mixed, ground using a mortar and pestle with the reagents, and the mixture was pressed into pellets with a hand press and sealed under vacuum (<10^{-4} Torr) in Pyrex tubes. Reactions were carried out at 400 $^{\circ}$C for 10 days for the iron compound and at 350 $^{\circ}$C for 21 days for nickel compound. Final products were washed with copious amounts of distilled water in combination with suction filtration to get rid of the exchanged bromide byproducts; samples were then rinsed with acetone and dried at 150 $^{\circ}$C for a minimum of 30 minutes. The iron product was brown in color and the nickel compound was yellow-green.

The synthesis of Ca$_{0.5}$LaTa$_2$O$_7$ followed a procedure similar to that described by Cushing *et al.*[16] Ca(NO$_3$)$_2$· 4H$_2$O (Aldrich, 99%) was placed to Pyrex tube, heated under dynamic vacuum for 24 hours at 150 $^{\circ}$C to dehydrate the compound, and was transferred to an argon filled glovebox to prevent rehydration. NaLaTa$_2$O$_7$ and dried Ca(NO$_3$)$_2$ at a 1:2 molar ratio were ground with a mortar and pestle in a glove box and the mixture was pressed into pellets that were evacuated (< 10^{-4} Torr) in a Pyrex tube (12 mm o.d.). The reaction tube was heated at 400 $^{\circ}$C for 5 days, after which the reaction tube was opened in a fume hood. The product was washed with distilled water and collected using a Büchner funnel through suction filtration, rinsed with

acetone, and dried in an oven at 150 $^\circ$C for 24 hours. ***Note:** The reaction tube has to be opened in a fume hood due to the production of NO_x gases (Figure 4.1) during the reaction; these gases are toxic.*
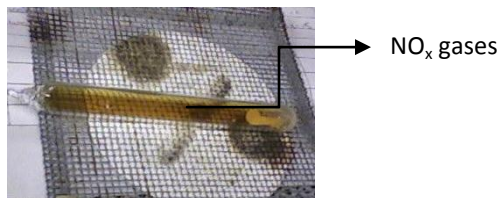
Figure 3.1 Reaction tube after ion exchange with $Ca(NO_3)_2$ showing the NO_X gases present

For vanadyl exchange, reactions were carried out in aqueous solutions where $ALaTa_2O_7$ (A = Na, K, Rb) was mixed with $VOSO_4 \cdot 2H_2O$ in a 2:1 molar ratio. A round bottom flask was filled with 100 mL of distilled water and the reagent was added and dissolved followed by the addition of starting material and a stir bar. The flask was placed into an oil bath where the temperature was kept between 55 - 60 $^\circ$C for two days. After the reaction time, the powder was isolated and added to a fresh $VOSO_4$ solution under the same conditions. The final green product was collected through centrifugation and washed with water followed by a rinse with acetone and was placed in an oven at 150 $^\circ$C overnight.

Reactions to obtain $Cu_{0.5}LaTa_2O_7$ were carried out in a similar way as reported in literature.[18] About 0.5 grams of $(CuCl)LaTa_2O_7$ was loaded into a quartz (fused silica) tube (12.8 mm o.d.) that was placed under dynamic vacuum and heated to 500 - 550 $^\circ$C for 5 to 24 hours. The reaction tube was cooled to room temperature and transferred to a glovebox and the sample was initially treated as air-sensitive. High temperature X-ray powder diffraction was done on $(CuCl)LaTa_2O_7$ on the under nitrogen flow.

41

Reductive Intercalation of $M_{0.5}LaTa_2O_7$: Rb (Alfa Aesar, 99.75%) was intercalated into both exchanged products $Ni_{0.5}LaTa_2O_7$ (Ni0.5-Ta) and $Fe_{0.5}LaTa_2O_7$ (Fe0.5-Ta). Cs (Alfa Aesar, 99.75%) was also intercalated into $Ni_{0.5}$-Ta. Reactions were carried out at 1:1.6 molar ratio using similar techniques used by Choi *et al.*[27] $M_{0.5}LaTa_2O_7$ compounds were pressed into pellets with a hand press, placed in a Pyrex tube (12 mm o.d.) before flame drying the samples under dynamic vacuum to remove any moisture. Alkali metals were weighed out in a small glass ampoule (6 mm o.d.) and were transferred to the bigger tube. ***Note: Caution should be taken when handling and disposing the alkali metals due to their violent reaction when in contact with moisture.*** The evacuated tube ($< 10^{-4}$ Torr) were then sealed and placed in a tube furnace at 250 $^{\circ}$C and 290 $^{\circ}$C for the rubidium and cesium metal samples, respectively. The reactions were carried out for 4 days, during which time the pellets crumbled on reaction. After 4 days, a temperature gradient was applied to transport any unreacted metals by putting one end of the Pyrex tube outside of the tube furnace (~ RT). The reaction tubes were transferred and opened in an argon-filled glovebox. The final products were black and were treated as air-sensitive.

Oxidative Intercalation: The products obtained after reductive intercalation underwent oxidative intercalation using chlorine gas (Matheson 99.99%). ***Note: Chlorine gas should be handled using an appropriate apparatus and protective equipment due to its corrosive and toxic nature.*** The chlorination procedure was similar to that used by Choi et al.[27] A Schlenk line with features like those described by Jolly,[28] was set up under a fume hood to avoid any exposure to chlorine gas. Concentrated sulfuric acid was used to remove any water from the gas and a saturated aqueous AOH solution (A = Na, or K) was used to scrub out excess chlorine gas. $A_xNi_{0.5}LaNb_2O_7$ sample was loaded into scintillation vials fitted with TFE/silicone septum cap

and cooled to in an ice-bath. The vial was then connected to the Schlenk line system via a disposable 21G stainless steel needle. The system was purged with nitrogen as reaction vials were cooled in an ice-bath. The samples were then reacted with chlorine gas – the chlorine flow was maintained for about two hours before purging the system for at least 4 hours under nitrogen to remove excess chlorine gas.

3.2.2 Characterization

Compounds were characterized by X-ray powder diffraction using a Philips X'Pert PW 3040 MPD system equipped with a graphite monochromator (Cu Kα radiation, λ = 1.5448 Å). High termperature XRD was carried out on an Anton Parr HTK-16 sample stage. Routine scans were collected in continuous mode for one hour over a 2θ range of 3 to 75° with a scan rate of 0.02 deg/sec. Air-sensitive samples were prepared for X-ray data collection in an argon-filled glovebox and sealed under a polypropylene film with silicone grease. ChekCell[29] was used to refine the lattice parameters after the peak positions were determined using the program PROFILE FIT.[30]

Compositional analysis was carried out by energy dispersive spectroscopy (EDS) on a JEOL JSM 5410 scanning electron microscope (SEM) equipped with an EDAX-DX PRIME microanalytical system. The morphology of the samples and structure information were obtained using a Leo 1530 VP field emission scanning electron microscope (FESEM), and JEOL 2010 transmission electron microscope (TEM). TEM samples were dispersed on Lacey Formvar Carbon grids (300 mesh) with alcohol.

Thermal behavior was monitored using a differential scanning calorimeter (DSC) on a

Netzsch 404S thermal analysis instrument in flowing argon and a TA-SDTQ600 thermal analyzer

in the temperature range 25 - 1000 ^{o}C under nitrogen atmosphere. Samples were heated in

alumina pans from 500 to 1000 ^{o}C at a rate of 10 – 50 ^{o}C/min

3.3 Results and Discussion

ALaTa$_2$O$_7$ (where A = Na, K, Rb, Cs) parent compounds were synthesized and confirmed

single phase by X-ray diffraction. RbLaTa$_2$O$_7$ and CsLaTa$_2$O$_7$ were used as starting materials to

make Ni$_{0.5}$LaTa$_2$O$_7$ (Ni-0.5/Ta) and Fe$_{0.5}$LaTa$_2$O$_7$ (Fe-0.5/Ta), respectively, through ion exchange.

EDS data indicated that some Rb and Cs still remained present indicating that the exchange was

partial, especially for cesium in the iron compound. Residual alkali metals were also observed in

the metal-0.5 of the niobate series (M-0.5/Nb).[18] Figure 4.2 shows the XRD patterns and Table

4.1 presents the refined unit cells of both the parents and products. All the peaks were indexed

on a tetragonal cell with space group *P4/mmm.* A decrease in *c*-parameter is observed for Ni-

0.5/Ta, which is consistent with the M-0.5/Nb and also expected due to the smaller size of the

transition metal. However, Fe-0.5/Ta showed only a slight decrease in the c-parameter,

consistent with partial exchange of cesium in these systems. A pattern was simulated for the

new M0.5-Ta compounds and is shown in Figure 4.3 followed by the model structure in Figure

4.4. Even though the Fe0.5-Ta might be partially exchanged the powder XRD indicates that it is

isostructural to its sister compound Ni0.5-Ta and they are both in fairly good agreement with
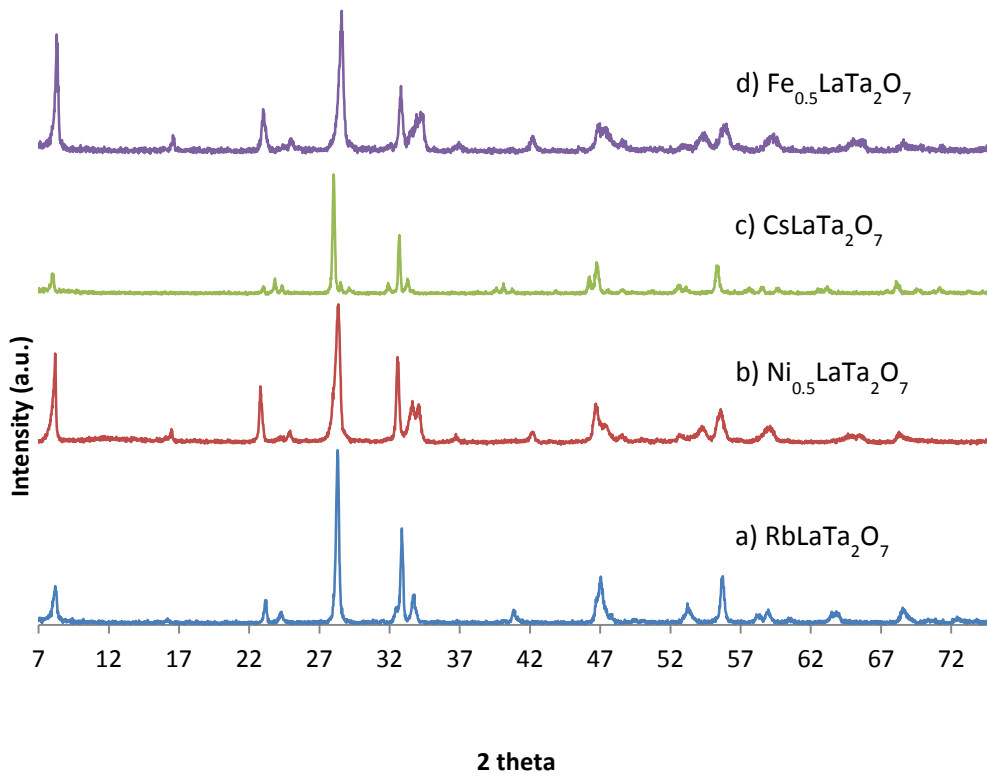
Figure 3.2 Diffraction pattern of parent a) $RbLaTa_2O_7$ versus b) $Ni_{0.5}LaTa_2O_7$, and parent c) $CsLaTa_2O_7$ versus product d) $Fe_{0.5}LaTa_2O_7$

Table 3.1 Unit cell parameters

	a (Å)	c (Å)
$RbLaTa_2O_7$[a]	3.8820(1)	11.1053(5)
$Ni_{0.5}LaTa_2O_7$	3.867(5)	10.6912(9)
$CsLaTa_2O_7$	3.891(5)	11.2346(7)
$Fe_{0.5}LaTa_2O_7$	3.891(9)	11.130(1)

[a]unit cell values in good agreement with literature.[23]
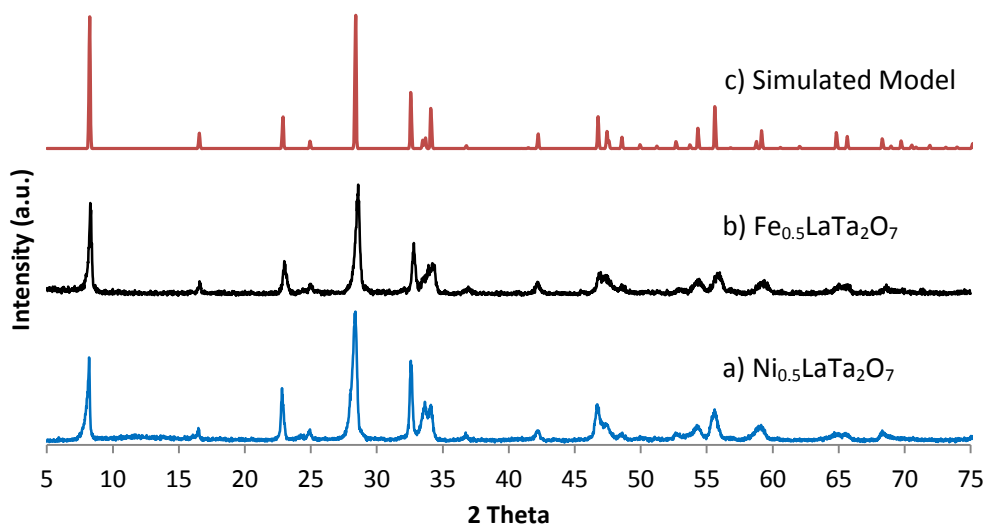
Figure 3.3 Diffraction pattern of the isostructural compounds a) $Ni_{0.5}LaTa_2O_7$ and b) $Fe_{0.5}LaTa_2O_7$ compared to the c) simulated model pattern
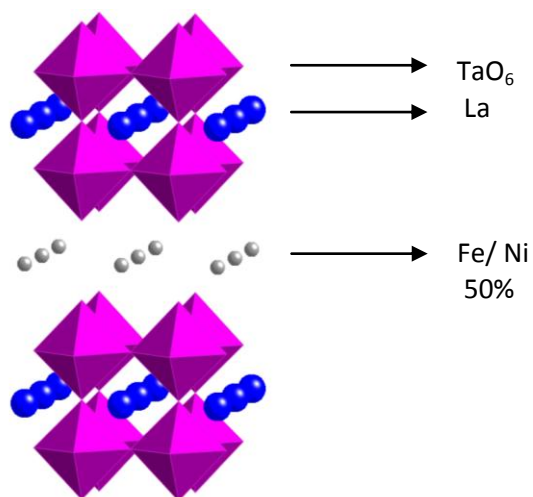
Figure 3.4 Model structure of $M_{0.5}LaTa_2O_7$

the proposed XRD model based on the parent, $RbLaTa_2O_7$. This indicates that the layered

structure of the parent compound is maintained where the perovskites slabs are oriented in the

eclipsed form. This correlates with what is observed in the M0.5-Nb (M = Fe, Ni) niobate series

but not with what is seen by other researchers where the perovskites layers shift to

accommodate the coordination around the smaller cation present after the exchange.[1,16] The

fact that there is still alkali metal left over after the exchange could account for the non-

structural change in these M0.5-Ta compounds. The partial exchange in the Fe0.5-Ta

compound could specifically be explained by the immobility of the Cs metal because of its

bigger size compared to rubidium. The size difference within the interlayer can cause local

stress within the crystallites and could cause a loss of crystallinity which is observed in XRD. In

the structure model, iron or nickel are assumed to be on the same site as rubidium in

$RbLaTa_2O_7$ but further analysis including Rietveld refinements are needed to pinpoint the exact

structure of the M0.5-Ta's. EDS has proven to be mainly a qualitative tool; the data showed a

significant compositional variance within the compounds synthesized.

FESEM images (Figure 4.5) collected by Ms. Yuan Yao, were taken to look at the morphology

of the Ni0.5-Ta and the parent compound $RbLaTa_2O_7$. Some charging was experienced during

the image collection of Ni0.5-Ta so a higher magnification image was not collected, however it

can be seen that the crystallites are still plate-like in shape before and after reaction. TEM

images were also collected of Ni0.5-Ta and the images are seen in Figure 4.6 a. Based on the

visible lattice planes, the d-spacing was measured, compared to the calculated value, and it was

determined that the crystallite is oriented along the (0 1 2) plane.
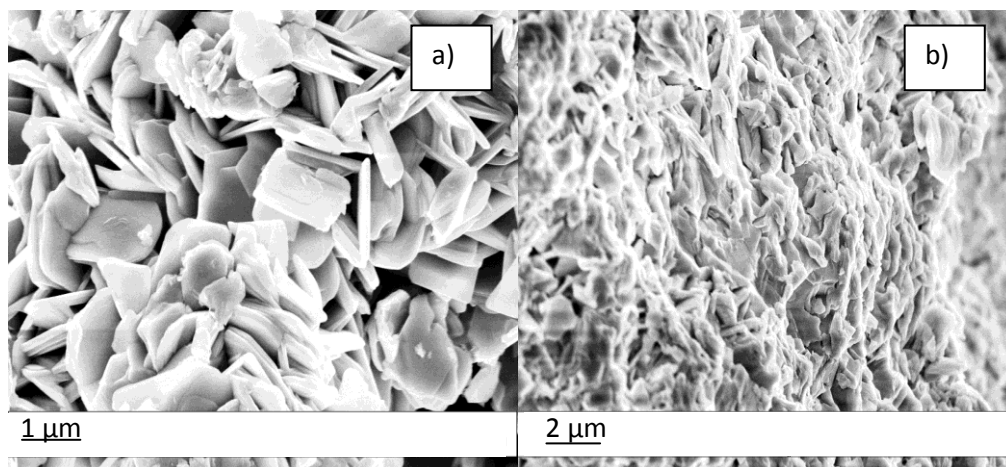
Figure 3.5 FESEM images showing the morphology of a) $RbLaTa_2O_7$ and b) $Ni_{0.5}LaTa_2O_7$
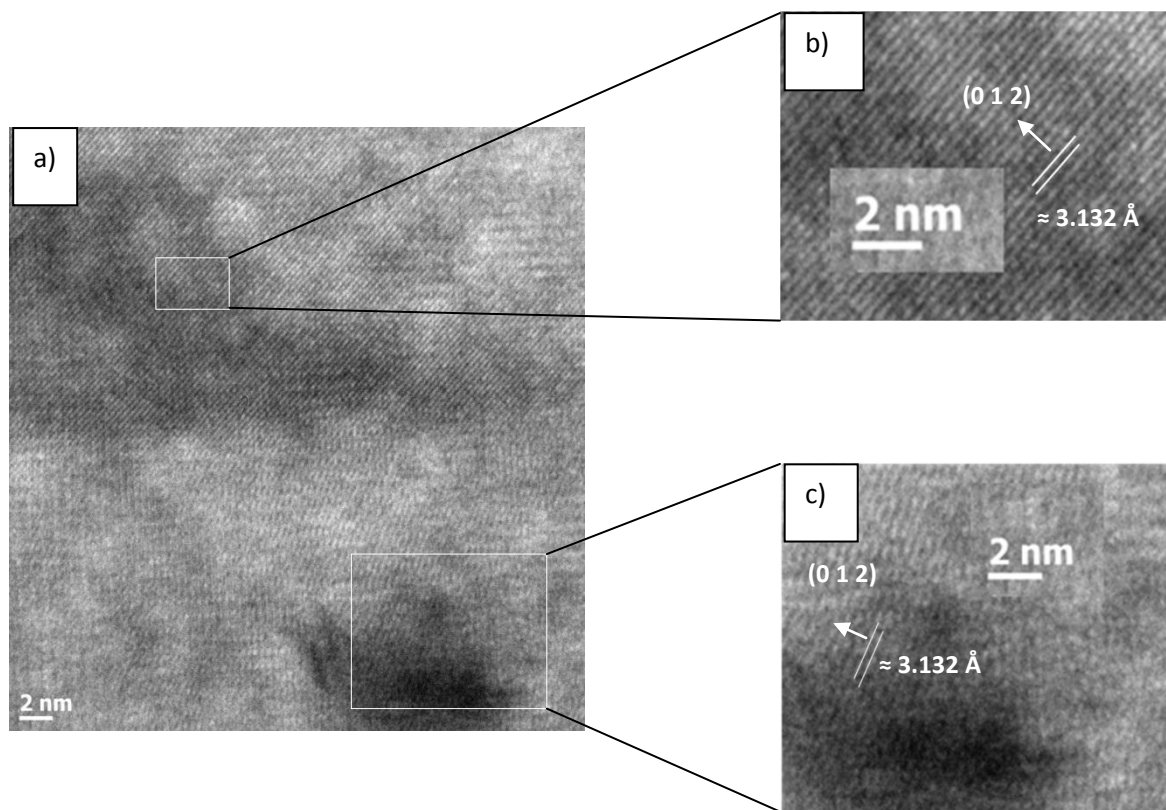
Figure 3.6 High Resolution TEM Images of a) Ni0.5-Ta crystallite and high magnification of specified regions b) and c)

No thermal event was seen in DSC collected for Ni0.5-Ta and the XRD data of the product after DSC indicated that the compound is decomposing but the decomposition products could not indentified due to the complexity of the XRD data. An onset of decomposition around 500 °C is observed in TGA under nitrogen indicating that the compound is stable at least up to that temperature and XRD data after analysis is the same as seen in the DSC data.

An attempt was made to make $Ca_{0.5}LaTa_2O_7$ from $NaLaTa_2O_7$ based on the approach reported by obtained from Cushing *et al*. on the double-layered niobate.[16] Evidence of exchange is observed but the crystallinity of the product was poor and the reaction was incomplete. The reaction conditions need to be revisited but the results are promising.

Appendix D covers the ion exchange of vanadyl units into layered niobate perovskites. Vanadyl exchange was also explored in the layered tantalate series using the solution technique by Neiner et al.[19-20] $ALaTa_2O_7$ (A = Na, K, Rb) underwent ion exchange with $VOSO_4 \cdot H_2O$ in solution and the powder diffraction data collected for each parent versus its product can be seen in Figure 4.7. The products appear to be isostructural to each other no matter which parent compound is used as starting material. EDS data on the samples showed little evidence of vanadium and IR data collected does not support the presence of vanadyl in the stretch range accepted of 950 – 1035cm^{-1}. The pH of the vanadyl solution was tested and was around 3 which is consistent with what is reported in literature as the acidity of VO^{2+} solutions.[31] Based on this is expected that the final products are all $HLaTa_2O_7$ and that little of the vanadyl has exchanged into the interlayer. This interpretation is a reasonable one since the synthesis of the $HLaTa_2O_7$ is carried out using similar acidic conditions. There seems to be a bigger drive to

intercalate the hydrogen ions compared to the vanadyl ions and there could be a couple of
factors involved.
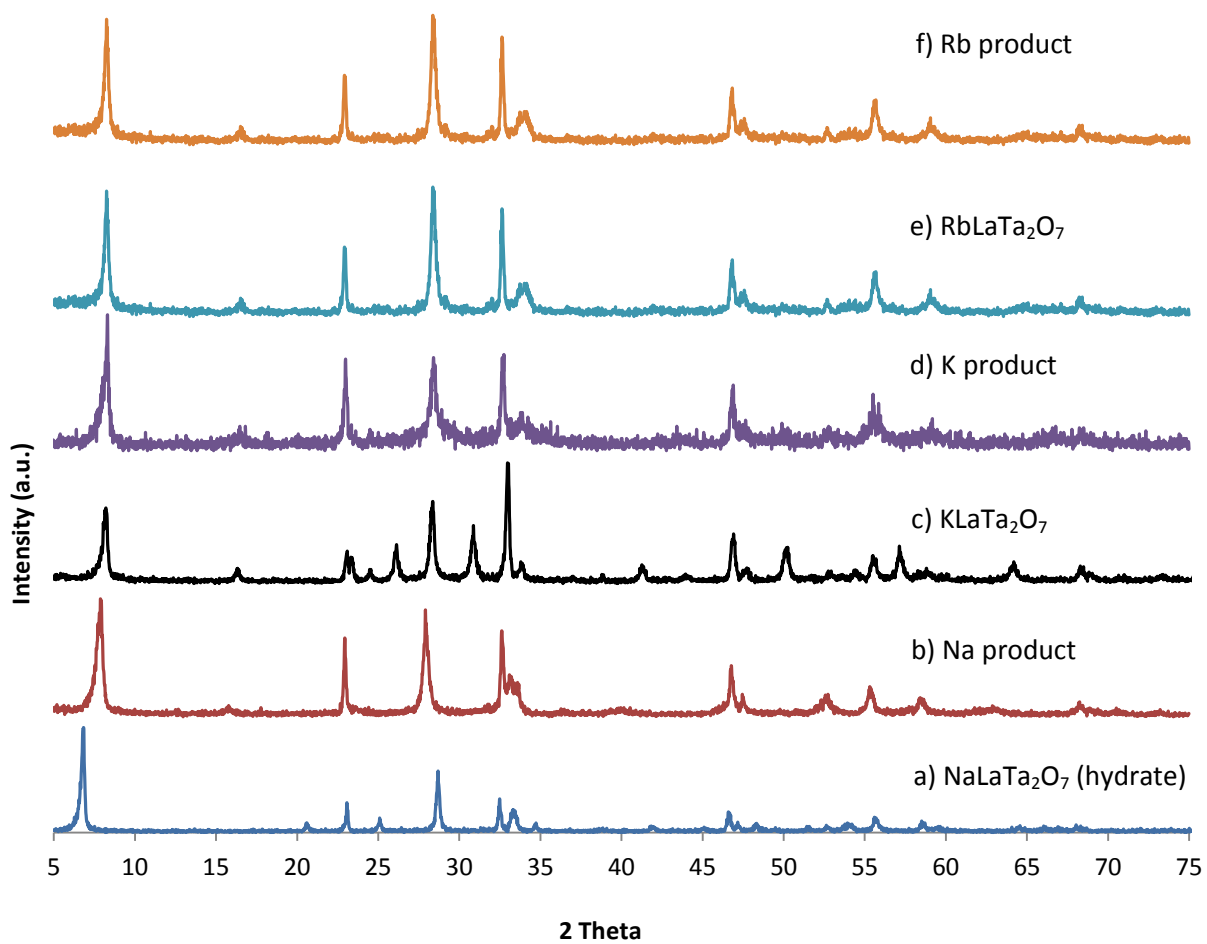
Figure 3.7 XRD data comparing each parent versus product after vanadyl exchange

One, the solution is highly acidic indicating the strong presence of the hydrogen ions in
solution and two, hydrogen's size, relative to vanadyl ion, might also play a role due to its

potential higher mobility. Figure 4.7 diffraction data shows a comparison of the $KLaTa_2O_7$

vanadyl exchange product to $HLaTa_2O_7$. XRD patterns are in good agreement; that argument

along with the lack of vanadium in the EDS data, support the formation of $HLaTa_2O_7$ from

reaction with the acidic vanadyl solution.

(CuCl)$LaTa_2O_7$ was heated under dynamic vacuum to try to produce $Cu_{0.5}LaTa_2O_7$ through

deintercalation of $CuCl_2$. The target compound could not be obtained no matter how the

reaction conditions were varied, and in some cases a new phase was observed, which was not

indicative of the formation of Cu0.5-Ta. To better understand the decomposition of the

compound, HTXRD was carried out under N_2 flow and showed that the compound is stable up
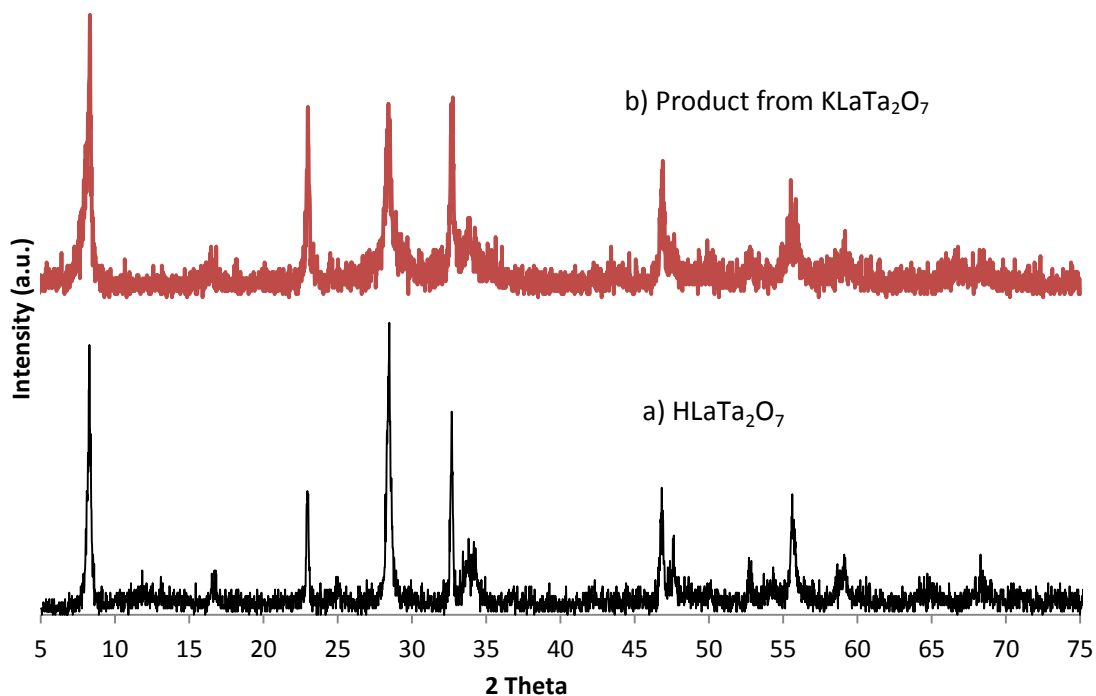
Figure 3.8 Comparison of a) $HLaTa_2O_7$ versus b) the vanadyl exchange product obtained with $KLaTa_2O_7$

to around 750°C where it possibly decomposes to a form of $Cu_xTa_2O_6$ however no evidence is seen for the formation of $LaTaO_4$. Interestingly the XRD pattern seen at 750 °C under N_2 flow is similar to the pattern observed after heating the sample under vacuum at 550 °C for an extended period of time. It is to be noted here that unlike the niobate compounds where the decomposition of $(CuCl)LaNb_2O_7$ forms the intermediate, $Cu_{0.5}LaNb_2O_7$, before it fully decomposes, in the tanatalate series this intermediate is not seen.[18] The intermediate compound might not be thermodynamically stable in the tantalate series and therefore not observed. There might be a bigger drive to form the more stable compound $Cu_xTa_2O_6$ instead. The decomposition of the tantalate series is under investigation by other researchers in the group and the details will be reported elsewhere.

Further topotactic manipulations were carried out on the Ni0.5-Ta compound and the host compound underwent reductive intercalation with rubidium and cesium metal (A-M0.5-Ta). The diffraction pattern of the products (Figure 3.9) obtained do not show significant changes on intercalation but evidence is seen for a low angle reflection indicative to reactivity in air. This phenomenon is also observed in other reductively intercalated compounds that are sensitive to air.[27] The yellow-green samples do turn black in color which is usually an indication of a change in oxidation state due to reductive intercalation. The oxidation change in these compounds is expected to result from tantalum going from 5+ to 4+/5+ mixed valency if reduction was successful. Evidence of intercalation is not so clear but is supported by the following. The sample was initially treated as air-sensitive and was left in air for about two months and scanned periodically to see if there was any change in the diffraction pattern. The black color
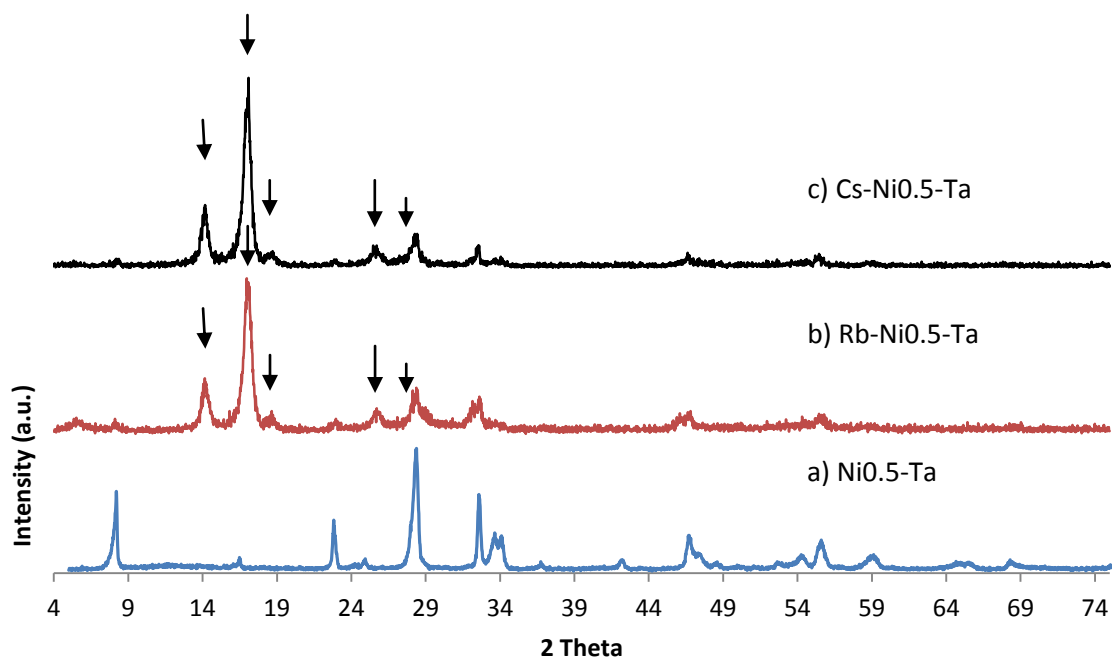
Figure 3.9 Host a) Ni0.5-Ta vs. b) Rb-Ni0.5-Ta and c) CsNi0.5-Ta. The polypropylene film is indicated by the symbol (↓)

also fades over time to become charcoal grey. It was concluded that even though there was a color change on intercalation the extent of insertion was relatively minor compared to that of the niobates due to the re-emergence of the host as the sample is exposed to air/moisture over an extended period of time; in decomposition of the corresponding niobates, the parent structure does not survive this process. Subsequent oxidative intercalation was carried out on Rb-Ni0.5-Ta with no clear indication of insertion into the host structure as seen in the niobates. Only RbCl byproduct was observed in the XRD data indicating deintercalation of the rubidium intercalated in the preceding step.

3.4 Conclusions

Ion exchange was used as a tool to insert divalent cations within layered perovskites. It has been proven to be a successful tool in the creation of vacancies within the interlayer of layered compounds allowing for further chemistry. Herein the new compound $Ni_{0.5}LaTa_2O_7$ was synthesized through ion exchange. Synthesis of the corresponding iron compound was also investigated but only evidence for minimal exchange was observed. Further efforts of topochemical manipulation on each of these compounds were explored but both reductive and oxidative intercalations were not successful. An attempt was also made to make other M-0.5 exchange products, ones that are known to form in the niobates or other perovskite compounds. In the case of the vanadyl, no evidence for ion exchange is seen and for the calcium, the quality of the products was poor, but this system may warrant further study. This chemistry is a clear indication that the tantalate series behaves in a different manner than the niobate series and could be in due part due to the greater stability of the higher oxidation state of tantalum, making its +5 state the most stable form and therefore resistant to further chemistry.

3.5 References

1. Gopalakrishnan, J.; Bhat, V.; Raveau, B. *Mater. Res. Bull.* **1987**, *22*, 413.
2. Dion, M.; Ganne, M.; Tournoux, M.; Ravez, J. *Rev. Chim. Miner.* **1984**, *21*, 92.
3. Hong, Y. S.; Kim, K. *Chem. Lett.* **2000**, 690.
4. Caruntu, G.; Spinu, L.; Wiley, J. B. *Mater. Res. Bull.* **2002**, *37*, 133.
5. Toda, K.; Kameo, Y.; Kurita, S.; Sato, M. *J. Alloys Compd.* **1996**, *234*, 19.
6. Ollivier, P. J.; Mallouk, T. E. *Chem. Mater.* **1998**, *10*, 2585.
7. Kodenkandath, T. A.; Wiley, J. B. *Mater. Res. Bull.* **2000**, *35*, 1737.

8. Crosnier-Lopez, M. P.; Le Berre, F.; Fourquet, J. L. *J. Mater. Chem.* **2001**, *11*, 1146.

9. Sato, M.; Toda, K.; Watanabe, J.; Uematsu, K. *Nippon Kagaku Kaishi* **1993**, 640.

10. Toda, K.; Watanabe, J.; Sato, M. *Mater. Res. Bull.* **1996**, *31*, 1427.

11. Ranmohotti, K. G. S.; Josepha, E.; Choi, J.; Zhang, J. X.; Wiley, J. B. *Adv. Mater.* **2011**, *23*, 442.

12. Gondrand, M.; Joubert, J. C. *Rev. Chim. Miner.* **1987**, *24*, 33.

13. Mahler, C. H.; Cushing, B. L.; Lalena, J. N.; Wiley, J. B. *Mater. Res. Bull.* **1998**, *33*, 1581.

14. Lalena, J. N.; Cushing, B. L.; Falster, A. U.; Simmons, W. B.; Seip, C. T.; Carpenter, E. E.; O'Connor, C. J.; Wiley, J. B. *Inorg. Chem.* **1998**, *37*, 4484.

15. McIntyre, R. A.; Falster, A. U.; Li, S. C.; Simmons, W. B.; O'Connor, C. J.; Wiley, J. B. *J. Am. Chem. Soc.* **1998**, *120*, 217.

16. Cushing, B. L.; Wiley, J. B. *Mater. Res. Bull.* **1999**, *34*, 271.

17. Hyeon, K. A.; Byeon, S. H. *Chem. Mater.* **1999**, *11*, 352.

18. Viciu, L.; Liziard, N.; Golub, V.; Kodenkandath, T. A.; Wiley, J. B. *Mater. Res. Bull.* **2004**, *39*, 2147.

19. Neiner, D.; Golub, V.; Wiley, J. B. *Mater. Res. Bull.* **2004**, *39*, 1385.

20. Neiner, D.; Sweany, R. L.; Golub, V.; Wiley, J. B. *J. Mater. Chem.* **2006**, *16*, 186.

21. Galven, C.; Fourquet, J. L.; Suard, E.; Crosnier-Lopez, M. P.; Le Berre, F. *Dalton Trans.* **2010**, *39*, 4191.

22. Galven, C.; Fourquet, J. L.; Suard, E.; Crosnier-Lopez, M. P.; Le Berre, F. *Dalton Trans.* **2010**, *39*, 3212.

23. Toda, K.; Sato, M. *J. Mater. Chem.* **1996**, *6*, 1067.

24. Toda, K.; Uematsu, K.; Sato, M. *J. Ceram. Soc. Jpn.* **1997**, *105*, 482.

25. Toda, K.; Honma, T.; Ye, Z. G.; Sato, M. *J. Alloys Compd.* **1997**, *249*, 256.

26. Kodenkandath, T. A.; Lalena, J. N.; Zhou, W. L.; Carpenter, E. E.; Sangregorio, C.; Falster, A. U.; Simmons, W. B.; O'Connor, C. J.; Wiley, J. B. *J. Am. Chem. Soc.* **1999**, *121*, 10743.

27. Choi, J.; Zhang, X.; Wiley, J. B. *Inorg. Chem.* **2009**, *48*, 4811.

28. Jolly, W. L. *The Synthesis and Characterization of Inorganic Compounds*; Prentice-Hall Inc.: NJ, . 1970.

29. Laugier, J.; Bochu, B.; http://www.inpg.fr/LMGP: Domaine Universitaire BP 46, 38402 Saint Martin d'Hères, France.

30. ProFit; Philips Analytical X-ray: Netherlands, 1996.

31. Cotton, F. A.; Wilkinson, G. *Advanced Inorganic Chemistry, 4th Ed.*; John Wiley and Sons: New York, 1980.

Chapter 4

Topochemical Manipulation of a Series of Ruddlesden-Popper Layered Perovskites

4.1 Introduction

The discovery of high temperature superconductivity in the Ruddlesden-Popper (RP) layered ruthenate, Sr_2RuO_4,[1] has opened the door for some extensive research on the family, $(A_{n+1}Ru_nO_{3n+1})$ (A = alkaline earth metal; n = 1, 2, 3). Interest in these compounds is due to electric and magnetic properties observed like the ferromagnetism found in the n = ∞, 3 members, $SrRuO_3$ and $Sr_4Ru_3O_{10}$, respectively.[2-5] The n= 2 compound, $Sr_3Ru_2O_7$, has been found to behave differently depending on the sample preparation.[6-9] In terms of intercalation chemistry, Greaves *et al.* have shown that fluorine ions can be intercalated into the cationic layers between perovskite blocks of $Sr_3Ru_2O_7F_2$ opening the door to new significant properties. Our group has investigated the formation of alkali metal halide layers within Dion-Jacobson (DJ) layered perovskites by a two-step method.[10-11] Reductive intercalation with an alkali metal, followed by oxidative intercalation with chlorine gas, led to the formation of compounds of general formula, $(A_2Cl)LaNb_2O_7$ (A = Rb, Cs).[12] In an effort to expand intercalation processes for building metal - halide layers, we are now investigating oxidative intercalation followed by reductive intercalation in other perovskite related compounds (RP). This could lead to the development of new perovskite systems with other important electronic and magnetic properties.

Following the Greaves *et al.*[10] approach we have investigated the oxidative intercalation (Ru^{4+} goes to Ru^{5+}) of chloride and fluoride ions between the perovskite layers of Ruddlesden-Popper series

$A_{n+1}M_nO_{3n+1}$ (A = Ca, Sr; M = Ru; n = 1, 2, or 3). Additionally, a subsequent reductive intercalation step with alkali metals (A) like Li, Rb, and Cs was investigated in an attempt to build "layers within layers".

4.2 Experimental

4.2.1 *Synthesis*

The hosts used for the oxidative intercalation reactions, Ca_2RuO_4 Sr_2RuO_4, $Sr_3Ru_2O_7$ and $Sr_4Ru_3O_{10}$,[1,3-7,13-14] were prepared by high temperature solid state methods. Ru metal powder (Alfa Aesar, ~ 200 mesh, 99.95%) and $AeCO_3$ (Ae = Ca, Sr) (Alfa Aesar, 99.994 %) in a 1 : 2 molar ratio were mixed and ground in a dry box and heated to a 1200 ^{o}C for 12 - 24 hours in an alumina crucible in air to prepare Ae_2RuO_4. The n = 2 ruthenate member was synthesized as the n = 1 but the molar ration there was 2 : 3 with a 1 % excess of $SrCO_3$ and heated to 1400 ^{o}C in air for 48 hours with intermediate grinding until a single phase was obtained. It is very important to mention here that we were not able to prepare pure samples of the n = 2, therefore we were not able to obtain pure products after the intercalation reactions. $Sr_4Ru_3O_{10}$ was provided by Prof. Zhiqiang Mao's group from Tulane University and $Sr_3Ru_2O_7F_2$ was prepared by published methods.[10]

Oxidative Intercalation:

Oxidative intercalation was then carried out using a series of fluorine, chlorine, bromine, and iodine sources listed in Table 4.1. Details on the reaction conditions are listed for the double layered ruthenate (Table 4.2); the same or similar conditions were carried out for the

Table 4.1 Reagents used for oxidative intercalation

Reagent	Purity and Supplier
CuF_2	Anhydrous, 99.5%, Alfa Aesar
$(CH_2CF_2)_n$	Alfa Aesar
NH_4F	98%, Alfa Aesar
Cl_2	99.99%, Matheson Trigas
NH_4Cl	99.999%, Alfa Aesar
$CuCl_2$	Ultra dry, 99.995%, Alfa Aesar
ICl_3	Sigma – Aldrich, 97%
PCl_5	Sigma – Aldrich, 95%
$CuBr_2$	Anhydrous, 99%, Alfa Aesar
NH_4Br	99.999%, Alfa Aesar
I_2	99.8%, Merck KGA, Germany

Table 4.2 Reaction conditions for the oxidative intercalation of halogens in $Sr_3Ru_2O_7$

Reagent	Reaction Conditions
CuF_2	1:2 molar ratio, mixed and ground together in an argon filled glove box and heated in air in an alumina boat at 220-260 ^{o}C for 20 to 24 hours
NH_4F	1:2 molar ratio, mixed and ground in an argon filled glove box, heated in air in an alumina crucible at 150 ^{o}C for 24 hours
Cl_2	Heated in a sand bath at 100-220 ^{o}C under inert atmosphere using a Schlenk line (Figure 4.1)
NH_4Cl	1:6 molar ratio total (1:2 increments with intermediate grinding), mixed and ground in an argon filled glove box and heated in air in an alumina boat at 320 ^{o}C for 12 to 48 hours
$CuCl_2$	Two techniques: a) 1:2 molar ratio, ground in an argon filled glove box and heated in air in an alumina boat at 220-260 ^{o}C for 12 to 24 hours. b) 1:2 molar ratio weighed and ground in an argon filled glove box, sealed in a Pyrex tube under vacuum and heated for 3 days, followed by an acetonitrile wash to remove the CuCl byproduct
ICl_3	1:1 and 1:10 molar ratio at RT, 50, and 120 ^{o}C; for 12 h to 3 days in Pyrex tubes sealed under vacuum
PCl_5	1:1 molar ratio, mixed and sealed under vacuum in Pyrex tubes and heated at 150 ^{o}C for 3 days. Reactions were carried out both mixed and separate (Figure 4.2)
$CuBr_2$	1:1 and 1:2 molar ratio, mixed and ground in an argon filled glove box and heated in air in an alumina boat at 250-400 ^{o}C for 12-24 hours
NH_4Br	1:6 molar ratio total (in 1:2 increments with intermediate grinding), mixed and ground in an argon filled glove box and heated in an alumina boat at 400-420 ^{o}C in air for 24 hours

intercalation reactions involving the other hosts. *Caution: Extreme care should be used in dealing with these reagents especially the fluorine reagents and the chlorine gas, by wearing protective gear like gloves, coats, and facemasks and executing the reactions in a well-ventilated hood or area.* The Schlenk line (Figure 4.1) used was similar to the one suggested by Jolly.[12,15] The aqueous KOH solutions were used to remove excess chlorine gas on the outlet. A second scrubber was added to the setup to make sure that most of the poisonous gas was scrubbed. Scintillation reaction vials (20 mL) with fitted TFE/silicone caps were used, however a serrated natural rubber septa fitted to an appropriately sized vial was also effective. The Cl_2 gas was allowed to flow at a rate of 10 cc/min and the line was purged overnight with N_2 gas after each reaction to remove the unreacted gas.

Reductive Intercalation:

Rb (Alfa Aesar, 99.75%), Cs (Alfa Aesar, 99.75%), and Li (Aldrich 1.6 and 2.5 M *n*-butyllithium in hexanes), were intercalated into the products, $Sr_3Ru_2O_7X_y$ (where X = F, Cl; y ~ 2) using the same techniques used by Choi et al.[12] The reactions using the alkali metals were carried out at 1:2 molar ratios in an argon filled dry box due to their reactivity to oxygen and/or moisture. The now halogenated compounds were pressed into pellets with a hand press (Aldrich Quick Press), placed in a Pyrex tube (12 mm o.d.) and flamed dried under dynamic vacuum. Then stoichiometric amounts of alkali metals were weighed out in a small glass ampoule (6 mm o.d.) and this was combined with the $Sr_3Ru_2O_7X_y$ pellets. ***Caution:*** *Care should be taken when handling the alkali metals due to their violent reaction when in contact with moisture, so good care should be taken during handling and disposal of the metal.*
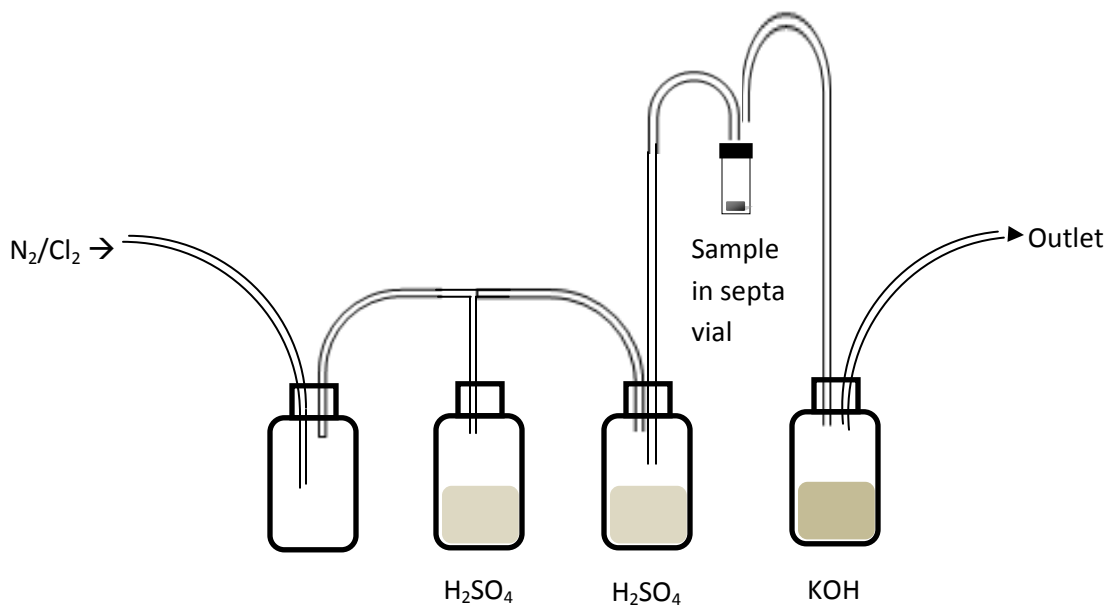
Figure 4.1 Reaction set up for Cl$_2$ reactions.
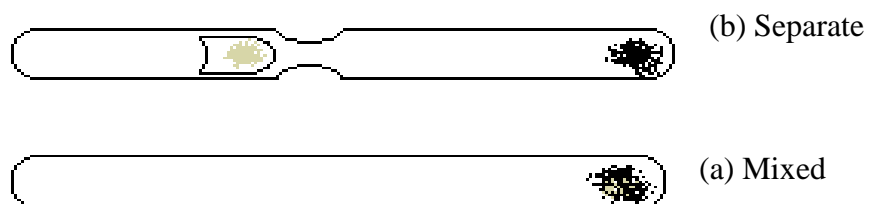
(b) Separate

(a) Mixed

Figure 4.2 Host and reagent were (a) mixed or (b) separate in Pyrex tubes.

The reaction tube was then sealed under vacuum (< 10^{-4} Torr) and placed in a tube furnace at 200 -

220 ^{o}C. The reactions were carried out for 4 days, during which time the pellets crumbled on reaction

due to volume changes in the products. After 4 days, to remove any unreacted metals, a temperature

gradient was applied by sliding one end of the Pyrex tube outside of the tube furnace (close to RT).

Reactions with *n*-butlyllithium were carried out at room temperature in an argon filled solution dry box at 1:5 and 1:10 molar ratio using 1, 1.6, and 2.5 M solutions. 1 M n-butyllithium was prepared through simple dilution of 2.5 M stock sample with anhydrous hexane. Stoichiometric amounts of halogenated samples and the reducing source were added into a vial that was stirred for 24hours to 2 days in the dry box. The products obtained were filtered by gravity filtration, washed with anhydrous hexane, and let to dry overnight into the dry box. All the reductively intercalated products were treated as air-sensitive samples during analysis.

4.2.2 *Characterization*

Powder X-ray diffraction data for all materials were collected on a Philips X-pert PW 3040 MPD X-ray powder diffractometer (XRD) using Cu *K*α radiation (λ = 1.5448 Å). Data were collected over the range of $3^o < 2\theta < 95^o$ in a continuous mode with a speed of 0.02deg/sec. Air-sensitive samples were prepared for X-ray data collection in an argon-filled glove box and sealed under a polypropylene film with silicone grease. Data analysis was carried out with the program POLSQ[16] to obtain refined unit cell parameters and LAZY[17] to simulate X-ray powder data. Compositional analyses were carried out by energy dispersive spectroscopy (EDS) on a JOEL JSM 5410 scanning electron microscope (SEM) equipped with an EDAX-DX PRIME microanalytical system. Thermal behavior was monitored using a differential scanning calorimeter (DSC) on a Netzsch 404S thermal analysis machine in flowing argon and 8% H_2/Ar balance mixture gas. Samples were heated in alumina pans to 1000 °C at a rate of 10 °C/min. Thermogravimetric analysis data was collected on TA Instruments Thermal Analyst-2000 apparatus using a platinum boat under argon flow heated to 1000 °C. Crystal structure refinements of the final compounds were investigated by the Rietveld technique with the GSAS program.[18] The morphology of the samples and structure information were obtained using a Leo 1530 VP field emission scanning electron microscope

(FESEM), and JEOL 2010 transmission electron microscope (TEM). TEM samples were dispersed on Lacey Formvar Carbon grids (300 mesh) with alcohol.

4.3 Results and Discussion

Oxidative Intercalation of $Ae_{n+1}Ru_nO_{3n+1}$ (Ae = Ca, Sr; n = 1, 2,3):

The as-synthesized Ae_2RuO_4 (Ae = Ca, Sr) samples were confirmed to be single phase through XRD. Oxidative intercalation of fluorine and chlorine was investigated using different sources. Reactions showed no evidence of intercalation and under some conditions deintercalation of strontium was observed to form SrX_2 (X = F, Cl). On longer reaction times or higher temperatures with $CuCl_2$ in air, Sr_2RuO_4 would totally decompose and evidence of Cu_2OCl_2 and $SrCl_2$ were observed in XRD along with a loss in crystallinity.

$Sr_3Ru_2O_7$ was successfully synthesized and the diffraction data is seen in Figure 4.3 with the
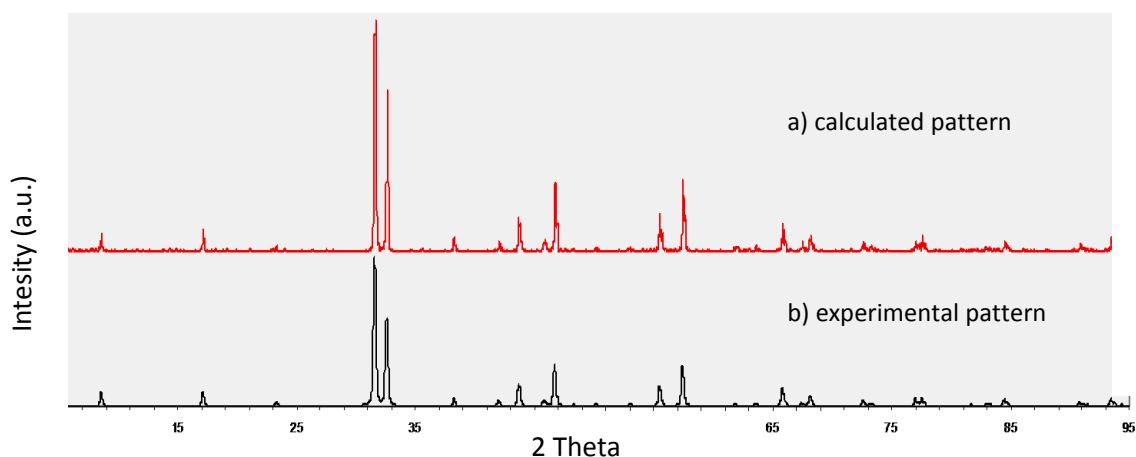
Figure 4.3 Diffraction of a) calculated pattern and b) experimental pattern for $Sr_3Ru_2O_7$.

corresponding refined unit cell parameters in Table 4.3. The host underwent oxidative halide insertion

Table 4.3 Unit cell parameters of reference versus experimental for $Sr_3Ru_2O_7$

Unit cell parameter	a (Å)	c (Å)
Literature values[10]	3.892	20.72
Experimental	3.8883(6)	20.729(2)

with several reagents and under different conditions (Table 4.2). Those based on chlorine intercalation,

showed clear evidence of insertion (Table 4.4) and were the best reagents of choice. Other fluorine

Table 4.4 Results of intercalation reactions with the host $Sr_3Ru_2O_7$

Reagent Used	Results
Cl_2	Intercalation with poor crystallinity and Sr deintercalation
NH_4Cl	Intercalation
$CuCl_2$	Intercalation
ICl_3	No intercalation
PCl_5	Intercalation with poor crystallinity and reaction incompletion
$CuBr_2$	No intercalation
NH_4Br	Intercalation combined with decomposition of product

sources were attempted to see if $Sr_3Ru_2O_7F_2$[10] could be synthesized with alternative reagents other than

CuF_2 to avoid CuO as an impurity; while compounds intercalated, only partial intercalation occurred

under these conditions. Initial attempts of chlorination were done using chlorine gas but extensive

deintercalation was observed in the form of $SrCl_2$ and the crystallinity of the compound significantly

decreased. It is thought that the reason for this could be that the pure gas is just too harsh of a reagent.

Exploratory reagents like ICl_3 and PCl_5 were also attempted under conditions such that they would decompose to produce some amount of chlorine gas; this approach also resulted in significant loss of crystallinity. NH_4Cl and $CuCl_2$ (in open air and in a sealed tube) were the best reagents for the intercalation of chlorine, with $CuCl_2$ under static vacuum giving the best results overall in terms of reaction completeness and retention of crystallinity. Figure 4.4 shows the X-ray powder diffraction data
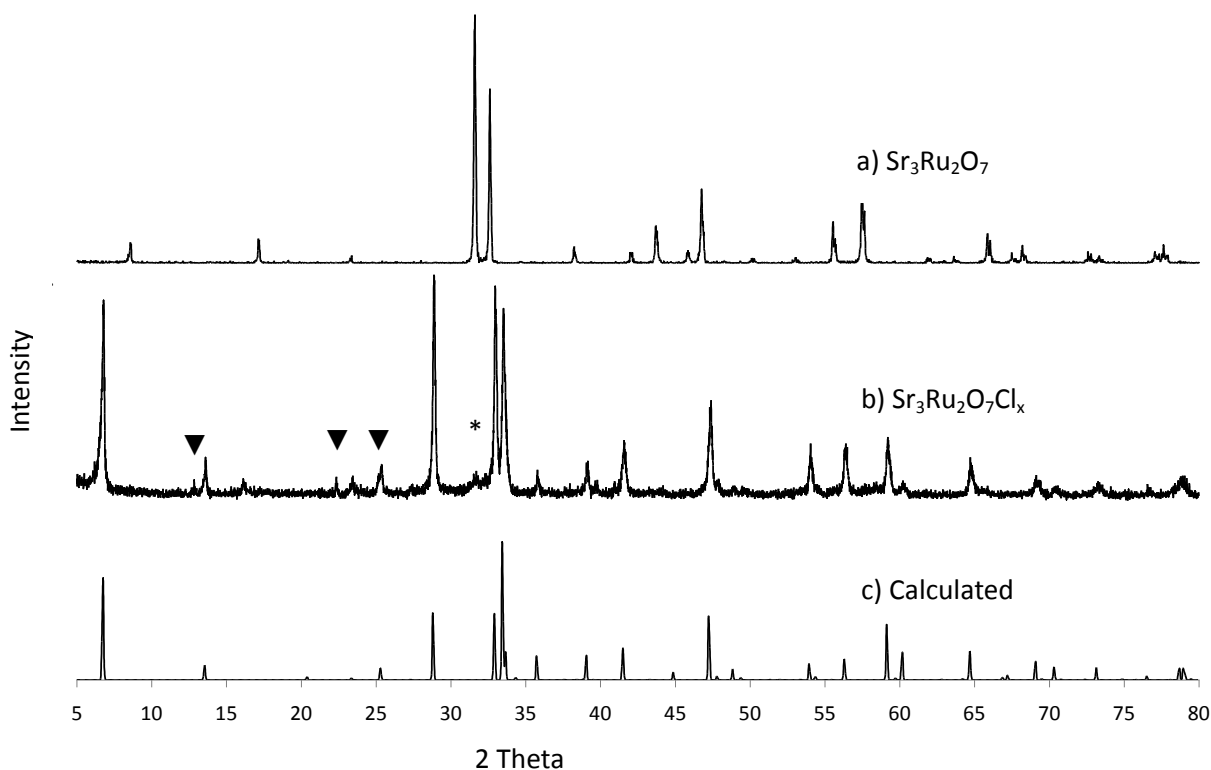
Figure 4.4 XRD of (a) $Sr_3Ru_2O_7$, (b) $Sr_3Ru_2O_7Cl_x$ made with $CuCl_2$ in air, and (c) calculated pattern based on model described in text. Asterisk (*) indicates unreacted starting material and inverted triangle (▼) a minor impurity, $SrCl_2 \cdot 6H_2O$ (JCPDS 6-0073).

for the parent, $Sr_3Ru_2O_7$, and its intercalation product, $Sr_3Ru_2O_7Cl_x$. An initial model was proposed for the

new compound and a XRD pattern was simulated and can also be found in the figure. The simulated

pattern is in reasonable agreement with the observed one. Unreacted starting material (*) and

strontium chloride hydrate (▼) are also observed as minor components in the powder pattern. In some

cases deintercalation of strontium is observed combined with the insertion of the chloride, specifically

at temperatures above 230 °C or if an excess of the reagent was added. However the amount of

formation of the byproduct could be controlled by optimizing the reaction conditions. EDS data

confirmed the presence of chlorine within the sample and indicated that x was around 2. Table 4.5

Table 4.5 Refined Lattice Parameters of $Sr_3Ru_2O_7Cl_x$

Unit Cell	a(Å)	b(Å)	c(Å)	V(Å³)	Layer Spacing (Å)
$Sr_3Ru_2O_7$[10]	5.5016(1)	5.5016(1)	20.7194(5)	627.127	10.36
$Sr_3Ru_2O_7F_2$[10]	5.4231(4)	5.4168(4)	24.2505(8)	712.379	12.13
$Sr_3Ru_2O_7Cl_x$	5.4323(5)	5.4327(5)	26.0732(9)	769.47(1)	13.04

presents the refined unit cell parameters for the two compounds in comparison to $Sr_3Ru_2O_7F_2$. A clear

layer expansion of about 5.4 Å relative to the parent can be seen after oxidation with the chlorine

reagent. After fluorine intercalation, the layer expansion is about 3.5 Å. In comparison to the

fluorinated ruthenate,[10] the increase in c-parameter is consistent with the increase in size going from

fluoride (1.17Å) to chloride (1.67Å).[19] Furthermore, the increase indicates that the lattice expansion

supports the insertion of chlorines into both layers of the ruthenate unit cell, as opposed to occupying

alternate layers. Initial efforts to index the powder pattern of $Sr_3Ru_2O_7Cl_x$ indicated the need for an

orthorhombic unit cell. This result was consistent with data published for both $Sr_3Ru_2O_7$[6] and

$Sr_3Ru_2O_7F_2$[10] where orthorhombic distortions were observed in these compounds due to twisting of the

RuO_6 octahedra. A separate study, however, published by Shaked *et al.*[8] showed that $Sr_3Ru_2O_7$ could be

modeled on a tetragonal cell in the orthorhombic space group *Bbcb*. Following the Shaked structural

model in combination with the interlayer halide structure reported by Greaves *et al.*,[10] we carried out

Rietveld structure refinement calculations. The refinement was carried out by Dr. Sanjaya Ranmohotti

using the XRD data. The observed, calculated, and difference plots for the refinement are shown in

Figure 4.5 and the structural information is provided in Table 4.6. The selected bond distances are

shown in Table 4.7. Based on the refinement data, the structure model of the final compound is

presented in Figure 4.6. The structure was refined with $SrCl_2 \cdot 6H_2O$ as an impurity phase. After the

oxidative intercalation, the chlorines sit in between the perovskite slabs in tetrahedral sites, $ClSr_4$. The

strontium chloride bond distance (2.999 Å) obtained through refinement is in good agreement with the

bond distance observed in $SrCl_2$ (3.031 Å).[20] The Sr-O bond lengths are also close to the reported values

for similar compounds in the ruthenate family like for example the parent compound $Sr_3Ru_2O_7$ where
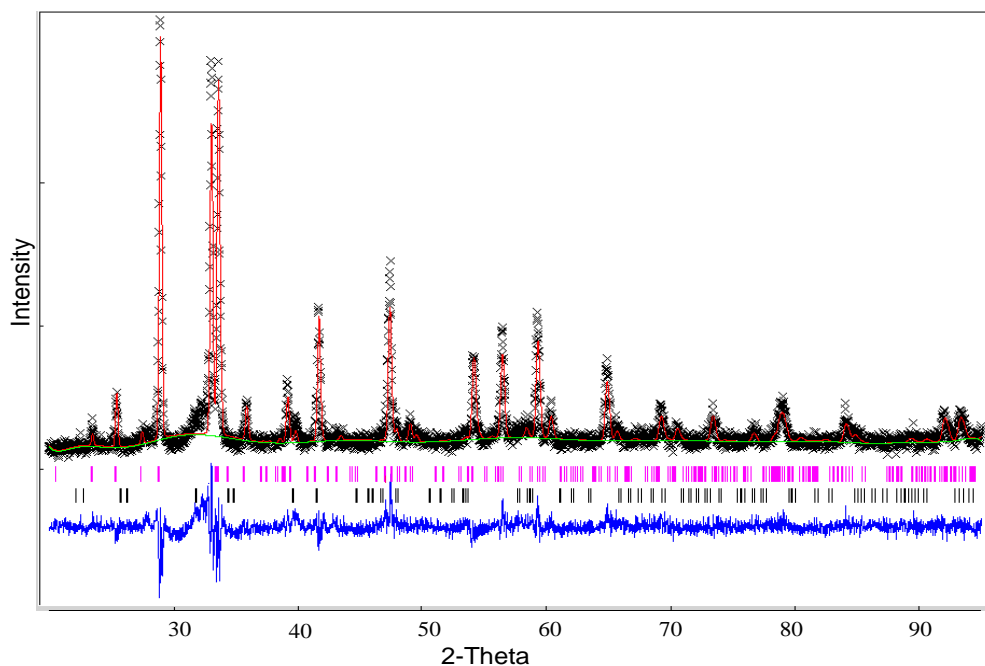
Figure 4.5 Results of Rietveld refinement for the structure of $Sr_3Ru_2O_7Cl_{0.7}$. The measured (crosses), calculated (solid line) and the difference (bottom) profiles are shown. Bragg positions are indicated by tic marks

Table 4.6 Crystallographic data for $Sr_3Ru_2O_7Cl_{0.7}$

	x	y	z	g
Sr1	¼	¼	0	1
Sr2	¼	¼	0.1617(2)	1
Ru	¼	¼	0.4206(3)	1
O1	¼	¼	½	1
O2	¼	¼	0.351(1)	1
O3	0.63(1)	0.98(1)	0.083(2)	1
Cl	½	½	¼	0.36(3)

[a]Space group: Bbcb (#137), R_p= 0.1272, R_{wp} = 0.1628, χ^2 = 1.748, U_{iso} were all constrained to 0.010

Table 4.7 Selected Bond Distances (Å) for $Sr_3Ru_2O_7Cl_{0.7}$

Bond	Length (Å)
Ru-O1	2.0616 (x1)
Ru-O2	1.8348 (x1)
Ru-O3	1.8949 (x2)
Ru-O3	1.9720 (x2)
Sr1-O1	2.721 (x2)
Sr1-O1	2.716 (x2)
Sr1-O3	2.750 (x4)
Sr1-O3	3.007 (x4)
Sr2-O2	2.735 (x2)
Sr2-O2	2.739 (x2)
Sr2-O3	2.704 (x2)
Sr2-O3	2.964 (x2)
Sr2-Cl	2.999 (x4)
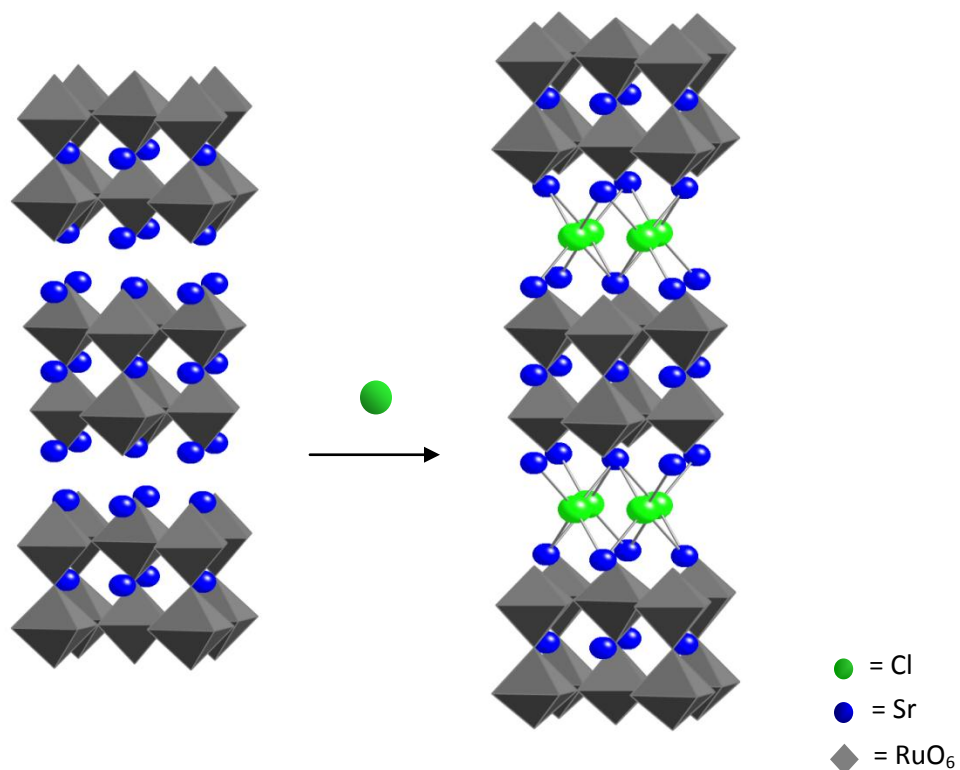
Figure 4.6 Structural representation of (left) $Sr_3Ru_2O_7$ vs. (right) $Sr_3Ru_2O_7Cl_{0.7}$

the bond length ranged from 2.459-2.962 Å.[10] Rietveld showed that the occupancy is 0.7

correspondingly indicating that even though the compound is isostructural to $Sr_3Ru_2O_7F_2$ mix valency is

present which is not seen in the fluorinated compound where ruthenium has a +5 charge. The change in

oxidation state is supported by the shorter bond distance observed in the external apical bonds (Ru -

O3) pointing towards the interlayer. The bond is much longer in the parent compound (2.025 Å) where

the Ru is in a +5 oxidation state.

FESEM images were taken by Ms. Yuan Yao to look at the morphology of the parent versus the product (Figure 4.7) for the CuCl2 treatment of $Sr_3Ru_2O_7$.   As can be seen in the images, the morphology of the crystallites remains the same, plate-like, after the reaction.

To explore the possibility of insertion of larger halide ions, bromine intercalation was also investigated. Evidence of bromine insertion was observed with NH_4Br as a reagent but not with $CuBr_2$ under the conditions tried. XRD data shows that even though bromination occurs, a simultaneous reaction to form $SrRuO_3$ is also observed, suggesting a possible instability in the reaction products, limiting the usefulness of this approach.
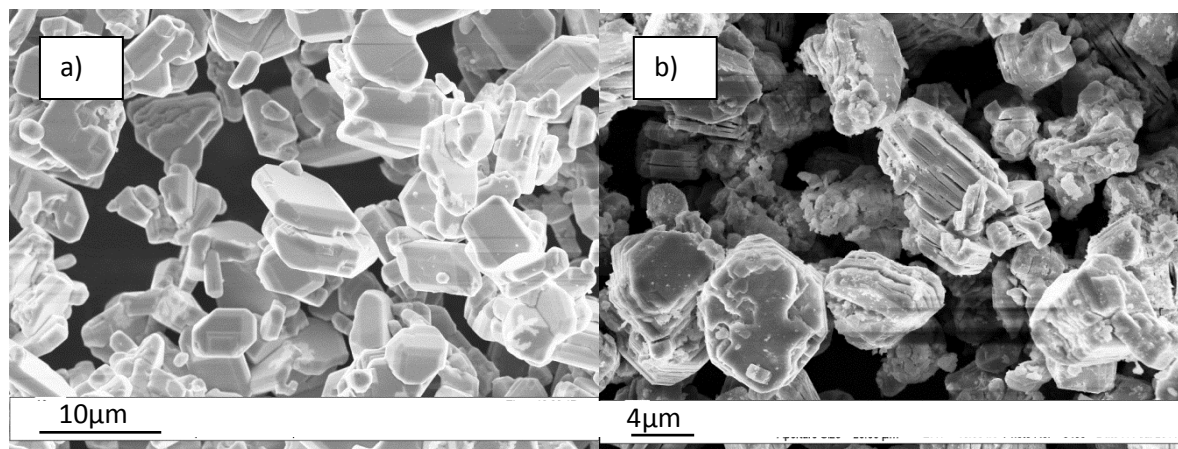
Figure 4.7 FESEM images showing the morphology of a) $Sr_3Ru_2O_7$ and b) $Sr_3Ru_2O_7Cl_x$.

Intercalation in the ruthenates was also applied to the n = 3 layered compounds, $Sr_4Ru_3O_{10}$. Since we were not equipped to readily synthesize the starting material, some sample was provided by Professor Mao's group at Tulane University, though the parent compound was not a pure phase and contained some amount of $Sr_3Ru_2O_7$ impurity (Figure 4.8). The unit cell parameters of the parent compound were calculated and refined based on the XRD data collected on the sample and are presented in Table 4.8. Oxidative intercalation was attempted using CuF_2, $CuCl_2$, NH_4Cl, and NH_4Br under similar conditions as

described in Table 4.2. The differences in reaction conditions varied mainly in molar ratio and reaction times. Evidence of fluorine and chlorine intercalation with the n = 3 compound was observed but bromine showed no intercalation. Further, due to the presence of the n = 2 impurity, additional peaks
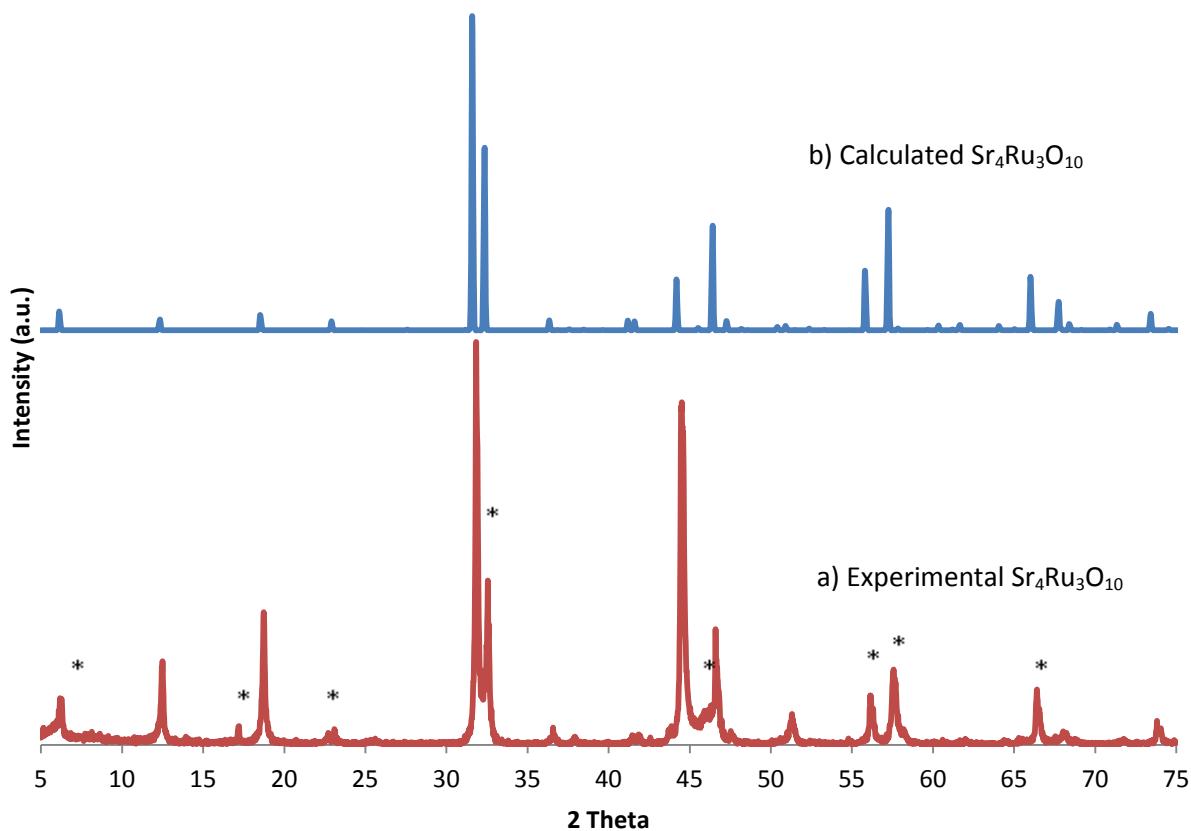
Figure 4.8 XRD pattern of a) experimental and b) calculated $Sr_4Ru_3O_{10}$. $Sr_3Ru_2O_7$ impurities are indicated by the symbol (*).

Table 4.8 Refined unit cell parameters for $Sr_4Ru_3O_{10}$.

Lattice parameter	Experimental	Literature[4]
a = b(Å)	3.8885(2)	3.9001(3)
c(Å)	28.42943(3)	28.573(3)
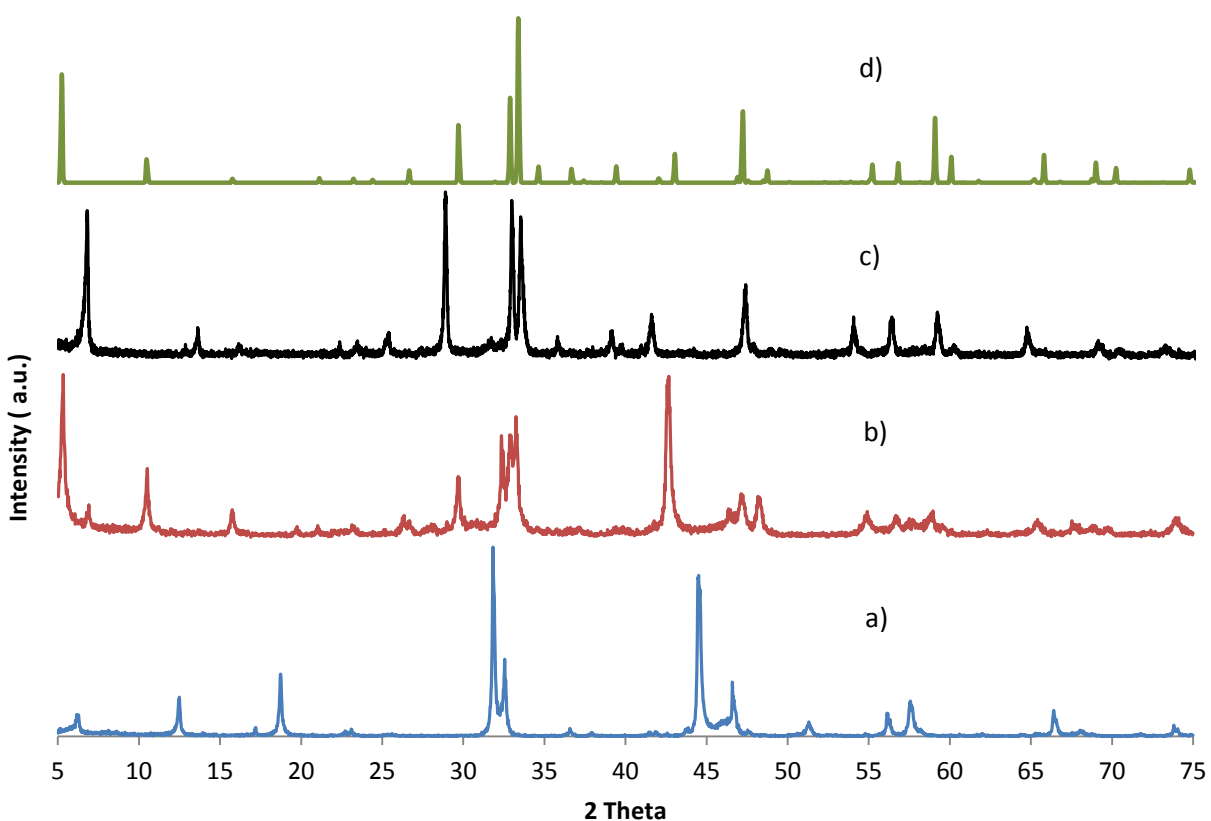
Figure 4.9 Diffraction data for a) $Sr_4Ru_3O_{10}$, b) product after chlorine intercalation, c) $Sr_3Ru_2O_7Cl_{0.7}$, and d) the simulated pattern.

were observed corresponding to the halide intercalated products based on this secondary phase. Figure 4.9 shows an example of the chlorinated sample with NH_4Cl. Additional peaks were also observed that are due to the incompletion of the reaction. Based on expected results, a model structure is simulated with the corresponding XRD (Figure 4.9d). Due to the $n = 2$ phase as an impurity the pattern is very complex yet it is can be pointed out that there is evidence for intercalation, as seen with the increase in the c-parameter. The reflections for the proposed model structure can be seen in the experimental data further confirming that oxidative intercalation was successful. Unit cell parameters were estimated and

Table 4.9 Unit cell parameters of oxidative intercalation products of $Sr_4Ru_3O_{10}$.

	a (Å)	b(Å)	c(Å)	Volume(Å^3)	Layer expansion (Å)	Layer Spacing (Å)
$Sr_4Ru_3O_{10}$	5.5280(11)	5.5260(11)	28.651(6)	875.2(2)	---	14.33
$Sr_4Ru_3O_{10}F_x$	5.4348(6)	5.3921(4)	31.51853(5)	923.7(1)	3.09	15.76
$Sr_4Ru_3O_{10}Cl_x$	3.8406(6)	---	33.53783(7)	494.7(1)	5.11	16.77

refined based on the diffraction pattern choosing the peaks that corresponds to the new phase, as shown in Table 4.9. The peaks were refined on a tetragonal cell and all the peaks were indexed. As can be seen in the Table 4.9, a layer expansion 3.09 Å is observed for the fluorine compound and 5.11 for the chlorine compound relative to the parent. These values are consistent with the layer expansion values seen in the n = 2 layered perovskite after halide intercalation (Table 4.5). A structure model was simulated of the chloride intercalated product (Figure 4.10).

Unlike the n = 2 and 3 phases, the n = 1 phase Ae_2RuO_4 (Ae = Ca, Sr) is not receptive to intercalation of halides. The reason for this is not completely obvious, though one possible explanation could be that the overall charge distribution within in the single perovskite slabs is more localized and this produces a more rigid interlayer that is less receptive to intercalation. In the other phases the existence of the multiple slabs allows for greater distribution of layer therefore a weaker interaction with the interlayer and a correspondingly greater receptiveness to topochemical manipulations.
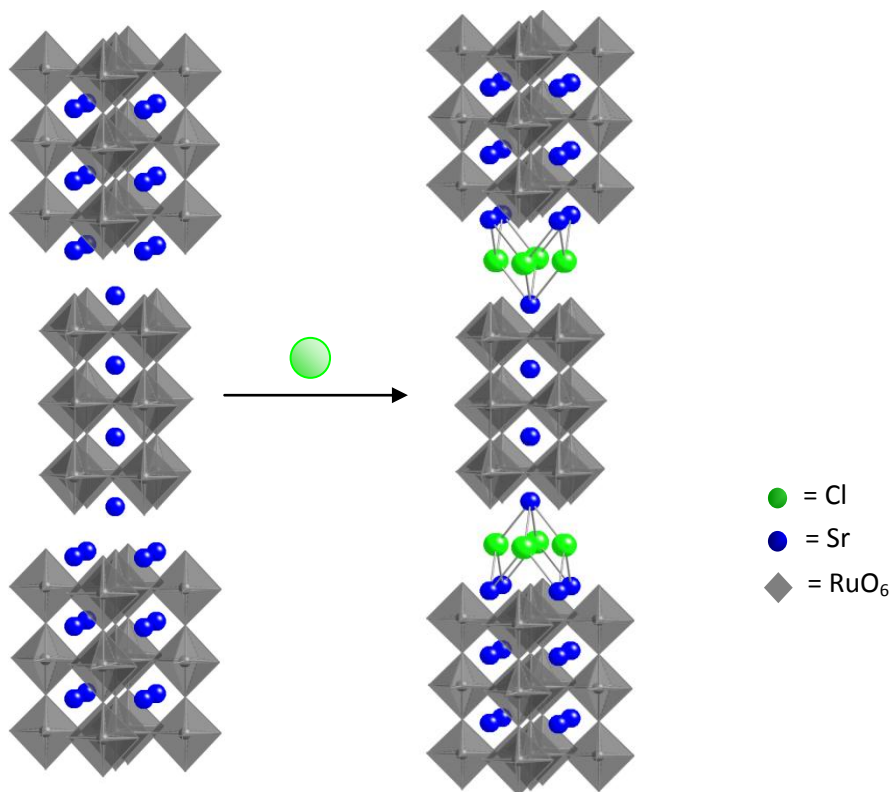
Figure 4.10 Structure model of (left) $Sr_4Ru_3O_{10}$ and (right) the simulated product after chlorination $Sr_4Ru_3O_{10}Cl_x$

Reductive Intercalation of $Sr_3Ru_2O_7X_y$:

Initial reductive intercalation reactions of the alkali metals Li, Rb, Cs into the hosts, $Sr_3Ru_2O_7Cl_x$ and $Sr_3Ru_2O_7F_2$, were carried out. While most of the reactions resulted in deintercalation of the halide (Table 4.10) to form the corresponding alkali-halide, evidence for lithium intercalation with n-butyllithium was observed on reaction with $Sr_3Ru_2O_7F_2$; a layer expansion of about 3 Å was seen but with a great loss of crystallinity (Figure 4.11). The ability to intercalate Li but not the larger alkali metals could be due to a size limitation of the interlayer. Looking at the large oxidation state possibilities for ruthenium it seems highly possible to be able further oxidize or reduce the cation but yet the

Table 4.10 Results of reductive intercalation reactions

Reagent	$Sr_3Ru_2O_7Cl_x$	$Sr_3Ru_2O_7F_2$
LiI	No attempt	De-intercalation of F
C_4H_9Li	No reaction	Intercalation*
Rb^o	De-intercalation of Cl	De-intercalation of F
Cs^o	De-intercalation of Cl	De-intercalation of F

*product showed a large loss of crystallinity

interlayer stability dictates whether further topochemical manipulations are possible. Cation mobility

might play a role here and is supported by the deintercalation of the fluorine/chlorine from the

interlayer and the important factor here could be just a greater affinity to form the more stable

compounds AX.
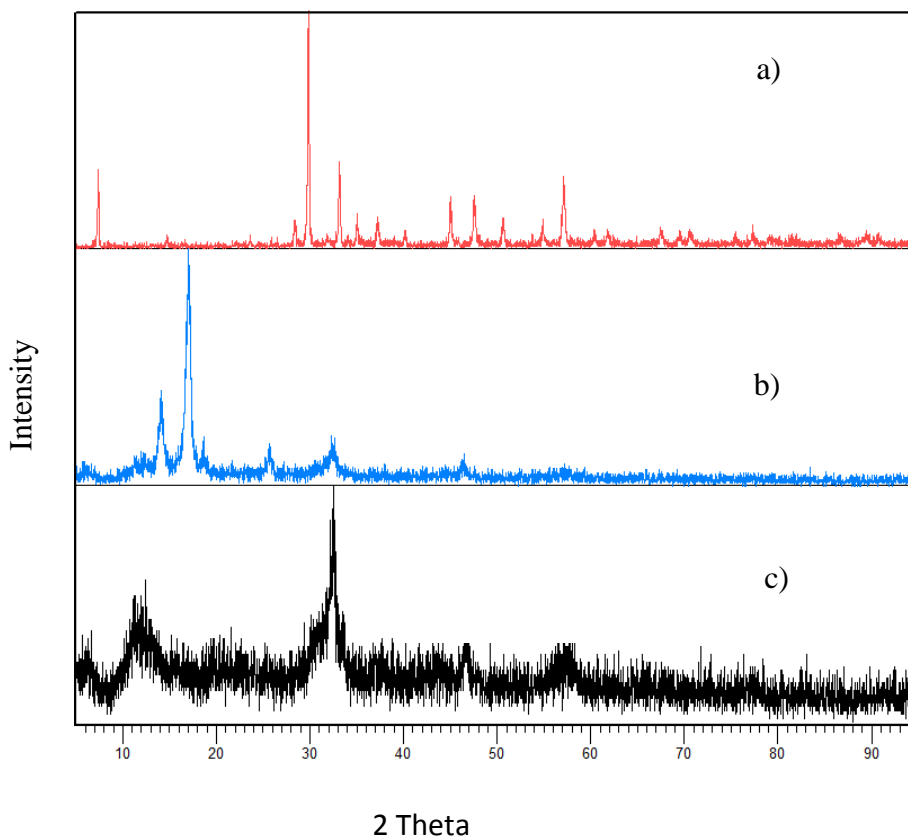
Figure 4.11 X-ray diffraction of a) $Sr_3Ru_2O_7F_2$, b) $Sr_3Ru_2O_7F_2$ and 2.5 M n-butyllithium at 1:5 ratio with film, and c) the product from b), without film.

4.4 Conclusions

Oxidative intercalation of a series of RP compounds, $Ae_{n+1}Ru_nO_{3n+1}$ (Ae = Ca, Sr; n = 1, 2,3), was investigated. $Sr_3Ru_2O_7$ lead to the formation of the new mixed valence compound, $Sr_3Ru_2O_7Cl_{0.7}$ after intercalation using a novel method of chlorination. The method developed showed to be effective on other systems and is a new synthetic application that can be applied to the further design of compounds that could have significant properties. Initial attempts were made to reductively intercalate alkali metals into $Sr_3Ru_2O_7Cl_x$ and $Sr_3Ru_2O_7F_2$; most reactions were unsuccessful.

4.5 References

1. Maeno, Y.; Hashimoto, H.; Yoshida, K.; Nishizaki, S.; Fujita, T.; Bednorz, J. G.; Lichtenberg, F. *Nature* **1994**, *372*, 532.
2. Allen, P. B.; Berger, H.; Chauvet, O.; Forro, L.; Jarlborg, T.; Junod, A.; Revaz, B.; Santi, G. *Phys. Rev. B* **1996**, *53*, 4393.
3. Cao, G.; McCall, S. K.; Crow, J. E.; Guertin, R. P. *Phys. Rev. B* **1997**, *56*, R5740.
4. Crawford, M. K.; Harlow, R. L.; Marshall, W.; Li, Z.; Cao, G.; Lindstrom, R. L.; Huang, Q.; Lynn, J. W. *Phys. Rev. B* **2002**, *65*.
5. Cao, G.; Balicas, L.; Song, W. H.; Sun, Y. P.; Xin, Y.; Bondarenko, V. A.; Brill, J. W.; Parkin, S.; Lin, X. N. *Phys. Rev. B* **2003**, *68*.
6. Cava, R. J.; Zandbergen, H. W.; Krajewski, J. J.; Peck, W. F.; Batlogg, B.; Carter, S.; Fleming, R. M.; Zhou, O.; Rupp, L. W. *J. Solid State Chem.* **1995**, *116*, 141.
7. Cao, G.; McCall, S.; Crow, J. E. *Phys. Rev. B* **1997**, *55*, R672.
8. Shaked, H.; Jorgensen, J. D.; Chmaissem, O.; Ikeda, S.; Maeno, Y. *J. Solid State Chem.* **2000**, *154*, 361.
9. Stone, M. B.; Lumsden, M. D.; Jin, R.; Sales, B. C.; Mandrus, D.; Nagler, S. E.; Qiu, Y. *Phys. Rev. B* **2006**, *73*.
10. Li, R. K.; Greaves, C. *Phys. Rev. B* **2000**, *62*, 3811.
11. McCabe, E. E.; Greaves, C. *J. Fluorine Chem.* **2007**, *128*, 448.
12. Choi, J.; Zhang, X.; Wiley, J. B. *Inorg. Chem.* **2009**, *48*, 4811.
13. Nakatsuji, S.; Maeno, Y. *J. Solid State Chem.* **2001**, *156*, 26.
14. Mackenzie, A. P.; Maeno, Y. *Reviews of Modern Physics* **2003**, *75*, 657.
15. Jolly, W. L. *The Synthesis and Characterization of Inorganic Compounds*; Prentice-Hall Inc.: NJ, . 1970.
16. Keszler, D. A.; Ibers, J. A. Department of Chemistry, Northwestern University, Evanston, IL 1983.
17. Yvon, K.; Jeitschko, W.; Parthe, E. Laboratoire de Crystallographic Aux Rayon-X, Univ. Geneva, Switzerland, 1977.

18. Larson, A. C.; Von Dreele, R. B.; Los Alamos National Laboratory: Los Alamos, NM: 2000.
19. Shannon, R. D. *Acta Crystallogr. Sect. A* **1976**, *32*, 751.
20. Mark, H.; Tolksdorf, S. *Zeitschrift fur Physik* **1925**, *33*, 681.

Chapter 5

Concluding Remarks

The topic of this dissertation is the topochemical manipulation of layered perovskites wherein the concept of rational design of new materials has been demonstrated. A great effort has been made to control the synthesis of new compounds by designing new techniques. Topotactic methods allow one to obtain compounds, sometimes metastable ones, not accessible through traditional high temperature solid state routes. The structural variety obtained within perovskites and perovskite-related compounds through topotactic methods is what makes these compounds so important to this field. In turn, the additional promise of new significant properties, including those of technological importance, is also an important consideration.

Herein, a multistep approach was developed towards the synthesis of the new compounds $(A_xM_{0.5}Cl_y)LaNb_2O_7$ (where A = Rb, Cs; M = Fe, Ni; $x \approx 1.5$; $y \approx 1$) at temperatures below 400 ^{o}C. This multistep approach is a strategy to form mixed-metal halide layers, specifically with divalent cations, within layered perovskites. The reaction series was also applied to the tantalate layered oxides, leading to the formation of the new compound $Ni_{0.5}LaTa_2O_7$ through ion exchange; the further multistep topochemical manipulation of this new compound was not successful and was indicative of the difference in chemical behavior of the tantalates versus the niobates.

We have also investigated the oxidative intercalation of halogens into a series of Ruddlesden-Popper (R-P) ruthenate oxides with the formula $Ae_{n+1}Ru_nO_{3n+1}$ (Ae = Ca, Sr; n = 1, 2, 3) with the use of several sources of fluorine, chlorine, and bromine. A new method was developed to intercalate chlorine into layered systems; this approach avoids the use of highly toxic chlorine gas and opens the door for several ways to chlorinate beyond the conventional way. The new mixed-valence phase $Sr_3Ru_2O_7Cl_{0.7}$ was synthesized by the new method and further topotactic manipulations were explored.

Topochemical methodologies offer extensive control over structure and therefore the properties. The ability to use such approaches to consciously direct the structuring of compounds is an especially powerful tool. It is expected that through combinations of these various methods (ion-exchange, oxidative intercalation and reductive intercalation), the long-term impact of topochemical reaction strategies will be felt. Expansion of the methods available and the number of hosts on which to apply them will certainly result in the ability to design and fabricate new materials of both fundamental and technological interest.

Appendix A

Initial Synthesis and Characterization of New Layered Mixed-Metal Bismuth Oxyhalides

A.1 Project motivation

Sillén and others[1] have reported a large number of complex bismuth oxyhalides of the family MBiO$_2$X. The characteristic feature of these structures is that they consist of M$_2$O$_2$ layers separated by single, double, or triple halide layers. The Sillén-derived compounds are of interest because they show attractive properties[2] such as catalytic activity, ferroelectricity, high temperature superconductivity, and ionic conductivity. Our group focuses on soft chemical methods (*chimie douce*) that allow for the manipulation of solid-state compounds at low temperatures (< 500 ^{o}C). With this aim we are examining bismuth oxyhalides as precursors to form new, more expanded layered structures. Our intention is to insert CsCl layers into hosts, AeBiO$_2$Cl (Ae= Ca, Sr, Ba).[3]

A.2 Experimental

A.2.1 Synthesis

AeBiO$_2$Cl samples where Ae = Sr, Ba, Ca were synthesized by solid state method using stoichiometric amounts of BiOCl and SrCO$_3$, BaCO$_3$, and CaCO$_3$, respectively.[3,4] The AeBiO$_2$Cl samples were used to synthesize compounds with the nominal composition CsAeBiO$_2$Cl$_2$

compounds. About 0.5 grams of $SrBiO_2Cl$ was mixed with a stoichiometric amount of CsCl in a molar ratio of 1: 1.5. The sample was ground well and pellets were prepared with a handpress. The pellets were then placed in quartz tubes that were sealed under vacuum. The sealed tubes were heated between 700 ^{o}C and 890 ^{o}C for 3 to 7 days. Samples were then washed before analysis.

A.2.2 Characterization

Powder X-ray diffraction data for all materials were collected on a Philips X-pert PW 3040 MPD X-ray diffractometer with Cu *K*α radiation. Data was collected over the range of $5^o < 2\theta < 95^o$. Data analysis was carried out with the programs POLSQ to obtain refined unit cell parameters and LAZY to simulate x-ray powder data. The structures were drawn using CrystalMaker.

A.3 Results and discussions

An attempt was made to make $CsAeBiO_2Cl_2$ where Ae = Sr, Ca, and Ba. Figure A.3.1 shows the XRD data collected for each parent and the nominal products obtained. As can be noted the series is isostructural. An expansion in the *c*-direction is seen of about 4 Å in each of the parent compounds that corresponds to the insertion of a single Cs layer in the halogen layer filling every other layer in the parent compound.

Table A.3.1 shows the c-parameter for each of the reactants and products. A clear layer expansion layer expansion for each compound on reaction with CsCl, consistent with the

insertion of a CsCl block. A proposed model for the structure of the products is presented in

Figure A.3.2. Here Cs is sitting in a cubic site (CN= 8) surrounded by chlorines similar to CsCl.

The cubic polyhedra exhibit face sharing, while the edge-sharing of M_2O_2 layers, as seen in the

parent compound, is maintained. This compound could be similar to one reported by Harris et

al.[5]
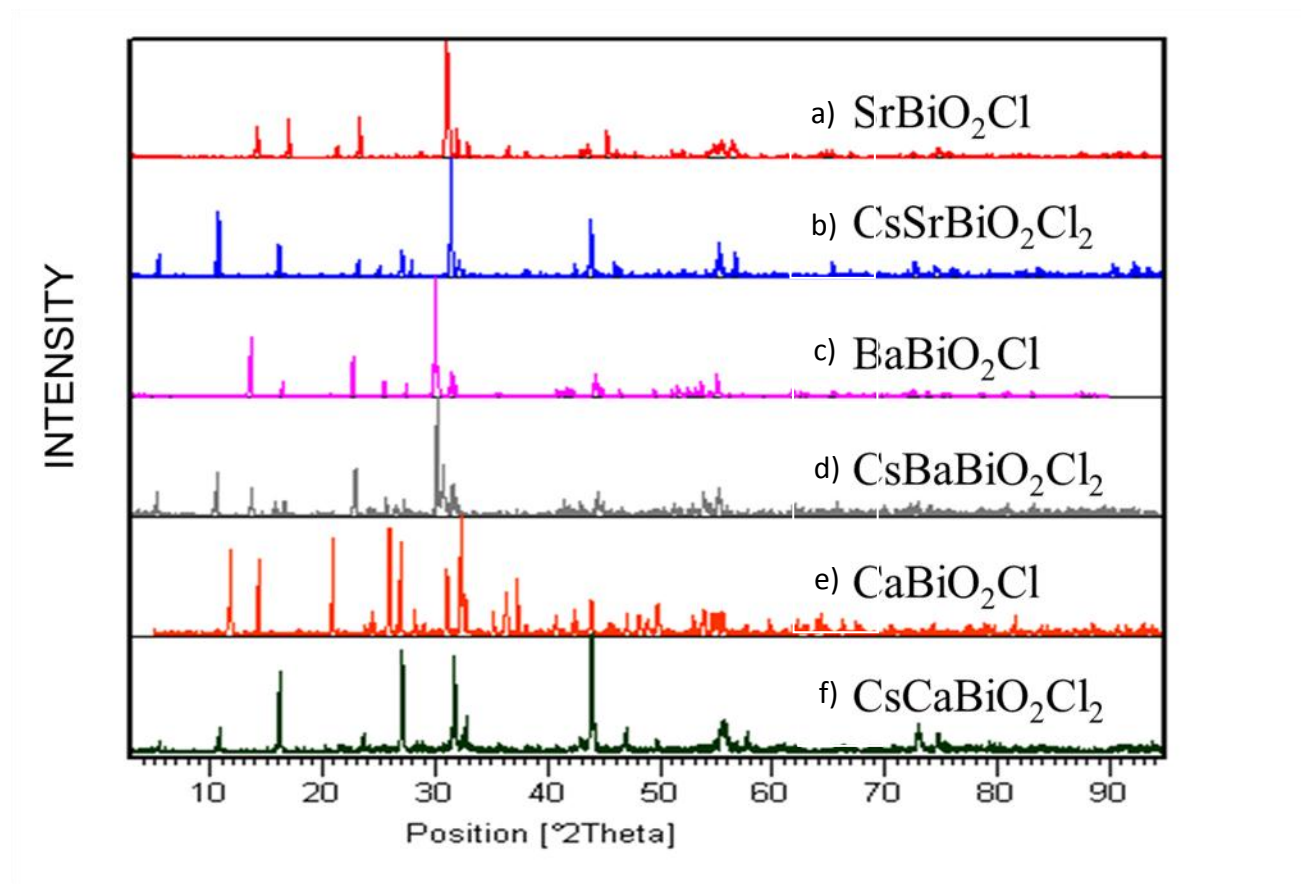
Figure A.1. X-Ray Diffraction Pattern for SrBiO$_2$Cl (a), CsSrBiO$_2$Cl$_2$ (b), BaBiO$_2$Cl (c), CsBaBiO$_2$Cl$_2$ (d), CaBiO$_2$Cl (e), CsCaBiO$_2$Cl$_2$ (f)

Table A.1. Unit cell expansion data

Nominal composition	Parameter c (Å)	Δ c (Å)
CaBiO$_2$Cl	12.796(2)[4]	
		3.77
CsCaBiO$_2$Cl$_2$	16.57(4)	
SrBiO$_2$Cl	12.4081(5)[4]	
		3.92
CsSrBiO$_2$Cl$_2$	16.33(2)	
BaBiO$_2$Cl	12.945(18)[3]	
		3.85
CsBaBiO$_2$Cl$_2$	16.19	

a) Structure of starting material   b) Structure of product
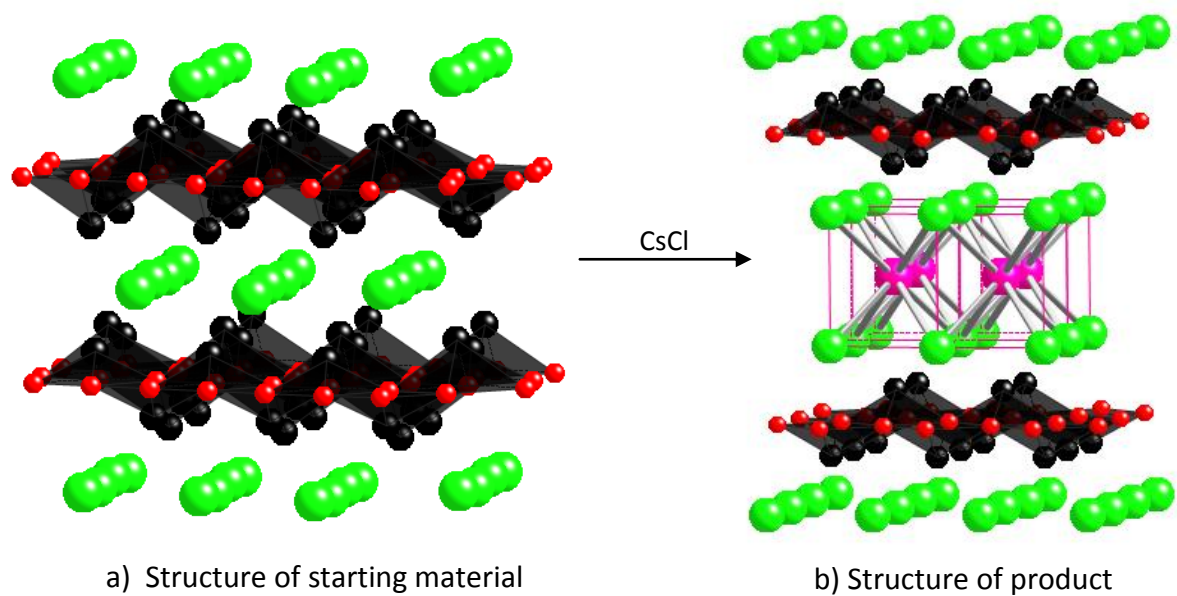
Figure A.2. Structures of starting material (a) and product (b)

Reactions carried out for longer time periods show evidence for another phase (Figure A.3.3). The cell parameters are presented in Table A.3.2. It is possible that the change in unit cell parameters corresponds to the insertion of CsCl in all of halogen layers.
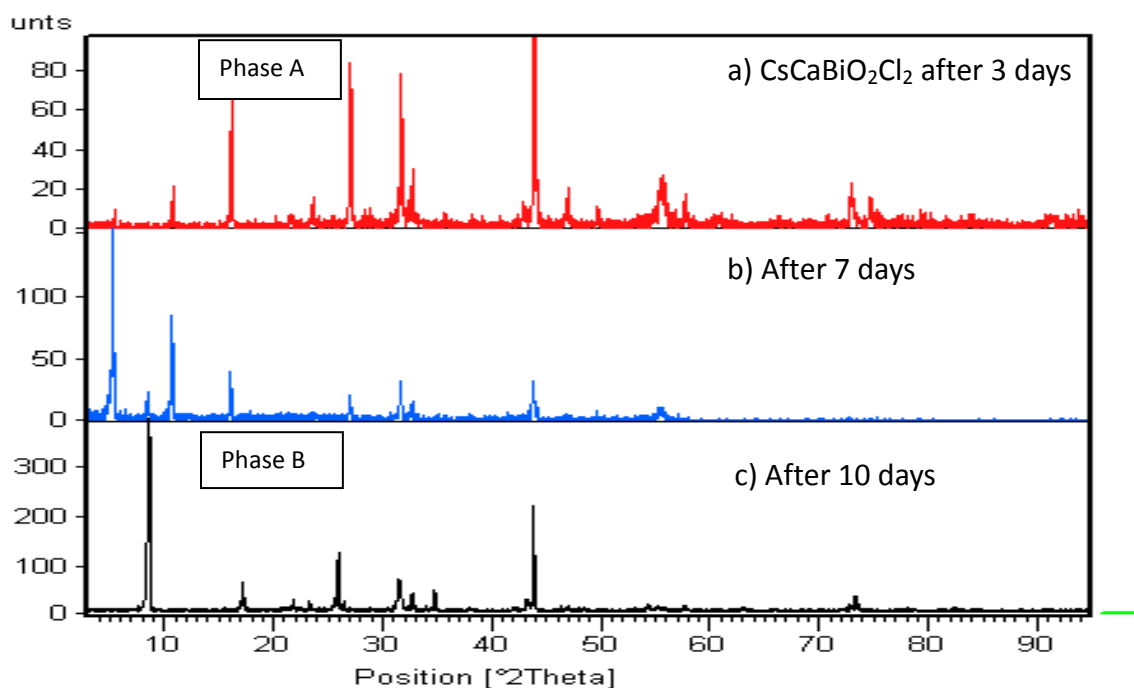
Figure A.3. Evidence for another phase. X-Ray diffraction pattern of phase a) $CsCaBiO_2Cl_2$ after 3 days (b), after 7 days (c), Phase B after 10 days

Table A.2. Layer spacing for insertion of additional CsCl layer

	$CsCaBiO_2Cl_2$ (Phase A)	$Cs_2CaBiO_2Cl_3$ (Phase B)
Unit Cell Parameter c (Å)	16.57(4)	10.16(2) (or 20.32)

A. 4 Conclusions

XRD clearly shows an expansion of the parent layer by ~4 Å consistent with the insertion of a single CsCl layer. The series of nominal composition, $CsAeBiO_2Cl_2$ (Ae = Ca, Sr, Ba) is isostructural. The initial model matches well with the powder data based for the insertion of a layer of CsCl into the parent structure. Here Cs would be on a cubic site (CN = 8) surrounded by chlorines and these cubic polyhedra exhibit face-sharing, similar to CsCl itself. The M_2O_2 layers of the parent are maintained in the reaction. A second compound was also observed; it appears that the change in unit cell parameters corresponds to the insertion of CsCl layers into every halogen layer of the parent.

A. 5 References

1.   L.G.Sillén, *Z. Anorg. Allg. Chem.* 248, 121 (1941).

2.   V.A. Dolgikh, L.N. Kholodkovskaya, *Russian J. Inor. Chem.*37, 5 (1992).

3.   S.M. Fray, C.J. Milne, C.J. Lightfoot, *J. Solid State Chem.* 128, 115 (1997).

4.   M.A. Kennard, J. Darriet, J. Grannec, A.J. Tressaud, *J. Solid State Chem.*117, 201 (1195).

5.   K.D.M. Harris, W. Ueda, J. M. Thomas, G.W. Smith, *Angew. Chem.*27, 1364 (1988).

6.   J.F. Ackerman, *J. Solid State Chem.*62, 92 (1986)

7.   H. Müller-Buschbaum, *Angew.Chem.* 16, 674 (1977)*.*

Appendix B

The Synthesis and Characterization of the New Layered Perovskite:
$(VO)_{0.5}LaNb_2O_7$

B.1 Project motivation

Our group focuses on topochemical methods, such as ion-exchange, intercalation and de-intercalation, that allow for the manipulation of solid-state compounds at low temperatures ($<500^{o}C$). The idea is to create or improve strategies for the formation of new-layered compounds while maintaining the overall structural features of the host.

Gopalakrishnan and coworkers initially reported on the vanadyl exchange in the triple layered perovskite $K_2La_2Ti_3O_{10}$.[1] Our group has also shown that monovalent exchange produced several other compounds like $M_{0.5}LaNb_2O_7$(M= Fe, Ni, Cu) and $Na_{0.1}(VO)_{0.45}LaTiO_4$.[2,3] With this aim we focused on the synthesis of $(VO)_{0.5}LaNb_2O_7$ through ion-exchange. The d^1 V^{4+} cation in the vanadyl, opens the door for some interesting properties.

Topochemical methods allow for the manipulation of layered compounds. An attempt was made to synthesize the new compound with the nominal composition $(VO)_{0.5}LaNb_2O_7$. A series of Dion-Jacobson (DJ) parents, underwent ion-exchange through solution using $VOSO_4 \bullet 2H_2O$. Details on the synthesis and the characterization of $(VO)_{0.5}LaNb_2O_7$ will be presented and the ability to manipulate this product topochemically will be briefly discussed.

B.2 Experimental

B.2.1 Synthesis

Target reaction equation:

$2 A\text{LaNb}_2\text{O}_7 + \text{VOSO}_4 \cdot 2\text{H}_2\text{O} \rightarrow 2 \text{(VO)}_{0.5}\text{LaNb}_2\text{O}_7 + A_2\text{SO}_4$ (where A = Li, Na, K, Rb, Cs, NH$_4$)
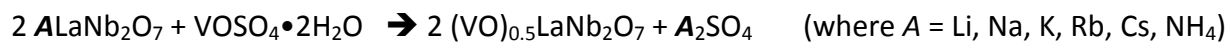
Table B.1 Reaction conditions

Sample Preparation	Host and reagent are weighed and mixed with 100mL of distilled water in a round bottom flask with a stir bar and placed in an oil bath (Figure B.1)
Molar Ratio	1:1, 1:2, 2:1
Reaction Time	About 6 days total where the solution was refreshed every 2days
Reaction Temperature	Between 55-60°C
Work up	Solid was isolated through suction filtration and through centrifugation depending on the particle sizes to increase the quantitative amount, washed with copious amount of distilled water, and rinsed with acetone before placed in the drying oven at 150°C

Figure B.1 Reaction Setup

B.2.2 Characterization

Powder X-ray diffraction data for all the materials were collected on a Philips X-pert Pw 3040 MPD X-ray diffractometer using Cu *K*α radiation. Data were collected over the range of $5^o< 2\theta<95^o$. Data analysis was carried out with the programs POLSQ to obtain refined unit cell parameters and Crystal Diffract to simulate the XRD pattern.

B.3 Results and discussion

Table B.2 Results

Parent	Results
$LiLaNb_2O_7$	Partial Exchange
$NaLaNb_2O_7$	Partial Exchange
$KLaNb_2O_7$	Exchange
$RbLaNb_2O_7$	Exchange
$CsLaNb_2O_7$	No Exchange
$NH_4LaNb_2O_7$	Exchange
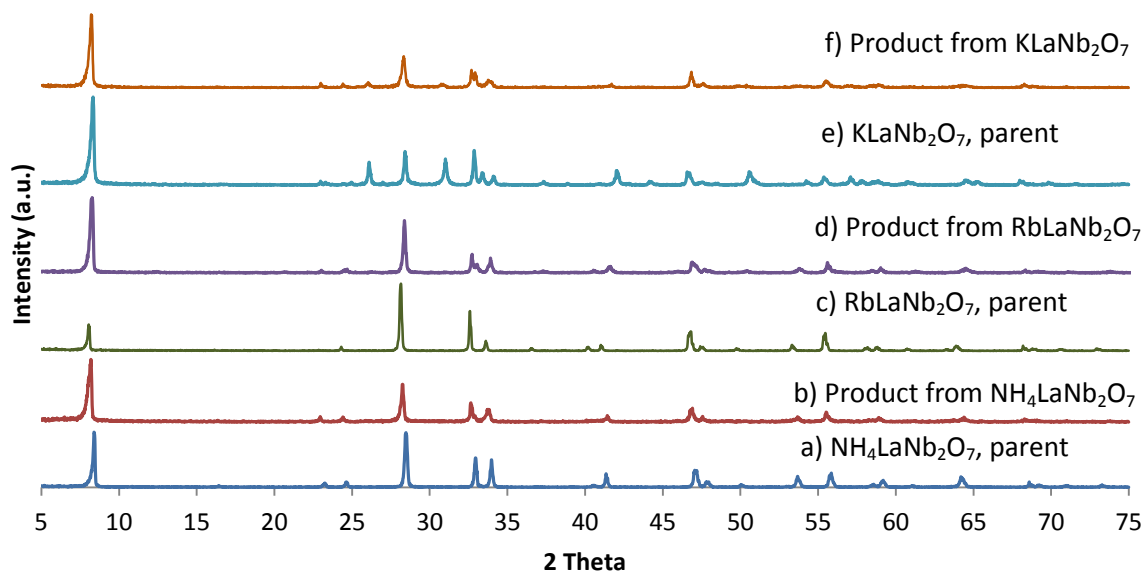
Figure B.2 XRD of products that underwent ion-exchange to become $(VO)_{0.5}LaNb_2O_7$
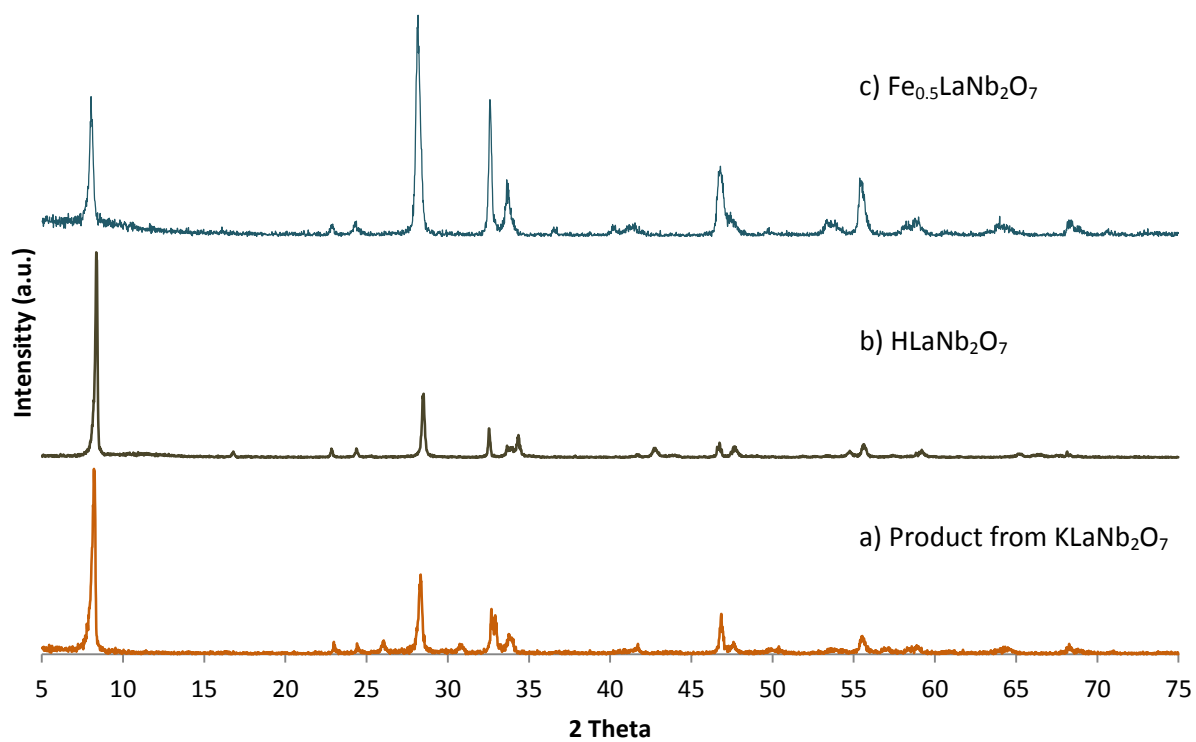
Figure B.3 XRD of a) product that underwent ion-exchange from $KLaNb_2O_7$ and comparison with b) $HLaNb_2O_7$ and c) $Fe_{0.5}LaNb_2O_7$

Table B.3 Refined unit cell parameters

	a(Å)	b(Å)
Parent, $NH_4LaNb_2O_7$[4]	3.879(7)	10.95(2)
Product	3.861(4)	11.04(2)
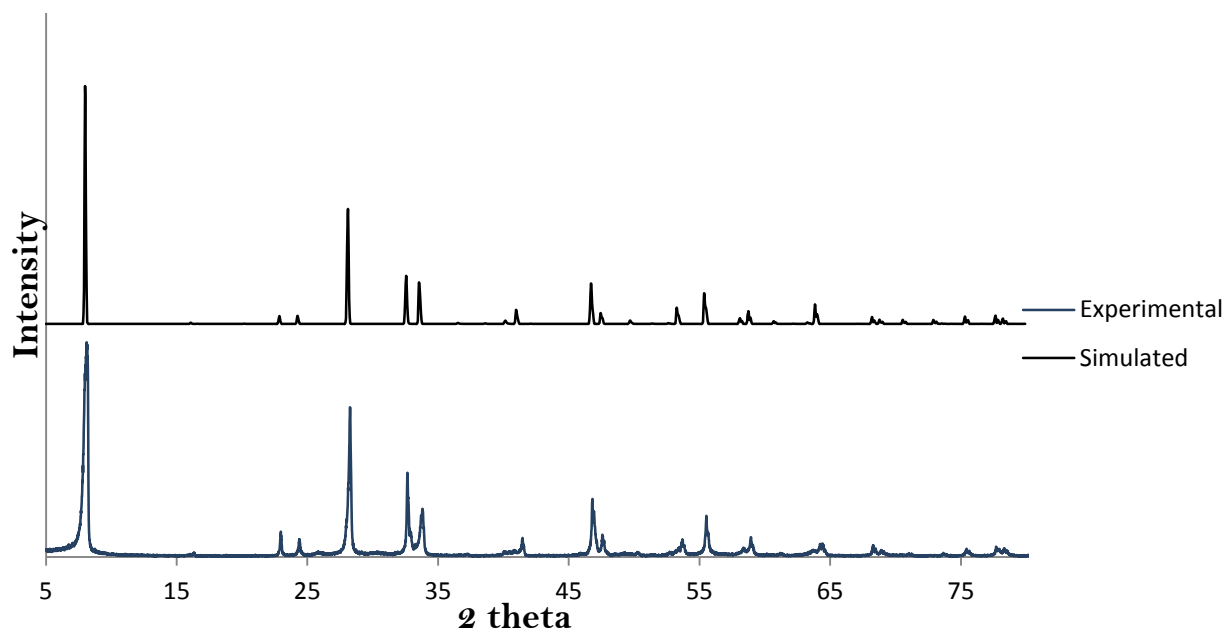
Figure B.4 Initial simulation of $(VO)_{0.5}LaNb_2O_7$

B.4 Conclusions

- IR and Raman data supports the presence of the VO unit in the structure. The stretching band is around 1014 cm^{-1}.

- EDAX indicates that V is present and initial analysis indicates La:V ratio of 1:0.5.

- The initial model is in good agreement with the experimental data

B.5 References

1. Gopalakrishnan, J.; Sivakumar, T.; Ramesha, K.; Thangadurai, V.; Subbanna, G. N. *J Am Chem Soc* 122, 26 (2000).
2.   Viciu, L.; Liziard, N.; Golub, V.; Kodenkandath, T. A.; Wiley, J. B. *Mat Res Bull* 39, 14-15 (2004).
3. Neiner, D.; Golub, V.; Wiley, J. B. *Mat Res Bull* 39, 10 (2004).
4. Gopalakrishnan, J.; Vasudeva, B. *Mat Res Bull* 22, 3 (1987).
5. Rao. C.N.R. and Gopalakrishnan, J. *New Directions in Solid State Chemistry* 2nd ed. Cambrige University Press: (1997).

Appendix C

Topotactic Manipulation of $Fe_{0.5}LaNb_2O_7$; An Attempt to fill Vacancies

C.1 Project Idea:

$Fe_{0.5}LaNb_2O_7$ + M (reductive) or X (oxidative) ➔ $Fe_{0.5}M/XLaNb_2O_7$ (M = Li; X = F, Cl)

Table C.1 Reagents and reaction conditions attempted

Reagent	Reaction Conditions
PVDF	1:3.6 molar ratio total (in 1:1.2 increments with intermediate grinding), mixed and ground in an argon filled glove box, pressed into pellets, sealed in a Pyrex tube under vacuum and heated at $400^{o}C$ for 19 h to 4 days.
NH_4F	1:2 molar ratio, mixed and ground in an argon filled glove box, heated in air in an alumina crucible at $150^{o}C$ for 15 hours
Cl_2	Heated in a sand bath at $230^{o}C$ under inert atmosphere using a Schlenk line
NH_4Cl	1:2 molar ratio, mixed and ground in an argon filled glove box and heated in air in an alumina boat at $320^{o}C$ for 17 hours
$CuCl_2$	Two techniques: a) 1:2 molar ratio, mixed and ground in an argon filled glove box and heated in air in an alumina boat at $225^{o}C$ for 17 hours. b)1:2 molar ratio mixed and ground in an argon filled glove box, sealed in a Pyrex tube under vacuum and heated for 3 days, followed by an acetonitrile wash to remove the CuCl byproduct
C_4H_9Li	1:5 molar ratio, under inert atmosphere in a 1.6M solution at RT for 15 hours, washed with hexane and dried under N_2
LiI	1:2 molar ratio, mixed and ground in an argon filled glove box, sealed in a Pyrex tube under vacuum and heated at 250, 350 or $400^{o}C$ for 7 days, temperature gradient for 2 days to remove I_2 byproduct

C.2 Results

Table C.2 Results

Reagent	Reaction Result
PVDF	Decomposition
NH_4F	No reaction
Cl_2	No reaction
NH_4Cl	No reaction
$CuCl_2$	a) No reaction in air b) Decomposition under vacuum
C_4H_9Li	No reaction/?
LiI	No reaction/?

VITA

The author was born in Oranjestad, on the island of Aruba. She graduated from Colegio
Arubano high school, Oranjestad in May 1998 and started her undergraduate studies at the
University of West Florida, UWF, in the fall of 1998 in Pensacola, Florida where she received her
B.S. degree in Chemistry in the spring of 2003. She also worked in the spring of 2003 as a
chemist doing analytical work for the WATER- EN ENERGIEBEDRIJF ARUBA N.V. (WEB). In the
fall off 2003 she joined the University of New Orleans Chemistry Department to start her
graduate career and was accepted in Prof. John B. Wiley's research group in December 2003 to
pursue a Ph.D. in Solid State Chemistry. In the spring of 2009, she received her MS in
Chemistry.